JAERI-M
82-077

ANNUAL REPORT ON NEUTRON SCATTERING STUDIES IN JAERI, SEPTEMBER 1, 1979 - AUGUST 31, 1981

July, 1982

[eds.] Masatoshi SATO,* Masakazu NISHI,*
Hideshi FUJISHITA,* and Masashi IIZUMI

日本原子力研究所
Japan Atomic Energy Research Institute

JAERI-Mレポートは，日本原子力研究所が不定期に公刊している研究報告書です。
入手の問合わせは，日本原子力研究所技術情報部情報資料課（〒319-11茨城県那珂郡東海村）あて，お申しこしください。なお，このほかに財団法人原子力弘済会資料センター（〒319-11茨城県那珂郡東海村日本原子力研究所内）で複写による実費頒布をおこなっております。

JAERI-M reports are issued irregularly.
Inquiries about availability of the reports should be addressed to Information Section, Division of Technical Information, Japan Atomic Energy Research Institute, Tokai-mura, Naka-gun, Ibaraki-ken 319-11, Japan.

編集兼発行　日本原子力研究所
印　　刷　いばらき印刷㈱

JAERI-M 82-077

Annual Report on Neutron Scattering Studies in JAERI
September 1, 1979 - August 31, 1981

(eds.) Masatoshi SATO*, Masakazu NISHI*,
Hideshi FUJISHITA* and Masashi IIZUMI

Division of Physics, Tokai Research
Establishment, JAERI

(Received June 7, 1982)

Neutron scattering studies carried out from September 1979 to August 1981 by Division of Physics, JAERI, and universities with JRR-2 and -3 neutron beam facilities are described : 61 summary reports, and a list of publications.

Key words: Neutron Scattering, Neutron Diffraction, Neutron Optics, Solids State Physics, Condensed Matters, Crystal Structure, Lattice Dynamics, Structural Phase Transition, Magnetic Structure, Magnetic Moment Distribution, Spin Wave, Liquid, Solution, Research Reactor, JAERI.

---

* The Institute for Solid State Physics, The University of Tokyo.

JAERI－M 82－077

日本原子力研究所における中性子散乱研究年次報告

（1979年9月1日～1981年8月31日）

日本原子力研究所東海研究所物理部

（編）佐藤正俊*・西　正和*

藤下豪司*・飯泉　仁

（1982年6月7日受理）

JRR－2，－3を使い，日本原子力研究所物理部および諸大学研究機関によって行なわれた中性子散乱研究の，2年間の成果をまとめたプログレス・レポートである。内容は，61篇の小論文と，出版された文献のリストを収録している。

* 東京大学物性研究所

PREFACE

The present report is the fourth issue of the series of publications which documents the current research activity in the neutron scattering at Tokai Research Establishment. Although this was originally intended to be issued annually, no publication was done last year because of the half year's break of the JRR-2 operation. Therefore this issue contains papers on the research works carried out in last two years from September 1, 1979 to August 31, 1981. All the research works reported here have been carried out by the use of the neutron facilities in JRR-2 and 3. The papers were prepared by individual authors.

The issuance of this report is not intended to constitute a publication in a usual sense. Final results will be submitted for publication in regular journals. Papers published during the period covered by this report are listed in the alphabetical order of the first authors at the end of this report.

CONTENTS

IV. MAGNETIC EXCITATIONS

V. LIQUIDS AND SOLUTIONS

VI. NEUTRON OPTICS and TECHNIQUES

目　　次

I1 Anharmonic Thermal Vibration of Cations in β-Ag_3SX (X=Br, I)

Takashi Sakuma* and Sadao Hoshino**

*Department of Physics, Faculty of Science, Ibaraki University and
** Institute for Solid State Physics, The University of Tokyo.

Ag_3SX (X=Br, I) is known to be a superionic conductor with a disordered distribution of Ag ions at room temperature. The crystal structure of β-Ag_3SX was studied by neutron and X-ray diffraction techniques and was analyzed using asymmetric anharmonic thermal vibration for cations.

Powder neutron diffraction measurements at room temperature were performed with ISSP ND-2 diffractometer installed at JRR-3 in Japan Atomic Energy Research Institute. The incident neutron wavelength of 0.95Å monochromatized with a germanium 311 reflection was used.

The structure refinement of β-Ag_3SX was carried out based on an anharmonic thermal vibration model for Ag ions.[1] Ag ions in β-Ag_3SX are distributed at random over the 12(h) sites with a site symmetry mm2. An effective anharmonic field of this position is

$$V=V_0+\mu u_3+\frac{1}{2}(\alpha_1 u_1^2+\alpha_2 u_2^2+\alpha_3 u_3^2)+\beta_1 u_1^2 u_3+\beta_2 u_2^2 u_3+\beta_3 u_3^3+$$
$$\cdots\cdots \text{(higher order terms)}.$$

u_1, u_2 and u_3 are the components of the displacement of cation from its equilibrium position due to the lattece vibration. Positions of X and S were fixed at 000 and $\frac{111}{222}$, respectively. The isotropic temperature factors were used for anions with the site symmetry m3m.

The detailed results have been published in J. Phys. Soc. Jpn 48(1980) 1036; ibid. 49(1980)678.

1) S. Hoshino, T. Sakuma and Y. Fujii: Solid State Commun. 22(1977)763.

I2 Crystal Structure and Phase Transition of $Ag_3SBr_{0.5}I_{0.5}$

Takashi Sakuma*, Hideshi Fujishita** and Sadao Hoshino**

* Department of Physics, Faculty of Science, Ibaraki Uneversity and

**Institute for Solid State Physics, The University of Tokyo.

Reuter and Hardel investigated[1] the solid solution of Ag_3SBr and Ag_3SI above room temperature by DTA method. They found that $Ag_3SBr_xI_{1-x}$ ($x=0\sim1$) is stable at room temperature, though $Ag_3SBr_{0.5}I_{0.5}$ decomposed near 300°C.

The phase transition and the structures of a superionic conductor $Ag_3SBr_{0.5}I_{0.5}$ were investigated by specific heat, X-ray diffraction, neutron diffraction and dielectric measurements. The ordered phase (γ-phase) concerning the Ag distribution was discovered below 115K.

Integrated intensities of Bragg reflections of the room temperature β-phase and the low temperature γ-phase were measured with powder sample. Neutron diffraction measurement was performed with ISSP ND-1 spectrometer installed at Japan Atomic Energy Research Institute. The incident neutron energy of 41 meV monochromatized with pyrolytic graphite 002 reflection was used.

The structures of the β-pase is simple cubic with the lattice constant $a= 4.842\pm0.003$Å and is isomorphous to that of β-Ag_3SI with the space group O_h^1-Pm3m.[2] The atomic positins are as follows:

$\frac{Br}{2}$ and $\frac{I}{2}$ in 000

S in $\frac{111}{222}$

3Ag in 12(h) $x\frac{1}{2}0$; $0x\frac{1}{2}$; $\frac{1}{2}0x$; $x0\frac{1}{2}$; $\frac{1}{2}x0$; $0\frac{1}{2}x$;
$\bar{x}\frac{1}{2}0$; $0\bar{x}\frac{1}{2}$; $\frac{1}{2}0\bar{x}$; $\bar{x}0\frac{1}{2}$; $\frac{1}{2}\bar{x}0$; $0\frac{1}{2}\bar{x}$.

The atomic position of Ag (x_{Ag}) and the Debye-Waller factors (B_{Ag}, B_S, $B_{Br+I/2}$) were determined by the least squares method. The obtained final values of the parameters with standard deviations are as follows:

$$x_{Ag} = 0.388\pm0.005$$

$$B_S = 0.24 \pm 2.41 \quad (A^2)$$

$$B_{\frac{Br+I}{2}} = 1.88 \pm 1.15 \quad (A^2)$$

$$B_{Ag} = 2.46 \pm 1.47 \quad (A^2)$$

The discrepancy index $R_I = \Sigma(|I_o - I_c|)/\Sigma I_o$ is 0.088.

The structure of γ-Ag $SBr_{0.5}I_{0.5}$ formed a face centered lattice with $a(\simeq b \simeq c) = 9.637 \pm 0.002$ Å at 99K which is almost twice of the lattice constant of the β-phase. The space group of γ-$Ag_3SBr_{0.5}I_{0.5}$ would be C_{2v}^{18}-Fmm2 and the atomic positions are as follows:

$$(000,\ 0\tfrac{11}{22},\ \tfrac{1}{2}0\tfrac{1}{2},\ \tfrac{11}{22}0)+$$

8S in 8(b) $\quad \tfrac{11}{44}z;\ \tfrac{13}{44}z,$

4Br and 4I in I 4(a) 00z (z=0),

II 4(a) 00z ($z \sim \tfrac{1}{2}$),

24Ag in I 8(d) x0z; $\bar{x}$0z,

II 8(c) 0yz; 0$\bar{y}$z;

III 8(b) $\tfrac{11}{44}z;\ \tfrac{13}{44}z.$

The leasrt squares refinement was carried out for ten structural parameters. The obtained final values and the discrepancy index R_I are as follows:

$$z_S = 0.229 \pm 0.047$$

$$z_{\frac{Br+I}{2}} = 0.494 \pm 0.020$$

$$x_{Ag_I} = 0.293 \pm 0.005$$

$$z_{Ag_I} = 0.249 \pm 0.014$$

$y_{Ag_{II}} = 0.231 \pm 0.007$

$z_{Ag_{II}} = 0.352 \pm 0.013$

$z_{Ag_{III}} = 0.519 \pm 0.019$

$B_S = 2.43 \pm 6.89$ ($\AA^2$)

$B_{\frac{Br+I}{2}} = 0.21 \pm 7.91$ ($\AA^2$)

$B_{Ag} = 1.29 \pm 1.03$ ($\AA^2$)

$R_I = 0.11$.

The γ-phase of $AgSBr_{0.5}I_{0.5}$ is not similar to that of Ag_3SBr and Ag_3SI.[3]

Detailes will be submitted to J. Phys. Soc. Jpn.

1) B. Reuter and K. Hardel: Z.für anorg. und allge. Chemie 310(1965)158.
2) S. Hoshino, T. Sakuma and Y. Fujii: J. Phys. Soc. Jpn. 47(1979)1252.
3) T. Sakuma and S. Hoshino: J. Phys. Soc. Jpn. 47(1979)1252.

I3 Neutron Scattering Study of Cation Distribution in α-AgI Type Superionic Conductors

Sadao Hoshino*,Takashi Sakuma**,Hideshi Fujishita* and Kaoru Shibata*

* Institute for Solid State Physics, The University of Tokyo,

** Department of Physics, Faculty of Science, Ibaraki University

The neutron diffuse scattering of α-AgI type superionic conductors, α-AgI, α-Ag_2S and α-Ag_3SI was measured using either powder sample or single crystal with a triple-axis type neutron spectrometer ISSP ND-1 installed at JRR-2. The purpose of this study was to examine a static state of order about the distribution of cations by the method of a separation of elastic disorder scattering from inelastic thermal scattering. The analyzer crystal was mounted at the fixed angle so as to measure only elastic part of the scattering though a part of quasi-elastic scattering was included due to the experimental energy resolution. The incident neutron energy of either 13.7meV or 30.5meV was used for the measurements.

Observed powder diffuse scattering curves indicated that the peak width became sharper with increasing cation concentration, that is, in the order of AgI, Ag_3SI and Ag_2S. This suggests that the interaction among cations becomes stronger when the concentration of cations is higher. The observed diffuse scattering intensity was compared with calculated ones with various models. A good agreement between experiment and calculation was obtained when we took account of the structure model of the twelve-position distribution with asymmetric anharmonic thermal vibration of cations. Short range order parameters were calculated also by the least squares fitting method and a resonable result was obtained.

The liquid phase of AgI was also investigated by neutron scattering. The result was analyzed with a hard sphere model and was examined in comparison with the diffuse scattering of the α-phase.

Details of this study has been reported at the XIIth International Congress of Crystallography, Ottawa, 1981 and will soon be submitted to J.Phys.Soc.Jpn.

I4 Reinvestigation of the Low Temperature Symmetry of $SrTiO_3$ by Neutron Diffraction

Sadao Hoshino and Hideshi Fujishita
Institute for Solid State Physics, The University of Tokyo

The space group of the low temperature phase of $SrTiO_3$ below 106K has long been believed as I4/mcm and the phase transition mechanism of this crystal has been discussed based on the symmetry consideration. Recently, Okazaki and Willis[1] reported that the space group was not I4/mcm as a result of their neutron diffraction data in which superlattice reflections prohibited by the symmetry were observed. This seems to be a very important report.

A reinvestigation was carried out for the intensity measurement of 1/2(111) reflection using an incident neutron energy of 13.7meV with a neutron spectrometer ISSP ND-1 at JRR-2. A single crystal of $SrTiO_3$ was cut and shaped so that the uniaxial stress could be applied along [110]. As reported by Okazaki and Willis, the prohibited 1/2(111) reflection was really observed in the present measurement too, but after the careful examination with various measurements under different conditions we finally found that the appearence of the prohibited reflections was due to the result of multiple reflections. The same crystal was sent to Brookhaven to examine with measurements varying the incident neutron energy, in particular, in the low energy region. The result clearly showed the same conclusion as stated above. Thus, it was concluded that the space group for the low temperature phase of $SrTiO_3$ was not to be changed.

1) A.Okazaki and B.T.M.Willis: Harwell Report HL80/2680,August,1980.

I5 Neutron Scattering Studies of the Ordered Structure of $C_{24}Rb$

Masatsugu Suzuki, Hironobu Ikeda, Hiroyoshi Suematsu*, Yasuo Endoh**, Hiroyuki Shiba*** and Michael T. Hutchings****

Department of Physics, Ochanomizu University, *Institute of Materials Science, University of Tsukuba, **Department of Physics, Tohoku University, ***Institute for Solid State Physics, University of Tokyo, ****Materials Physics Division, AERE Harwell

A neutron elastic scattering measurement has been performed on $C_{24}Rb$ at temperature between 106 K and 165 K. The observed extinction rule of the diffraction pattern can be explained on the basis of a simple model : Rb layers form a triangular lattice with fundamental wave vector G_R^0 =1.20 $\mathring{A}^{-1}$, which is modulated by the gaphite layers. The modulation is described by a static distortion wave, which manifests itself in the appearance of a satellite peak at $G_R^0 - G_0$ =1.78 $\mathring{A}^{-1}$, for example, where G_0 =2.95 $\mathring{A}^{-1}$ is the fundamental in-plane wave vector of graphite. This model leads to a prediction that the Rb layer is rotated relative to the graphite layer by 9°.

I6 Strain Waves in Cr and its Alloys

Satoshi Iida*, Masaharu Kohno** Yorihiko Tsunoda
and Nobuhiko Kunitomi

Department of Physics, Faculty of Science, Osaka University, Toyonaka 560

Chromium shows the spin density wave (SDW) state, in which the spin density varies sinusoidally in space and its period is incommensurate with the lattice periodicity. By X-ray diffraction experiments the sinusoidal periodic lattice strain (strain wave, SW) associated with SDW ordering was observed by Tsunoda et al.[1] in pure Cr. The period of the strain wave observed by them is one half of that of SDW. In the present work, we carried out neutron and X-ray diffraction measurements of the strain wave in pure Cr, CrMn and CrV alloys at various temperatures in order to elucidate the nature of the strain wave. These alloys were chosen because the physical properties concerning SDW were precisely measured hitherto and their physical properties are rather easier to interpret by considering the change of the d-electron number compared with the other Cr alloys.

The single crystals of pure Cr and Cr alloys with the volume of 50 ∿ 400 mm^3 are cut from the ingots which were made by the repeated arc-melting. The experiments were performed on the triple axis neutron spectrometer TUNS installed at JRR-2 in JAERI. The typical incident neutron energy used in this measurement was 39.13 meV (1.44Å). A pyrolytic graphite analyzer was used to eliminate the inelastic component. The collimator system was of 20'-30'-30'-30'.

Typical examples of the neutron diffraction patterns of (200), SDW and SW reflections for Cr-0.5 at.% Mn at 85 K and 324 K and for Cr-0.3 at. %V are shown in Fig. 1 and 2, respectively. The two different temperatures used for the measurments on Cr-0.5 at.% Mn correspond to the incommensurate and commensurate SDW states and the strain wave reflection was observed only in the former and not in the latter. The position of the strain wave reflection expected from the SDW satellite position is shown by the arrow.

From these figures, we can estimate the magnitude of SDW $\hat{S}$ and displacement amplitude Δ together with the modulation wave number δ and 2δ. In practice the determination of the absolute value of Δ was made from the observed ratio of I(SW)/I(SDW) and I(SW)/I(200). In the former, we used the value of $\hat{S}$ determined by previous worker by powder method and determined the absolute value of Δ. In the latter, we assumed equal

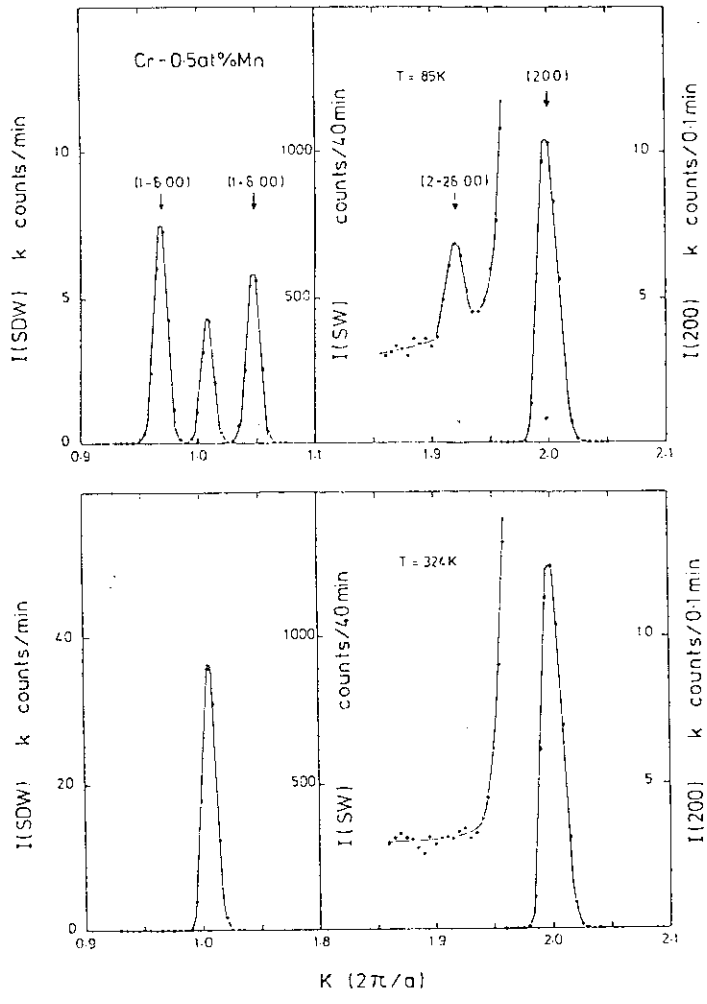

Fig. 1. The line profiles of SDW, SW and (200) Bragg reflections of Cr-0.5 at.% Mn.

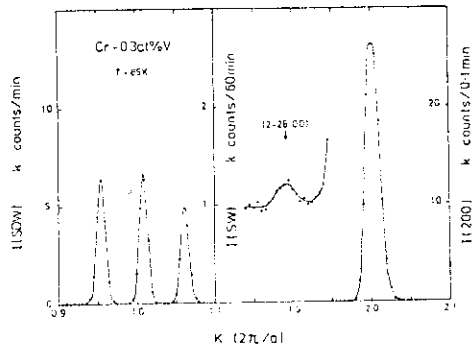

Fig. 2. The line profiles of SDW, SW and (200) Bragg reflections of Cr-0.3 at.% V.

distribution of the magnetic domains. In both cases, we neglected the secondary extinction effect which may be large in the latter. The displacement amplitude for various specimens are shown in Fig. 3 as a function of δ. The values determined by both methods coincide within the experimental error. The displacement amplitude increases with the decrease of δ. In vertical axis, the displacement is normalized by the lattice constant. The displacement amplitude Δ is converted to the strain amplitude Δa by

$$\Delta a = \Delta \sin(2\delta a)$$

and can be compared with the theoretical results. In Fig. 4, the observed value $(\Delta a/a)/\hat{S}$ for various specimens is summarized as a function of δ. Kotani[2] has carried out the theoretical calcu-

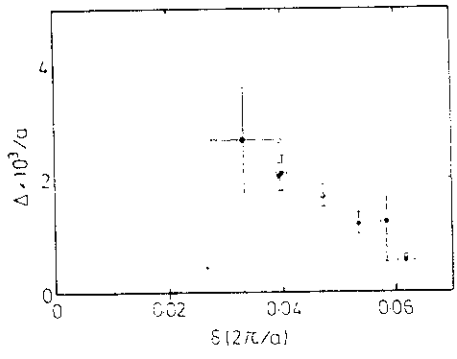

Fig. 3. The displacement amplitude as a function of δ.

lation of Δa on the basis of nesting model and his result is shown by a solid curve in the figure. The theoretical curve reproduces the experimental results in the sense that it increases first and then decreases with the decrease of δ.

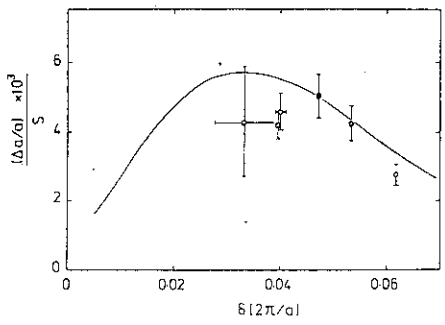

Fig. 4. The ratio of the strain wave amplitude to the primary SDW amplitude as a function of δ.

* Present Address ; Faculty of Science, Kwansei Gakuin University, Uegahara, Nishinomiya, Hyogo 662.

**Present Address ; Kobe Steel Ltd., Wakihama Chuoku, Kobe, Hyogo 651.

References

1) Y. Tsunoda, M. Mori, N. Kunitomi, Y. Teraoka and J. Kanamori ; Solid State Commun. 14 (1974) 287.

2) A. Kotani ; J. Phys. Soc. Japan 39 (1975) 851.

I7 Lattice Strain in Fe-Pt Alloys Observed by Polarized Neutron Method

Nobuhiko Kunitomi and Yutaka Nakai

Department of Physics, Faculty of Science, Osaka University
Toyonaka, Osaka, 560

The diffuse scattering cross section of a dilute alloy with a short range atomic order and a lattice distortion around an impurity atom is described as

$$\frac{d\sigma}{d\Omega} = c(1-c)[(f_i-f_h)^2 S(K) - 2f_h(f_i-f_h)D(K)] \qquad (1)$$

with

$$S(K) = \sum_j z_j \alpha_j \sin KR_j/KR_j \qquad (2)$$

and

$$D(K) = \sum_j z_j \frac{\delta_j}{R_j}\left(\frac{\sin KR_j}{KR_j} - \cos KR_j\right), \qquad (3)$$

where S(K) and D(K) corresponds to atomic short range order and lattice distotion terms, respectively. In these equations, c is the fractional impurity concentration, f_i and f_h are the impurity and host scattering amplitudes, the α_j's are the Warren-Cowley short range order parameter for j-th nearest neibors separated by R_j and δ_j's are radial diplacements from the host lattcie due to the impurity. Because of the small value of δ_j in a typical alloy, the D(K) term amounts for the order of a few millibarns and is very difficult to detect beyond the experimental errors.

Cable et al have developed a method to detect the diffuse scattering due to lattice distortion without the interference due to other sources of backgraound scattering by means of polarized neutron diffuse scattering . The difference cross section between spin-up and spin-down states is

$$\Delta\frac{d\sigma}{d\Omega} = 4c(1-c)[\Delta b\ \Delta p\ S(K) - (b_h\Delta p - p_h\Delta b)D(K)], \qquad (4)$$

where $b = b_i - b_h$ and $p = p_i - p_h$ (p the magnetic scattering amplitude). They applied this equation to the case of Pd-1 at.% Gd alloy and obtained S(K) and D(K). However, since the contribution from S(K) is the same order of the magnitude of that from D(K), the separation of these two terms is quite difficult and causes much error. If we uses an alloy with $\underline{\Delta b=0}$, the difference cross section becomes

$$\Delta\frac{d\sigma}{d\Omega} = -4c(1-c)\Delta p D(K), \qquad (5)$$

and the contribution from S(K) vanishes. In the present experiment, we used alloys of Fe-Pt which have the following four advantages:

(i) The nuclear scattering amplitudes of Fe and Pt are 9.51 fm and 9.5 fm, respectively, thus resulting $\Delta b=0$.

(ii) The alloy is ferromagnetic in Fe rich side and, therfore, the polarize neutron experiment is possible. Furthermore, the difference of Fe and Pt moment is fairly large ($\mu_{Fe} \simeq 2.2\ \mu_B$, $\mu_{Pt} \simeq 0\ \mu_B$), thus value of Δp becomes large.

(iii) The atomic radius of Pt is much larger than that of Fe, since Pt belongs to 5d sereis while Fe to 3d. The large difference of atomic radius makes δ_j and D(K) large.

(iv) The magnetic form factor $f_{Fe}(K)$ is larger than $f_{Pt}(K)$ in a wide range of K, thus making Δp large in a wide K range.

The experiment was made for $Fe_{90}Pt_{10}$ and $Fe_{95.3}Pt_{4.7}$ by using POLTO polalize neutron diffractometer and a part of which was carried out by using PANSI. The measurement was made at room temperature in a 2θ range from 5° to 22°. The contribution from multiple scattering was subtracted by the computer simulation method. The difference cross section thus obtained is shown in Figs. 1 and 2 for 4.7 and 10 at.% Pt specimens. In these figures are shown the calculated curves by Eq.(5) under the assumption that the contributions from the second and the further nearest neiboring atoms are negligible. The best fitted parameters for δ_1 are 0.13 and 0.16 A, respectively, for 4.7 and 10 at.% specimens. The strain produced by the introduction of Pt atom is about 5% of the lattice spacing

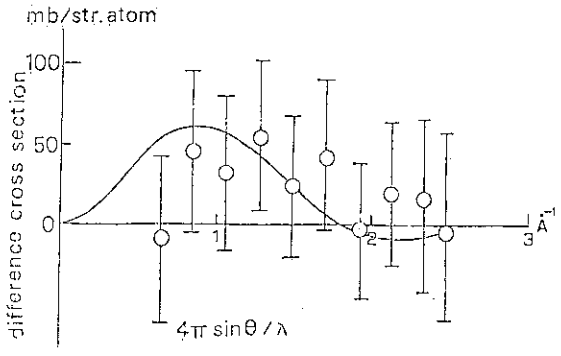

Fig.1 Polarize neutron difference cross section of $Fe_{95.3}Pt_{4.7}$ after multiple scattering corrected. Solid curve represents theoretical curve obtained by Eq.(5)

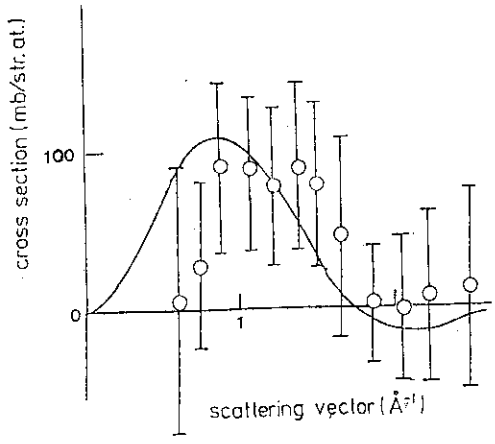

Fig. 2. Polarize neutron difference cross section of $Fe_{90}Pt_{10}$, after multiple scattering corrected. Solid curve is obtained by Eq. (5)

which is considered to be a reasonable value for these kinds of alloys.[3]

Although the statistical error is still high in this experiment, this polarize neutron method under the condition of $b_i = b_h$ is undoubtedly a unique technique for the study of the strain.

The authors would like to express their sincere thanks to Prof.Y.Ito of ISSP and his colleagues for their cooperations.

(1) J.W.Cable, R.E.Parra, H.R.Child; Solid State Comm. 27(1978)911
(2) Y.Nakai; J.Appl.Phys. Jpn. 13(1974)1061
(3) M.A.Krivoglaz; Theory of X-ray and Thermal Neutron Scattering by Real Crystals, Plenum Press, New York, 1969

I8 Anisotropic Precipitation of G.P. zone in an AlCu Alloy under Compressive Stress

Shuzo Kawarazaki and Nobuhiko Kunitomi

Department of Physics, Faculty of Science, Osaka University, Totonaka 560

An Al alloy containing dilute concentration of Cu is well known as a precipitation alloy in which precipitates of Cu called as a Guinier-Preston zone is formed in the early stage of aging. In the case of Al-Cu alloy, the precipitate is plate-like and grows so that the plate is parallel to the (100) plane. In the matrix of Al around this precipitate is induced the lattice strain which modulates the lattice spacing mainly in the direction perpendicular to the plate. Therefore, it is considered that the formation of the precipitates should be anisotropic if the external stress is applied on the specimen in the course of the aging. In order to observe this effect neutron diffraction method is more advantageous than x-ray because we can use a bulk specimen which is sufficiently rigid under the compression.

The specimen is an $Al_{98.2}Cu_{1.8}$ single crystal of a cylindrical form with the approximate size of 7mm-diameter x 8mm which was grown by strain annealing method. The cylindrical axis is parallel to the [100] direction. The specimen was annealed at 550 °C for 5 hrs and then ice-water quenched. The aging was done at 80 °C for 24 hrs under the compressive stress parallel to the cylindrical axis. The magnitude of the stress was that corresponding to 0.15 % strain of the specimen. After removing the applied stress, the neutron diffraction measurement was made on the TOG-ND installed at JRR-3 at room temperature. The diffuse tail around the 200 and 020 Bragg reflections was measured. The equi-intensity contour line is shwon in the Fig1.

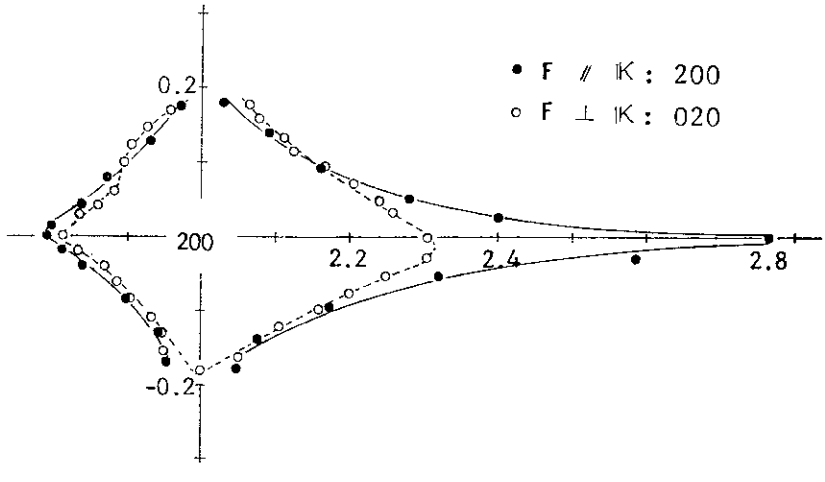

Fig.1 Equi-intensity contour of the diffuse tail around 200 and 020 Bragg position. For comparison the data for 020 have been plotted so that the [020] axis coinsides with the [200] axis.

As is apparent in the figure, the diffuse tail is longer in the case where the applied compression is parallel to the scattering vector than in the case of perpendicular. The intensity ratio of the diffuse tail along the [ζ00] reciprocal axis to that along the [0ζ0]axis was 4.0 between $2.1 < \zeta < 2.3$.

The present result indicates that the number of the precipitates grown in the crystal plane perpendicular to the compression largely increases as the result of the strain aging.

The further investigations such as the effect of the strain aging on the phonon anomaly previously observed[1] are now in progress.

1) to be published.

I9 Neutron Small-Angle Scattering Study of the Decomposition Kinetics in Fe-Cr Alloys

Susumu KATANO and Masashi IIZUMI

Physics Division, Japan Atomic Energy Research Institute

It has been established that Fe-Cr alloys separate at 550° C or lower into two phases. Vintaykin et al.[1] investigated the decomposition kinetics of Fe-Cr solid solutions by means of neutron small-angle scattering and correlated the experimental results in the very early stages with Cahn's linear theory[2] of spinodal decomposition. In recent years, however, there has been growing interest in the non-linear and non-equilibrium processes of the decomposition kinetics. A microscopic theory by Saito[3], a phenomenological theory by Binder and Stauffer[4] and computer simulations by Marro et al.[5] have disclosed the limitation of Cahn's theory and revealed more complicated aspects of the decomposition kinetics in the unstable state. In Fe-Cr alloys the decomposition takes place within a wide composition range and the elastic energy due to size difference of the components has little effect on the decomposition, therefore this alloy system is one of the ideal system to verify these new results. In order to investigate more extensively the decomposition kinetics of Fe-Cr alloys, we undertake neutron small-angle scattering measurements.

The Fe-Cr alloys containing 20 at.% Cr and 34 at.% Cr is prepared by melting in an arc furnace in argon atmosphere. The ingot was homogenized at 500° C up to 20 hr. All experiments were carried out at room temperature. The neutron small-angle scattering measurements were performed by a triple axis neutron spectrometer in the diffractometer arrangement with the neutron wavelength of 2.35 A. A background correction was made for the measured intensity. Magnetic and Nuclear scattering were not distinguished in this work.

In Fig.1 the evolution of the scattered intensity I of the Fe-Cr alloy containing 20 at.% Cr is shown as a function of the wave vector Q (= $4\pi \sin\theta/\lambda$) for increasing aging times up to 20 hr at 500° C. The scattered pattern little changes by aging. The result of the Fe-Cr alloy containing 34 at.% Cr is shown in Fig.2. In contrast to the result of the alloy containing 20 at.% Cr, aging changes the scattered pattern substantially : the intensity increases as a whole but also shows a maximum. It is considered that the distinct difference between the scattered patterns after aging of these alloys indicates that the alloy containing 20 at.% Cr locates outside the spinodal (in the metas-

table state) and the alloy containing 34 at % Cr inside the spinodal (in the unstable state).

In the case of the Fe-34 at.% Cr alloy, the intensity continues to increase and the maximum position shifts toward small wave vecotors with increasing aging time. According to Cahn's theory, the intensity at each wave vector Q changes exponentially with aging time and the peak position of the scattering pattern does not change during the time evolution. In sharp contrast to this theoretical conclusion, our experimental results show that the exponential law of I vs. aging time is not followed at any wave vector and in particular the peak position changes as was stated above. The overall change of the scattering patterns including the later stages of decomposition is rather in good agreement with those illustrated in the papers by Saito[3] and by Marro et al.[5]

In consistence with our results the new theories and computer simulations have revealed the non-exponential time evolution with shifting peak position. Two important parameters characterizing the evolution of I are position of the maximum Q_m and the height of the maximum $I(Q_m)$. The phenomenological theory by Binder and Stauffer[4] and the Monte Carlo simulations by Marro et al.[5] have pointed out that the time evolution of Q_m and $I(Q_m)$ follow the power laws $Q_m \propto t^{-a'}$ and $I(Q_m) \propto t^{a''}$. Binder and Stanffer's theory has predicted a' = 1/6 and a'' = 1/2

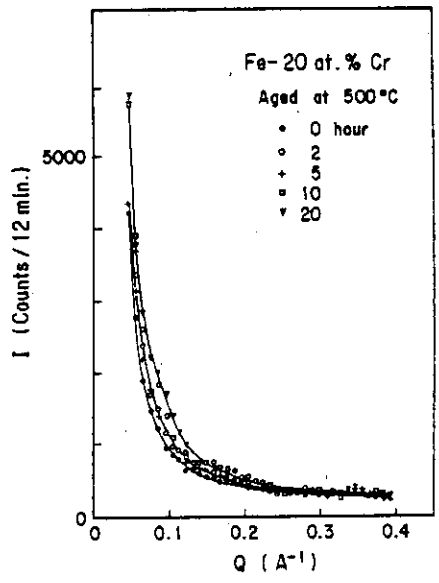

Fig.1. The scattered intensity of the alloy containing 20 at. % Cr as a function of the wave vector for various aging times at 500° C.

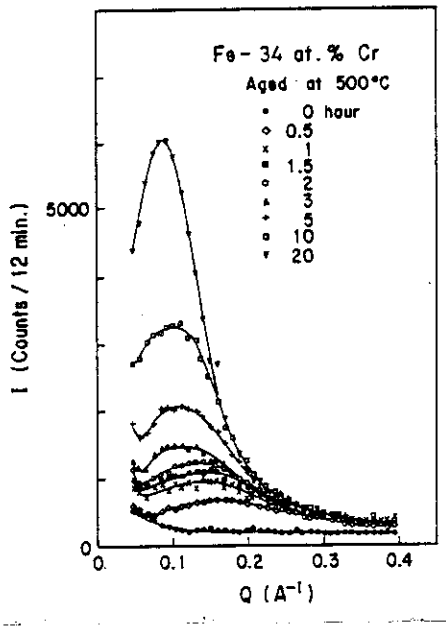

Fig.2. The scattered intensity of the alloy containing 34 at. % Cr as a function of the wave vector for various aging times at 500° C.

for low temperatures, and the computer simulations have given almost consistent results : a' ≃ 0.2 and a" ≃ 0.7 below the critical temperature. In Fig.3, Q_m and $I(Q_m)$ of the present experimental results are plotted as a function of the aging time. It shows that power laws are followed with a' = 0.17 (± 0.02) and a" = 0.6 (± 0.1). These exponents are in good agreement with the above mentioned predictions.

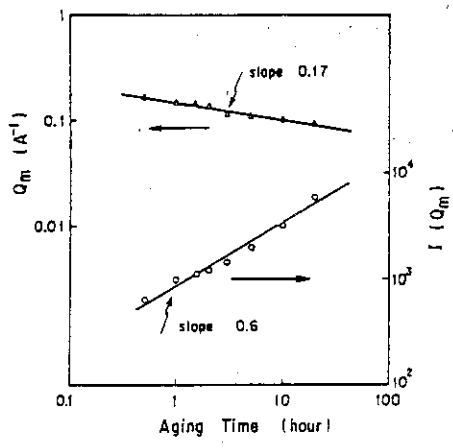

Fig.3. The maximum position Q_m and the maximum height $I(Q_m)$ of the scattered intensity as a function of aging time.

In conclusion, the time evolution of the scattered intensity of Fe-Cr alloys shows rather distinct behaviors depending on whether the alloy locates outside or inside the spinodal. The decomposition kinetics of the alloy in the unstable state agrees well with the predictions of the recent theories and of the Monte Carlo simulations.

References

1) YE. Z. Vintaykin, V. N. Dmitriyev and V. YU. Kolontsov: Fiz. Metal. Metalloved 29 (1970) 1257.

2) J. W. Cahn : Acta Metallurgica 9 (1961) 795.

3) Y. Saito : J. Phys. Soc. Jpn. 41 (1976) 1129.

4) K. Binder and D. Stauffer : Phys. Rev. Letters 33 (1974) 1106.

5) J. Marro, A. B. Bortz, M. H. Kalos and J. L. Lebowitz : Phys. Rev. B 12 (1975) 2000.

III Neutron Scattering Study of the Phase Transition of Ag_3SI

Sadao Hoshino*, Takashi Sakuma** and Hideshi Fujishita*
*Institute for Solid State Physics, the University of Tokyo
**Department of Physics, Faculty of Science, Ibaraki University

The low temperature phase transition of the superionic conductor Ag_3SI was studied by neutron scattering in order to examine the nature of this structural phase transition with order-disorder behavior of cations. Neutron scattering measurements were carried out with a triple-axis type spectrometer ISSP ND-1 at JRR-2. Measurements were performed by the constant Q mode operation with the incident neutron energy of 13.7 and 30.5 meV with PG filter. Single crystals of Ag_3SI with a mosaic spread of about 0.8^{o} were grown by the Bridgman method. Using a single crystal of about 0.5 cm^3, the temperature dependence of the phonon scattering was measured from $25^{o}C$ down to 100K.

At room temperature, the phonon dispersion relation for the TA mode toward [ζ00], [ζζ0] and [ζζζ] up to ζ≈0.2 was measured. However, the other phonons (especially the optical phonons) were highly over-damped and could not be observed. At low temperatur, a very low energy excitation peak with a transfer energy of about 2 meV was observed, suggesting the existence of a local vibrational mode for cations with a poor dispersion behavior. A multi-domain structure is realized in the low temperature phase with a possibility of forming sixteen domain orientations, and these domain orientations were not always realized with the same probability. In fact, the phonon measurements, especially for the [ζζζ] direction, showed somewhat different features when a different crystal was mounted on the cryostat. Thus the data taken in the low temperature phase in the present measurements could have been influenced by such a domain formation.

The present neutron scattering study together with the dielectric investigations of Ag_3SI and also of Ag_3SBr was reported at the Third International Meeting on Solid Electrolytes held in Tokyo on September, 1980 and the proceedings has been published as Solid State Ionics Vol.3/4, August, 1981.

II2 Phonon Dispersion Relations in $C_{24}Rb$

Satoru FUNAHASHI*, Tamotsu KONDOW** and Masashi IIZUMI*
*Physics Division, Japan Atomic Energy Research Institute,
**Department of Chemistry, University of Tokyo.

Among the great variety of graphite intercalation compounds, $C_{24}Rb$ is one of the most intensively investigated materials as a typical second stage compound.[1] The carbon and the alkali metal layers are stacked along the c-axis in the sequence A/AB/BC/CA/A (A,B and C refer to the carbon hexagonal planes and / refers to rubidium plane). Long range order of the rubidium layers develops below about 160K and further structural transition occur at about 100K and at about 50K.[2]

We measured dispersion relations of [001] L-phonons of this material with triple axis spectrometers CTNS and DMNS. The sample used was prepared from highly oriented pyrolytic graphite with the dual furnace method. The dimension of the sample was $1\times1\times0.8\ cm^3$ and the c-axis mosaic spread was about 1.8°.

Measurements were carried out for the three ordered phases namely at 120K, 80K and at 30K. We could observe three phonon branches in all along the c*-axis between 00 15 and 00 19.5 . Since the L-mode phonons along the c*-axis do not discriminate the different stacking of the carbon layers(A, B and C), the phonon dispersion periodicity corresponds to the one third of the unit cell length of /AB/BC/CA/. Fig.1 shows the result at 80K. Little difference from this result was observed in those of 30K and 120K. Zone boundary is corresponding to $q=\pi/(c/3)$. It should be remarked that the acoustic branch has a gap at $\hbar\omega\simeq5$meV. The behavior of the dispersion curves in this region suggests an interaction of the branch with some other degrees of freedom. This reminds us of a flat optic branch at 51K(i.e. 4.4meV) predicted by Kondow et al. from the Einstein-type low temperature specific heat.[3]

In order to analyze the result, we consider longitudinal vibrations of a linear chain illustrated in Fig.2. For rubidium atoms, however, we allow transverse vibrations as well to introduce the transverse Einstein oscillation mode described above. As shown in Fig.2, ϕ_1, ϕ_2 and ϕ_3 represent the nearest neighbor C-C, C-Rb and the second neighbor C-C(over Rb) force constants, respectively, while ϕ' is the force constant of the transverse oscillation of Rb. The introduction of the second neighbor force constant ϕ_3 is inevitable, otherwise the fitting of the calculated curves becomes very poor, especially at the zone boundary, and ϕ_1 becomes unreasonably large. We took a coupling potential into account in the form $U'=\mu u_3 v_3$, where u_3 and v_3 are

the longitudinal and the transverse displacements of a rubidium atom, respectively. The best fit parameters were determined by the least square calculation to be ϕ_1=2940, ϕ_2=2540, ϕ_3=360, ϕ'=338 and μ=158(dyn/cm). The best fit curves are drawn in Fig.1. The magnitude of ϕ_1 is nearly equal to that of the pristine graphite, and ϕ_2 agrees with the exponential formula proposed by Dresselhaus et al.[4] Though little attention has been paid to the second neighbor force up to present, our result indicates that ϕ_3 is as large as 12% of ϕ_1, and that the long range force should not be neglected. Another important feature is that a firm basis is provided to the flat optic branch which has been provisionally introduced in the interpretation of the specific heat.

References. 1)M.S.Dresselhaus and G.Dresselhaus, Advances in Phys.30(1981) 139.
2)H.Suematsu et al., J.Phys.Soc.Jpn. 49(1980)835.
3)M.Suganuma et al., Phys. Rev.B 23(1981)706.
4)G.Dresselhaus et al., Solid State Commun. 40(1981)229.

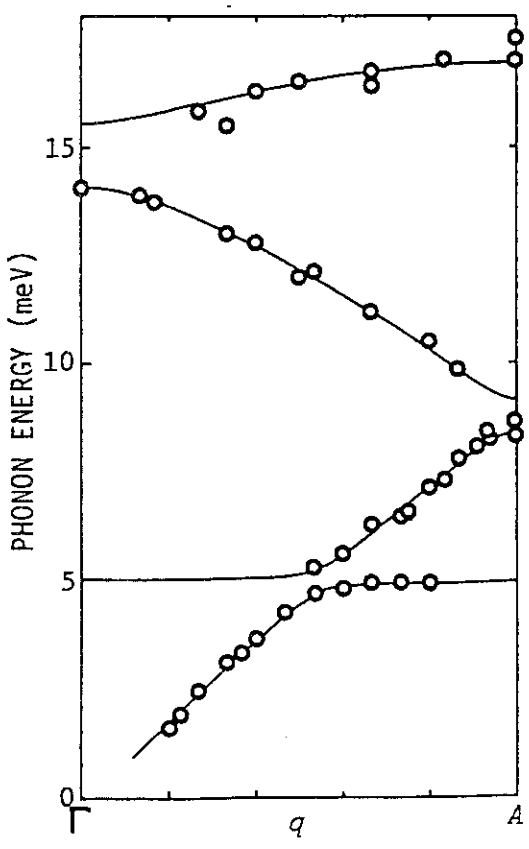

Fig.1. Dispersion relations of [001] L-mode phonons of $C_{24}Rb$ at 80K. Zone boundary(A) corresponds to $q=\pi/(c/3)$. Curves were calculated with parameters in the text.

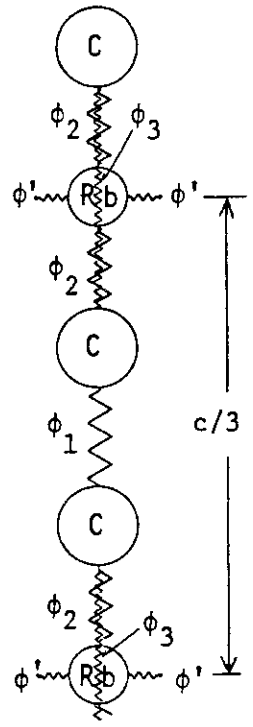

Fig.2. Linear chain model for $C_{24}Rb$. Longitudinal vibrations are considered. But we take transverse oscillations of Rb with force constant ϕ' into account via coupling potential $U'=\mu u_3 v_3$.

II3 Low lying phonon dispersion curves of Rb_xWO_3

Masatoshi Sato

The Institute for Solid State Physics, The University of Tokyo, Roppongi, Minato-ku, Tokyo

The abstract of the paper appeared in J. Phys. C13 L481 (1980) is cited below.

Phonon dispersion curves of Rb_xWO_3 has been measured by the neutron inelastic scattering technique. Nearly dispersionless phonon branches are found at the energy of about 6 meV. They can be considered as the local modes of Rb atoms which are loosely bound in the WO_3 skelton.

For the further work readers can find another reference [Evidence of structurul phase transitions in superconducting Rb_xWO_3 M. Sato et al. Phys. Rev. B25 NO.1 (1982)].

II4 Phonons in $Al_{98}Cu_2$ Alloy at a High Temperature

Hiroshi Shiraishi, Nobuhoko Kunitomi and Yorihiko Tsunoda

Department of Physics, Faculty of Science, Osaka University

In the previous note,[1] we reported the observation of an anomalously large resonance mode in ζ 0 0 T branch of an $Al_{98.2}Cu_{1.8}$ alloy. This mode vanishes in ζ ζ 0 T_1 branch and its origin may be attributed to the plate-like Guinier-Preston (G.P.) zone precipitated in pure Al. However, the G.P. zone developes at room temperature in a very short time and we were unable to observe the phonon of a complete solid solution as a reference. In this note, we report the phonon profile observed at 550° C where the Cu dissolves completely in Al matrix.

The specimen was prepared by the strain anneal method and was supplied by Prof. M. Osamura, Kyoto University. The measurement was made on TUNS-TAS with the incident energy of 40 meV.

Fig. 1 shows the dispersion relation of ζ00 T phonon at 550° C. The double peak structure of the phonon line profile which is the typical evidence of the resonance mode can hardly observed but an appreciable line broadening near ζ = 0.38 implies the existence of the resonance mode. In the inset of this figure, the half widths of line profiles are shown. The solid curve shown in the figure as a guide to eye also indicates the existence of the resonance mode. The observed magnitude of the anomaly is considered to be reasonable from the CPA calculation which is shown in the previous note.[1] The dispersion relation for $\zeta\zeta$0 T_1 branch observed at 550° C is shown in Fig. 2. Similar broadening of the line profile and the breaking of the dispersion curve are also found at about 2 meV. This result suggests that the observed resonance mode is isotropic and has typical nature of the phonon resonance in a dilute solid solution.

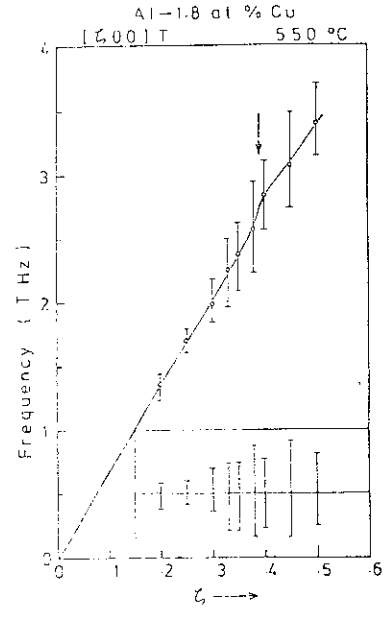

Fig. 1 Dispersion relation of ζ00 T phonon of $Al_{98.2}Cu_{1.8}$ at 550° C.

It is concluded, therefore, that the anomalous resonance mode reported in the previous report is due to the plate-like G.P. zone appeared in the early stage of the precipitation.

(1) N. Kunitomi, H. Shiraishi, Y. Tsunoda and M. Osamura; Ann.Rep. Neutron Scatt. JAERI-M 8719 (1979) 23.

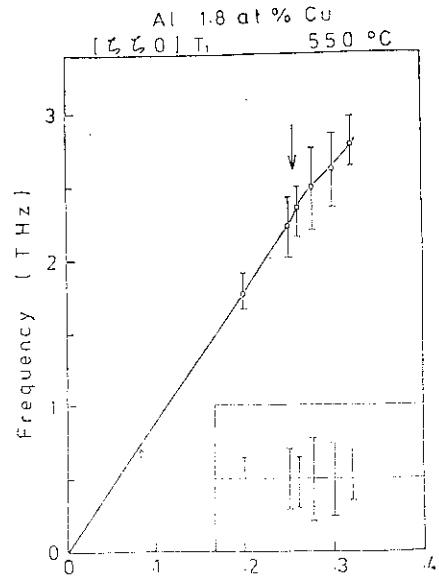

Fig. 2 Dispersion relation of $\zeta\zeta 0$ T_1 phonon of $Al_{98.2}Cu_{1.8}$ at 550° C. Arrows show FWHM of line profile.

II5 Phonon Dispersion Relations of BCC Thallium and the BCC to HCP Martensitic Phase Transformation

Masashi IIZUMI

Physics Division, Japan Atomic Energy Research Institute

Neutron inelastic scattering measurement of the phonon dispersion relations in the body-centered cubic phase has been completed. Experimental details and some preliminary results were described in the previous report.[1] Unique procedure of the measurement was to grow a single crystal within a furnace to be used in the measurement and to keep the crystal above the temperature (230° C) where the bcc to hcp martensitic phase transformation takes place.

The final result of the dispersion relations at 250° C is shown in Fig. 1. The relations show common features of the bcc metals such as remarkable dip of the longitudinal mode in the vicinity of $\vec{q} = (\frac{2}{3}, \frac{2}{3}, \frac{2}{3})$ and besides, some anomalous bend of the curves are seen in the vicinity of the H and N points. However, the most interesting feature of the lattice dynamics of the crystal is the low lying T_1 transverse mode ($\vec{e} \parallel [1\bar{1}0]$) along the [110] direction and in particular the downward bend of the branch in the vicinty of the zone boundary.

The bcc→hcp transformations is explained by Burgers to be carried out by the shuffling of the {110} planes of the bcc lattice i.e. the displacement of every other (110) plane in the $[1\bar{1}0]$ or $[\bar{1}\bar{1}0]$ directions. The shuffling of every (110) plane is accompanied by a secondary shear distortion within the plane to make it the basal (001) plane of the hcp lattice.

The displacement pattern of the shuffling is identical with the zone boundary mode of the T_1 branch which is the collective motion of the (110) planes in the $[1\bar{1}0]$ direction with the wave length of $\sqrt{2}a$, namely the alternate shift of the (110) planes. The observed lowering of the phonon energy of this mode implies that the crystal has a tendency to become unstable with respect to the shuffling type of motion. However it is not appropriate to apply the soft-phonon concept of the usual structural phase transition to this case. The temperature dependence of the zone boundary mode was measured to give no discernible evidence of the softening. Therefore we can only point out that this type of motion has a very small energy, that is, the restoring force for this type of collective atomic displacement is very weak.

It is of interest to Fourier-analyze the dispersion curve of the T_1 mode and to get the effective interplaner force constants between the {110} planes. The analysis has been carried out by the least square fit of the following relation to the observed $\hbar\omega(q)$ data.

$$M\left[\hbar\omega(q)\right]^2 = \sum_{n=1}^{N} \Phi_n \left(1-\cos n\pi q/q_{max}\right)$$

By the analysis we could determine the force constants up to N=3. They are compared with those for the sodium crystal in Table 1. The result indicates that the second neighbor interplaner force is attractive and is quite dominant, which means that the every other (110) planes are coupled with each other and have tendency to move together. This situation among the harmonic force constants for small amplitude oscillation of atoms presumably assists the shuffling motion which is large amplitude displacements of atoms over the anharmonic potential barriers.

This observation is the first which disclosed some sign of the lattice instability related to the bcc to hcp martensitic phase transformation.

1) M. Iizumi, JAERI-M-8719 (1980) p20.

Table 1 Inter planer force constants related to the [110] T_1 mode (10^2 dyne/cm)

	Φ_1	Φ_2	Φ_3	Error
Tl	5.5	4.9	-1.4	0.1
Na	6.7	0.4	-0.2	0.1

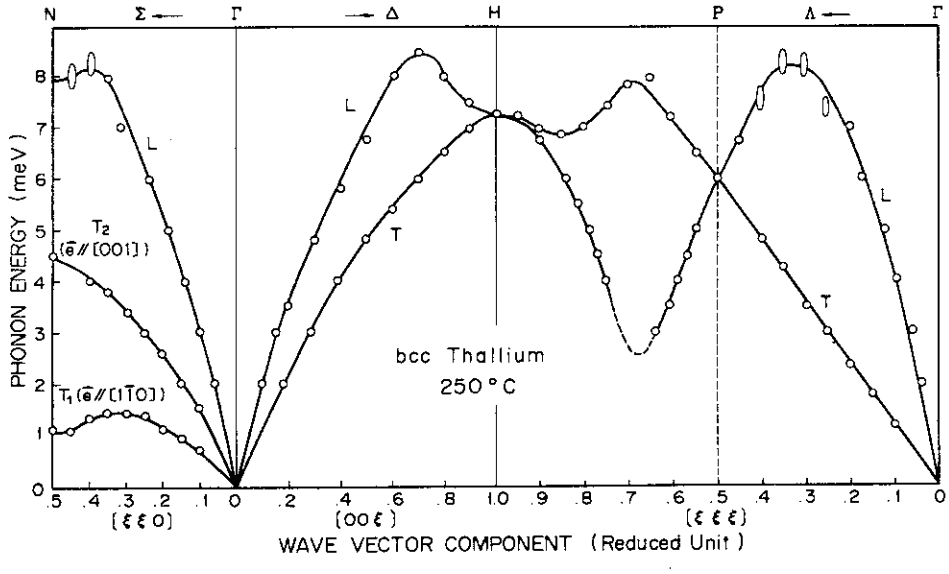

Fig. 1 Phonon dispersion relations of bcc Tl.

II6 Phonon dispersions in $FePt_3$

Yasuhisa Noda*, Yasuo Endoh, Masashi Iizumi**
and Susumu Katano**

Department of Physics, Tohoku University, *Sendai College of Radio Technology, Miyagi, ** Division of Physics, Tokai Establishment, JAERl

Fe-Pt alloy system has two similar metallic compounds of Fe_3Pt and $FePt_3$ of the AB_3 crystal structure with an almost same lattice parameter. We have found a lattice anomaly concomitant with the Invar character in Fe_3Pt[1]. However the anomaly starts at elevated temperatures near the ordering temperature. Therefore we initiate a systematic study of both $FePt_3$ and Fe_3Pt in order to understand the lattice properties associated with the Invar characters.

$FePt_3$ exhibits an antiferromagnetic long range order below T_N about 120K. The magnetic behavior in this compound is explained in terms of the quasi localized magnetic moment model where the localized moment at Fe sites orders antiferromagnetically via the RKKY type magnetic interactions by the conduction electrons donated mainly from Pt atoms[2]. However the complicated magnetic phase transitions associated with the lattice distortion are not fully understood, although much efforts have been devoted to these phase transition.

The measurements were performed on a large single crystal of $FePt_3$ prepared in the Ishikawa Laboratory of Physics Department, Tohoku University. The crystal was grown in an evacuated furnace using a Bridgman technique. The sample was annealed at about 900°c in order to develop the ordering and was cooled in the furnace. The chemical analysis indicated that this crystal contains 22.5 at.% Fe.

The phonon dispersion curves were obtained using two three axis spectrometers of CTNS and TUNS installed at JRR-2. The measurements were performed in $(1\bar{1}0)$, (100), $(11\bar{2})$ symmetry planes. Modes were assigned by the symmetry consideration as well as the calculation of the dynamical structure factors based on the BVK force constant model.

The full dispersion curves were determined along the $\langle 100 \rangle$, $\langle 110 \rangle$ and $\langle 111 \rangle$ symmetry directions. Note that some of measured phonon peaks are not

processed by the resolution correction, and moreover the dispersion curves presented in the figure is not analyzed by any specified model yet, although the fitting the data to BVK force constant model were initiated.

The dispersion curves at 297 show several anomalous features. The Λ_2 mode propagated along [111] direction is unusual such that the zone boundary frequency of R_{25} is substantially low. Simultaneously that of the acoustic mode is also suppressed. Although we do not study the temperature dependence, we anticipate further softening of these zone boundary modes. Because these modes of R_5 or M_5 would be responsible to the tetragonal distortion of this compound at low temperatues. We are planning to search very near future.

References

1) Y. Endoh: J.M.M.M. 10(1979)177.

2) M. Kohgi and Y. Ishikawa: J. Phys. Soc. Jpn. 49(1980)985.

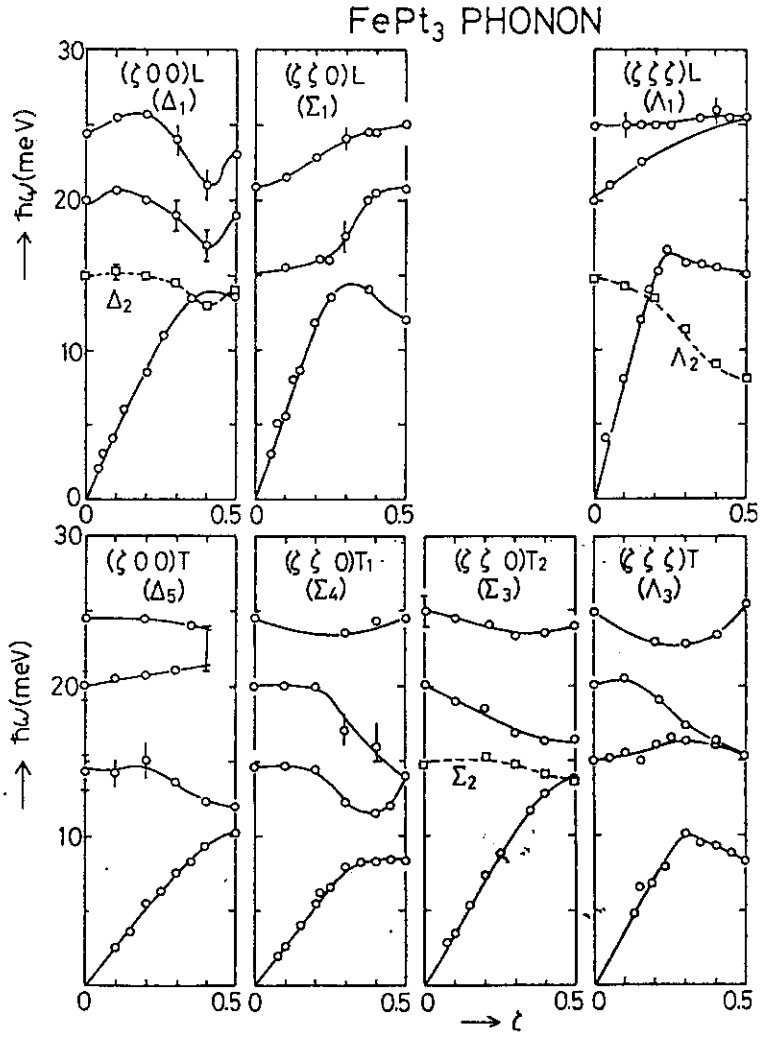

Phonon dispersion curves of $FePt_3$ along the [100], [110] and [111] symmetry directions at 297K. The curves are only guide to eye.

II7 Order-Disorder Transformation of $V_{1-x}Cr_xD_{0.5}$ and $V_{1-x}Ta_xD_{0.5}$

T. Kajitani, T. Konno*, H. Kaneko and M. Hirabayashi

The Research Institute for Iron, Steel and Other Metals, Tohoku University.

The phase transitions of $VD_{0.5}$ and $VH_{0.5}$ have attracted considerable interest[1,2,3]. In the present work, neutron diffraction studies have been carried out to investigate the effects of addition of Cr or Ta on the β-α phase transformation of $VD_{0.5}$.

The location sites of hydrogen and deuterium in the host lattice of vanadium change in the phase transitions of β-α of $VD_{0.5}$ and β_1-β_2-α of $VH_{0.5}$. In the disordered α and α' phases, deuterium and hydrogen atoms are located randomly at tetrahedral sites in the bcc host lattice. On the other hand, the interstitials in the ordered phases of β-$VD_{0.5}$, β_1- and β_2-$VH_{0.5}$ sit regularly at selected octahedral sites. In β_2-$VH_{0.5}$, hydrogens occupy O_z sites which have the neighboring vanadium atoms along the [001] direction. Deuteriums in β-$VD_{0.5}$ and hydrogens in β_1-$VH_{0.5}$ occupy alternative (101) planes of the O_z sites; the occupied O_z sites are named O_{z1} sites, and the others are O_{z2} sites.

Binary alloys of V-Cr and V-Ta were prepared from 99.8 wt% V, 99.99 wt% Cr and 99.9 wt% Ta by using an arc-furnace in a purified argon atmospere. Deuterium was introduced into the powdered alloys using a Sieverts' type apparatus. Powder neutron diffraction works from 78 K to 500 K were accomplished by the TOG diffractometer at the JRR-3 reactor. The neutron wavelength was chosen to be about 1.0 Å.

Integrated neutron intensities of 001, 110, 002 and 111 reflections of $V_{1-x}Cr_xD_{0.5}$ and $V_{1-x}Ta_xD_y$ were measured with changing temperatures. The observed intensities were analyzed assuming the occupation probability of deuterium in O_{z1}, O_{z2} and T_4 sites, where T_4 sites are special T-sites surrounding the O_{z1} and O_{z2} sites. Fig. 1 shows the transition temperatures of $V_{1-x}Cr_xD_{0.5}$ and $V_{1-x}Ta_xD_{0.5}$. The two-step (β_1-β_2-α) phase

---

* Present address; Electrical Steel Research Center, Process Technology R. & D. Laboratories, Nippon Steel Corporation.

transformation occurs in $V_{1-x}Cr_xD_{0.5}$ like in $VH_{0.5}$. In $V_{1-x}Ta_xD_{0.5}$, the order-disorder (β-α) transformation temperature of $VD_{0.5}$ is lowered appreciably with addition of Ta, and at the same time the β phase region shifts to the lower deuterium concentration side, as shown in Fig. 2. Reduction of the transformation temperature is induced by the homogeneous lattice expansion due to the addition of Ta. The shift of the β phase region may be ascribed to the fact that deuterium atoms can not sit at specific O_{z1} sites where a tantalum atom is nearby.

Fig. 3 shows the occupation probabilities of deuterium in O_{z1}, O_{z2} and T_4 sites at room temperature as a function of Cr or Ta concentration. Introduction of Cr leads to the atabilization of the β_2 phase which is isomorphic with the β_2-$VH_{0.5}$, and to the lowering of β_1-β_2 transformation temperature. It is noticed that the deuterium occupation at O_{z1}, O_{z2} and T_4 sites alters similarly in both β_1-$V_{1-x}Cr_xD_{0.5}$ and β-$V_{1-x}Ta_xD_y$.

References

(1) H. Asano and M. Hirabayashi: Z. Phys. Chem. (Neue Folge) 114 (1979) 1.

(2) H. Sugimoto and Y. Fukai: Phys. Rev. B22 (1980) 670.

(3) M. Hirabayashi and H. Asano: Metal Hydrides, NATO Advanced Studies, Plenum Press (1981), 53.

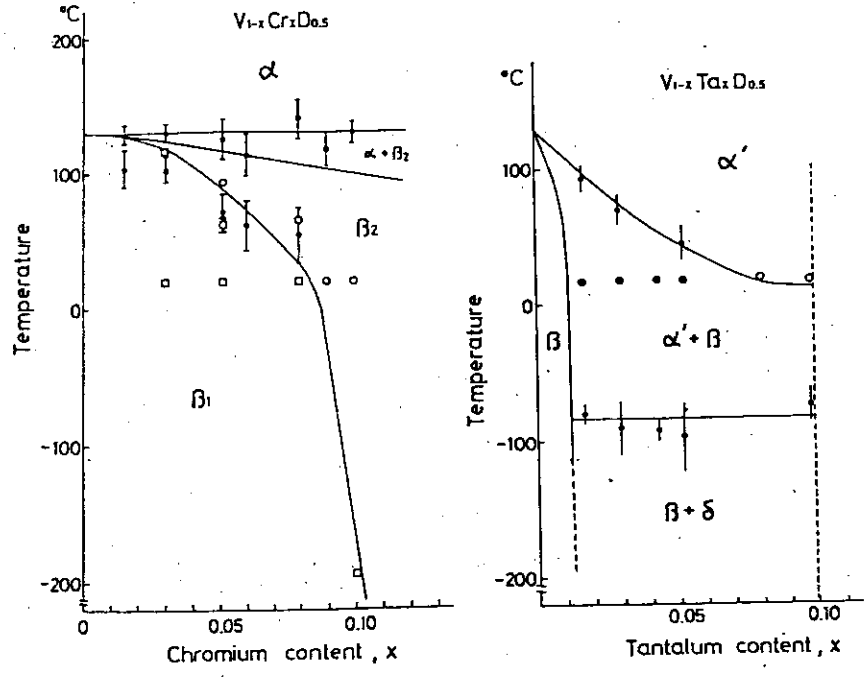

Fig. 1 Transformation temperature of $V_{1-x}Cr_xD_{0.5}$ and $V_{1-x}Ta_xD_{0.5}$ determined by X-ray and neutron diffraction and thermal analyses.

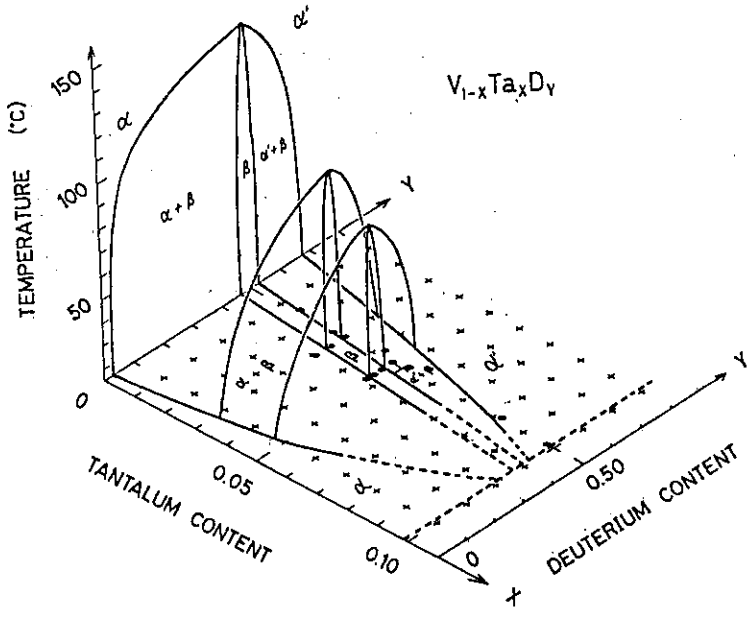

Fig. 2 Bird's eye view of phase diagrams of $V_{1-x}Ta_xD_y$ ($x = 0. \sim 0.10$, $y = 0. \sim 0.9$). Note that the β phase shifts toward lower D-content side in higher Ta-content region.

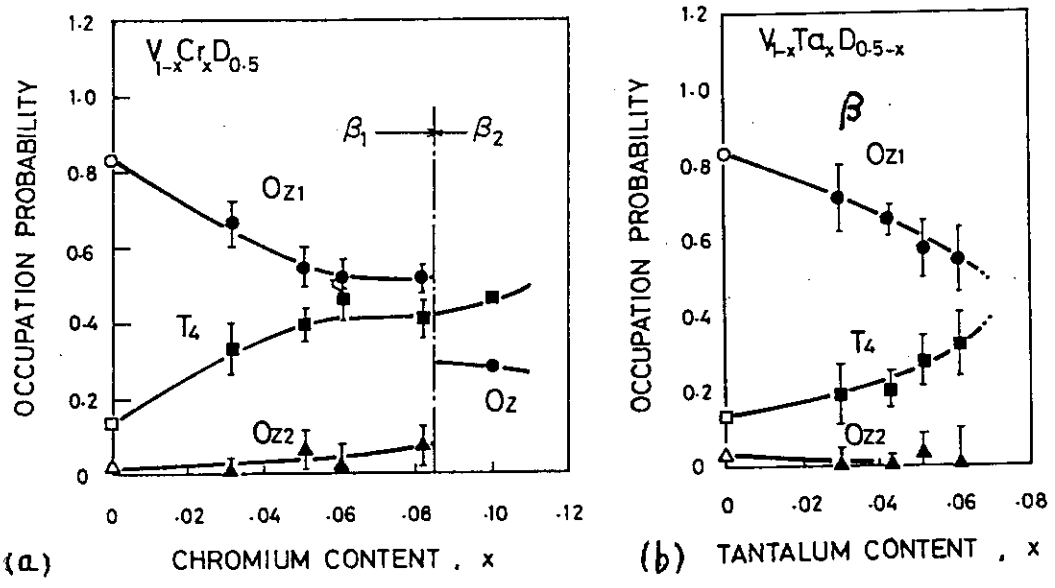

Fig. 3 Occupation probability of deuterium at O_{z1}, O_{z2} and T_4 sites in $V_{1-x}Cr_xD$ (a) and $V_{1-x}Ta_xD_y$ (b) at room temperature.

IIIl Diffuse Scattering in Mn-rich γ-MnCu Alloy Single Crystal

Yorihiko Tsunoda and Yutaka Nakai

Department of Physics, Faculty of Science, Osaka University

In the last two decades, metastable γ-Mn alloy has been intensively studied from the interests in both magnetism and metallurgy. One of the most complicated problems has been an interpretation of the strong diffuse peak observed around ((100)) Bragg angle in neutron powder diffraction patterns of various kinds of γ-Mn alloys. In the present paper, we report that the diffuse peak previously observed with powder samples contains several different origines and these contributions to diffuse scattering can be separately studied by the use of single crystal specimen of γ-MnCu alloy.

Measurements were performed by using TOG double axis diffractometer installed at JRR-3 and inelastic data were taken on TUNS triple axis spectrometer at JRR-2, JAERI, Tokai.

1) (001) elastic magnetic scattering

The existence of elastic peak at (001) point was confirmed by the triple axis spectrometer with the analyzer setting of ΔE=0 meV. As pointed out in the previous paper,[1] the (001) elastic peak comes from magnetic origin. The existence of (001) elastic magnetic peak indicates that the spin vectors of ferromagnetic sheets in AF-1 structure are inclined from [001] cube axis just as the case of γ-Fe precipitated in copper.

2) Magnon scattering

The purpose of the present magnon measurements is to throw light on the relation between the diffuse peak around (001) and magnon scattering. Inelastic scattering measurements were performed with constant-E mode of operation by using the incident neutron wave length of λ =1.43 A. Fig. 1 shows the magnon peaks observed for q [001] direction. From the line shape fitting to observed data, we can obtained the extraordinary large magnon line width Γ. This characteristic behavior agrees with the previous magnon data for γ-MnNi alloys studied by Haywood et al.[2] and Hennion et al.[2] and seems to be common feature of γ-Mn alloy. Fig. 2 indicates the intensity map around (100) reciprocal lattice point observed by the conventional double axis diffractometer. Sharp peak at (001) position is again elastic magnetic scattering due to the inclined spin axis. While a bowshape diffuse peak is ascribed to magnon scattering. The

curvature of the bow roughly coincides with the direction of scattered neutron wave vector which passes through around (001) reciprocal lattice point. Since the magnon dispersion curve has extremely large line width, wide region of the energy-momentum space is covered by magnon contribution. When the diffraction measurements have been made without energy analysis, the condition of energy and momentum conservation law on magnon scattering is fulfilled in the wide range of reciprocal lattice space and diffuse like peak comes out around (001) point where the thermal population of magnon is the largest.

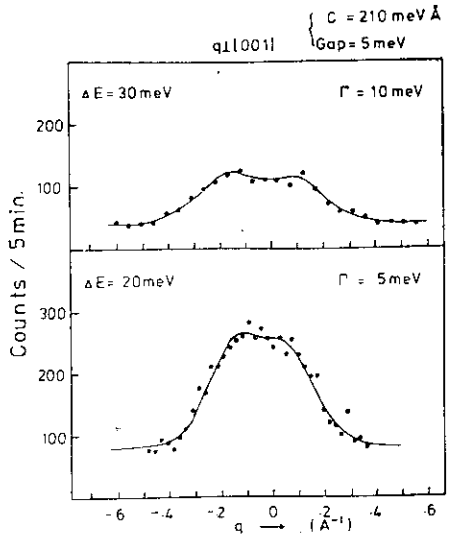

Fig. 1 Magnon peaks for q [001] direction. Solid lines are the calculated fitting curves.

We can conclude that there are mainly three contributions as origins of strong ((100)) diffuse scattering observed by powder sample. 1) Atomic short range order peak around (1 1/2 0) reciprocal lattice point. 2) Elastic magnetic scattering at (001) coming from the inclined spin axis. 3) Magnon contribution around (001) reciprocal lattice point. However, we cannot absolutely say which is the most important factor as the origin of diffuse scattering. It depends on the thermal history and the magnetic domain distribution of the sample, Cu concentrations, experimental conditions including the temperature and so on.

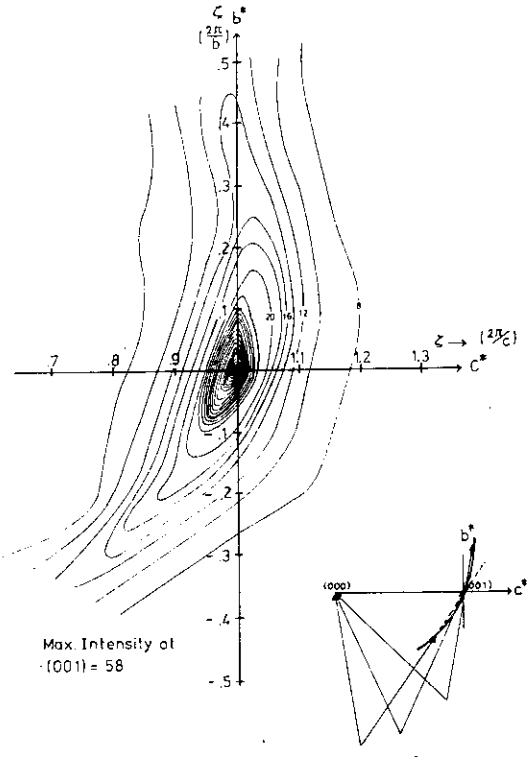

Fig. 2 Observed intensity map around (001) reciprocal lattice point by double axis diffractometer.

1) Y. Tsunoda and Y. Nakai; Solid State Commun. 34 413 (1980)
2) B.C.G. Haywood, R.D. Lowde, M.W. Stringfellow and W.B. Waeber; J. Phys. (France) C1 1186 (1971).
B.Hennion et al.; Conf. on Neutron Scatt. Gattlinburg (1976) 825.

III2 Inclined Spin Axis of Mn-rich γ-MnCu Alloy

Yorihiko Tsunoda and Yutaka Nakai

Department of Physics, Faculty of Science, Osaka University

The magnetic structure of Mn-rich γ-MnCu alloy proposed by Meneghetti and Sidhu[1] and confirmed by Bacon et al[2] is the first kind of antiferromagnetic structure (AF-1) in which the magnetic moments are aligned parallel to c-axis and form the (001) ferromagnetic sheets with alternately antiparallel configuration along c-axis. In this spin structure, there is no (001) magnetic reflection. In the present report on the neutron scattering measurements of Mn-rich γ-MnCu alloy single crystal, we show the existence of (001) elastic magnetic peak suggesting that the γ-MnCu alloy has also the inclined spin axis as well as the f.c.c. γ-Fe and γ-Fe alloys.

After growing the single crystal by the Bridgman method, sample was homogenized at 900 ℃ for 25 hours, then quenched rapidly into ice-water. The Néel temperature and the tetragonality c/a at room temperature were 320 K and 0.98, respectively.

Most of the measurements were performed by using TOG double axis diffractometer installed at JRR-3 and some inelastic data were taken on TUNS triple axis spectrometer at JRR-2, JAERI, Tokai. Since incident neutrons with rather short wavelength of 0.936 Å were used with the Er filter, λ/2 component was suppressed less than statistical errors of the background for double axis measurements.

Fig. 1 indicates an example of observed peaks by scanning along the scattering vector (θ-2θ scanning) in the neighborhood of (200) and (100) reciprocal lattice points. Double peaks around (200) were caused by the distribution of the domains with the f.c.t. structure appeared below T_N. While a single peak was observed exactly at (001) reciprocal lattice point,

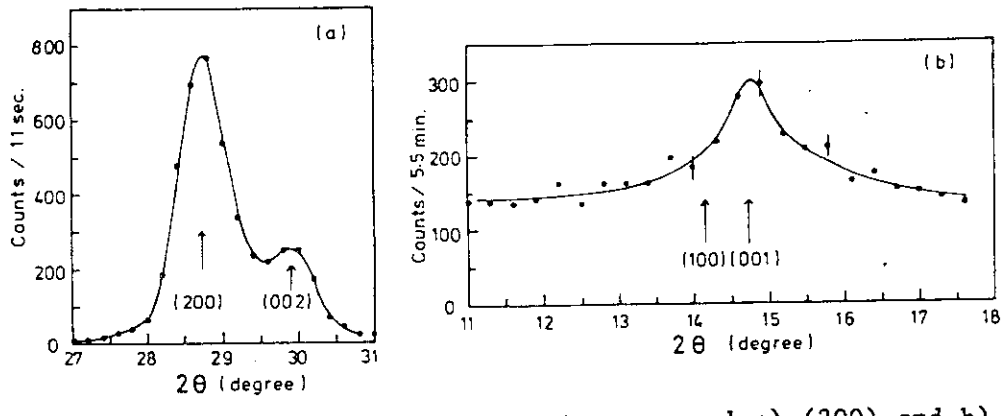

Fig. 1. Observed peaks at room temperature around a) (200) and b) (100).

but no peak at (100) position, though the (001) peak seems to have slightly broad line width.

There are several grounds to rely upon to conclude that the (001) peak observed here comes from magnetic origin. 1) There exists an intensity anomaly at T_N which was determined by the temperature dependence of (110) magnetic peak intensity and rapid decreasing of the scattering intensity above T_N. 2) The temperature dependence of the scattering intensity can be reproduced immediately even for the abrupt temperature variation. 3) No peaks were observed at (001) reciprocal lattice point by X-ray diffraction.

Energy analysis of the (001) peak was performed by using the incident neutron wavelength of 2.448 Å with graphite filter. The observed energy spectrum at (001) position is shown in Fig. 2. Although the peak at E = 0 meV contains remaining $\lambda/2$ component of 230 count due to incomplete filtering and incoherent scattering of 40 counts, the line width does not show any broadening beyond the instrumental resolution. We can conclude that the (001) magnetic peak observed here is due to elastic scattering. The existence of (001) elastic magnetic peak indicates that the spin vectors of ferromagnetic sheets in AF-1 structure are inclined from [001] cube axis just as the case of γ-Fe and other γ-Fe alloys. From the peak intencity, average canting angle is estimated as 5.3° (±0.2°) at 78 K. A broad peak around 5 meV seen in the inset of Fig. 2 can be identified with the spin wave energy gap at q = 0.

The contribution of (001) magnetic peak to the whole diffuse scattering around (100) Bragg angle observed in the most of γ-Mn alloy powder samples may be rather small but cannot be ignored to the cusp like and the temperature dependent parts of diffuse scattering.

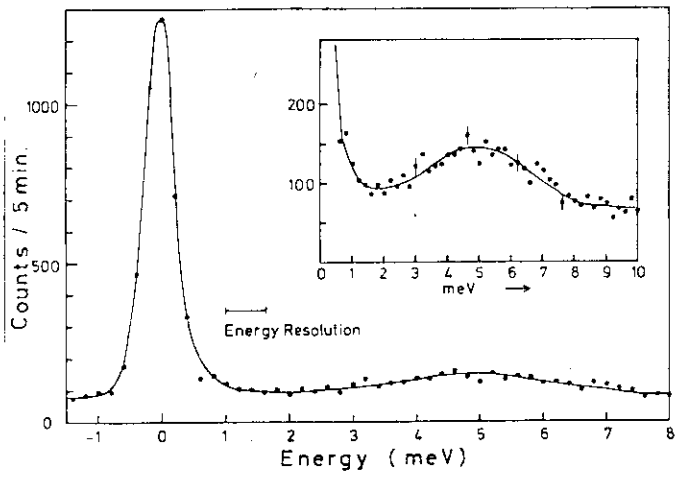

Fig. 2 Energy spectrum of scattered neutrons at (001) peak position

1) Meneghetti D. and Sidhu S. S. Phys. Rev. 105 130 (1957).
2) Bacon G. E., Dunmur I. W., Smith H. J. and Street R. Proc. R. Soc. A241 223 (1957).

III3 Magnetic Moment of Mn Atoms in Fe-Ni Alloys

S. Iida*, Y. Nakai and N. Kunitomi

Department of Physics, Faculty of Science, Osaka University.

The environmental effects of the magnetic moments of Mn atoms in various alloys were examined by many workers. The theoretical calculation by Jo[1] based on the CPA including the nearest neighbor environmental effect showed that the magnetic moment of an isolated Mn atom in a Fe-Ni alloy aligns parallel or antiparallel to the bulk magnetization, depending on the number of the nearest neighbor Fe atoms, n_{Fe}, and the composition of the Fe-Ni alloy.

We examined it for the specimens having 3 or 6 at. Mn in the Fe-Ni alloys by means of diffuse scattering of polarized neutrons. Because the nuclear scattering amplitude of Fe, b(Fe), is nearly equal to the one of Ni, b(Ni), the difference between the cross sections for neutrons with up spin and the ones with down spin are given as,

$$\Delta\frac{d\sigma}{d\Omega} = 4\left(\frac{\gamma e^2}{2mc^2}\right) y\cdot(1-y)(\bar{b}-b(Mn))(\bar{M}-M(Mn))f(K)(1+S(K))$$

$$+ \text{ small correction term due to the difference between } b(Fe) \text{ and } b(Ni), \qquad (1)$$

where y is the concentration of the Mn atoms and f(K) is the averaged form factor. The averaged values, $\bar{b}$ and $\bar{M}$ are the ones for the host Fe-Ni alloys without Mn impurities. The disturbance effect due to Mn atoms is expressed in S(K).

The measurements were performed at room temperature by the use of POLTO polarized neutron diffractometer installed in JRR-3. The experimental values of the M(Mn) as a function of the concentration of Fe, x, were estimated from the 1st term of eq. (1) and were compared with the theoretical ones and the experimental ones from NMR[2], as seen in Fig. 1. The experimental result for the Ni-Mn alloy by Cable and Child[3] is also displayed in Fig. 1. As Mn atoms in each specimen have various values of n_{Fe}, the M(Mn) should be compared with the averaged value of the calculated Mn moments as a function of n_{Fe}, assuming the binomial

---

*present address Department of Physics, Kwansei-Gakuin University.

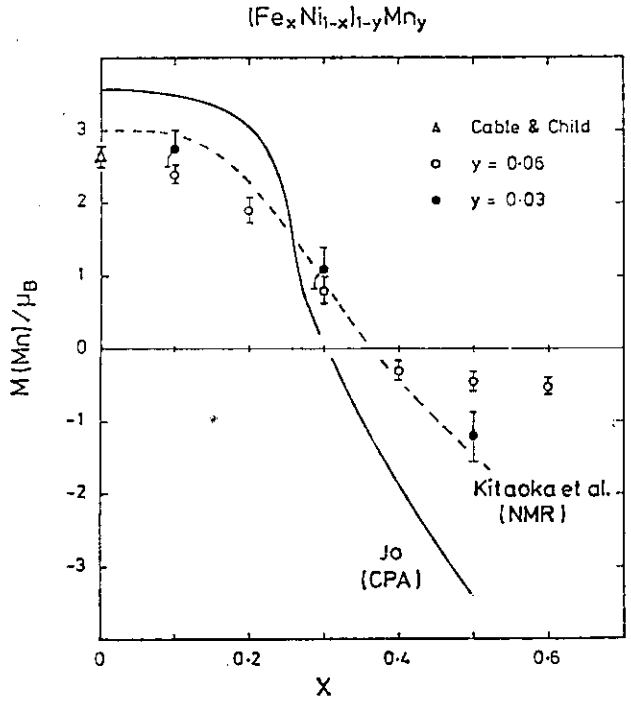

Fig. 1. Averaged Mn moments M(Mn) as a function of the Fe concentration, x.

distribution for n_{Fe}.

From the S(K) term, it can be concluded that the Mn atoms diminish the magnetic moments of the nearest neighbor atoms, but its quantitative explanation remains as the subject of the future investigation.

1)T.Jo: Physica 86-88B(1977) 747.
2)Y.Kitaoka, K.Ueno and K.Asayama: J. Phys. Soc. Jpn 44(1978) 142.
3)J.W.Cable and H.R.Child: Phys. Rev. 10(1974) 4607.

III4 Emperical Relation between Amplitude and Period of Spin Density Wave for Cr(V) and Cr(Mn) Alloys

Yutaka Nakai and Satoshi Iida*

Department of Physics, Faculty of Science, Osaka University.

It is well known that the ground state of metallic chromium is a spin density wave (SDW) state in which the magnetic moments on Cr atoms are modulated sinusoidally in space and the period is incommensurate with the period of the lattice. Recent experiments have revealed the existence of the harmonics component with the wave vector of 3Q in the SDW modulation, superposed on the primary wave with the wave vector of Q.[1] Moreover, the modulation of the lattice spacing with 2Q has been found.[2] These phenomena take place in the SDW state of the Cr alloys with the small amounts of V or Mn atoms.[3,4] For these alloys, Cr(V), Cr(Mn) and Cr(V,Mn), together with pure Cr, the most part of the experimental results for the magnetism could be explained by the two band nesting model on a rigid band approximation.[5,6]

Neutron diffraction experiments were performed for single or polycrystal specimens of the Cr(V) and Cr(Mn) alloys with 0.18 to 2.3 at.%V or 0.25 at.%Mn at TOG diffractometer installed in JRR-3. The magnetic moments M_1 and the wave vectors in the unit of $2\pi/a_0$, δ, at zero temperature were obtained by the smooth-extrapolation of the results at various temperatures.

The square amplitudes M_1^2 are plotted against the squares of the wave vectors δ^2, as seen in Fig. 1, including the data obtained by previous authors.[7-10]

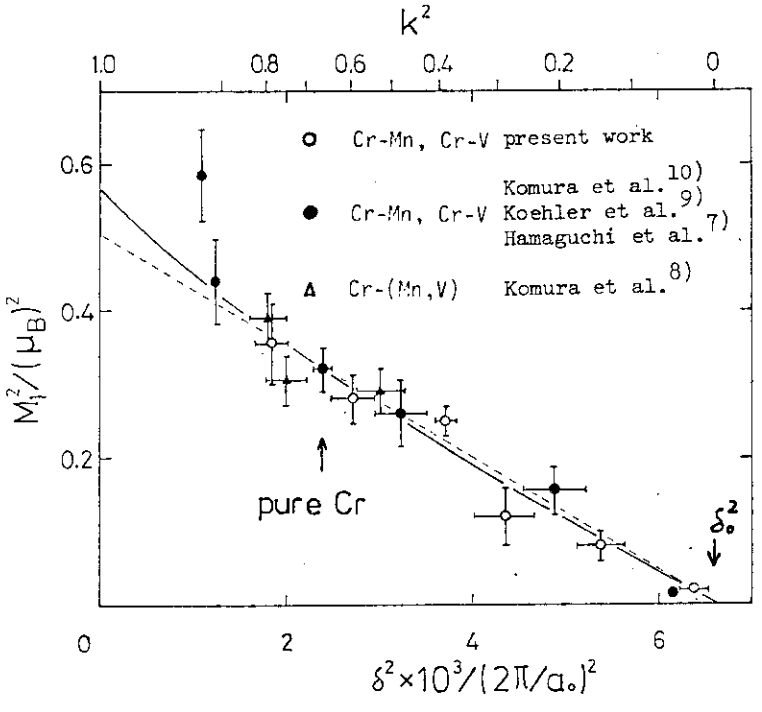

Fig. 1. M^2 against δ^2 at zero temperature

*Present address: Department of Physics, Kwansei-Gakuin University.

One salient feature of Fig. 1 is that there is approximately an linear relation of M_1^2 and δ^2, as shown by a broken line. With the variation of the composition M_1^2 and δ^2 vary but the relation is sustained. Only a variable is necessary to describe two quantities, M_1 and δ. It should be also pointed out that there is the maximum value of the wave vector, δ_o, in the stable SDW state of these alloys.

Considering the appearance of the harmonics in the SDW, the spatial variation of the sublattice magnetic moment along x-axis parallel to Q is assumed to be expressed as,

$$M(x) = (\sqrt{2}k/\sqrt{1+k^2})\, M_o\, sn(\delta_o/\sqrt{1+k^2}\, x,k) , \quad (1)$$

where M_o is a parameter corresponding to the maximum amplitude of the alloy system. The Jacobi's elliptic function with small modulus k, sn(x,k), can be approximated by sin x. Equation (1) can be expanded in series of sinusoidal functions. As the first and the second terms of the expansion correspond to the primary and the 3rd harmonic components of the SDW, M_1 and M_3, respectively, M_1, M_3 and δ are given as $(2\sqrt{2}\pi/K\sqrt{1+k^2})M_o\sqrt{q}/(1-q)$, $(2\sqrt{2}\pi/K\sqrt{1+k^2})M_o \cdot q^{3/2}/(1-q^3)$ and $(\pi/2K)\delta_o/\sqrt{1+k^2}$, respectively. Here the conventional notations are used for q and K, which depend on the modulus k only.

The precise relation between M_1^2 and δ^2 can be easily calculated. The results by using best-fitted M_o of 0.594 μ_B, displayed by the solid curve in Fig. 1, is resemble closely to the linear relation. The calculated ratio, M_3/M_1, as a function of δ agrees with the experimental one[4] by considering the existence of the lattice spacing modulation.

1)R.Pynn, W.Press, S.M.Shapiro and S.A.Werner:Phys. Rev. B13(1976) 295.
2)Y.Tsunoda, M.Mori, N.Kunitomi, Y.Teraoka and J.Kanamori:Solid State Commun. 14(1974) 287.
3)S.Iida, M.Kohno, Y.Tsunoda and N.Kunitomi:J.Phys.Soc. Jpn 50(1981) 2581.
4)S.Iida, Y.Tsunoda, Y.Nakai and N.Kunitomi:J.Phys.Soc. Jpn 50(1981) 2587.
5)A.Shibatani, K.Mochizuki and T.Nagamiya:Phys. Rev. 177(1969) 984.
6)A.Kotani:J. Phys. Soc. Jpn 39(1975) 851.
7)Y.Hamaguchi, E.O.Wollan and W.C.Koehler:Phys. Rev. 138(1965) A737.
8)S.Komura, Y.Hamaguchi and N.Kunitomi:J. Phys. Soc. Jpn 23(1967) 171.
9)W.C.Koehler, R.M.Moon, A.L.Trego and A.R.Mackintosh:Phys. Rev. 151(1966) 405.
10)S.Komura and N.Kunitomi:J. Phys. Soc. Jpn 20(1965) 103.

III5 Neutron Diffraction Study on the $Mo_{0.8}Al_{0.2}$ Alloy

Yoshiyuki Nakata and Shuzo Kawarazaki

Department of Physics, Osaka University

In a CrAl alloy, the Neel temperature remarkably increases with the increasing concentration of Al; it reaches 900 K for Al concentration of 20 at.%. The recent theory[1] explains this phenomenon as due to the enhancement of the antiferromagnetic susceptibility caused by the decreasing of Cr-Cr nearest neighbor coupling with addition of Al. On the other hand, Mo is an isoelectolonic element of Cr, and has approximately the same band structure as that of Cr. Therefore, if the same mechanism of the susceptibility enhancement works in MoAl alloys, it is expected that an antiferromagnetic phase appears in a MoAl alloy.

Recently we studied the electronic specific heat of $(Cr_{1-x}Mo_x)_{1-y}Al_y$ alloys.[2] The density of states at the Fermi level, $N(E_F)$, of the MoAl alloy initially decreases with the addition of Al. This fact is contrary to the tendency of $N(E_F)$ in virtual paramagnetic CrAl alloys determined by extrapolating $N(E_F)$ of paramagnetic (CrMo)Al alloys to CrAl. This result of the specific heat experiment also suggests the existence of the magnetic ordering in MoAl alloys at low temperature.

We carried out the elastic neutron diffraction measurement on the powdered $Mo_{0.8}Al_{0.2}$ alloy. The sample was prepared by the repeating argon arc melting. The diffraction measurement was done using the TOG Diffractometer at JRR-3. The neutron wave length was chosen as 0.919Å and an Er-filter was used for eliminating $\lambda/2$ scattering. The neutron scattering intensity along [q00] axis between $0.89 \leq q \leq 1.11$ was carefully measured at the liq. He temperature. However, no magnetic paek was found around (100) position beyond the experimental error of $0.14 \mu_B$.

References

1) Y.Teraoka and J.Kanamori; Inst. Phys. Conf. Ser. No.39 (1978) 588

2) to be published

III6 Neutron Diffraction Study on f.c.c. Fe precipitated in Cu

Toshiro Cey, Shigeki Meguro, Shuzo Kawarazaki, Nobuhiko Kunitomi

Department of Physics, Osaka University, Toyonaka, Osaka 560

It is well known that γ-Fe precipitates coherently in a Cu matrix by the proper annealing and the precipitates of γ-Fe show the antiferromagnetism in low temperature. Neutron diffraction measurement by Abrahams et al (1962)[1] shows that the Néel temperature of γ-Fe precipitated in copper is about 8 K and its spin structure is γ-Mn type with an average moment of 0.7 μ_B. On the other hand the Néel temperature determined by Mössbauer effect measurements[2] is about 70 K as well as N.D. measurements by Johanson et al(1970)[3].

Neutron diffraction measurements on Cu(Fe) single crystals in a temperature range from 4.2 K to 90 K was made by TOG-diffractometer in order to measure the Néel temperature of γ-Fe accurately.

Single crystal specimens grown by Bridgman method by using raw materials of 3N Fe and 5N Cu. In order to form γ-Fe the single crystals, $Cu_{.974}Fe_{.026}$, $Cu_{.982}Fe_{.018}$, were annealed at 650 °C for 1000 minutes and quenched into water, according to the experimental results by Takahashi et al.[4]

Fig.1 and Fig.2 show the temperature dependence of the magnetic (110) peak intensity of $Cu_{.974}Fe_{.026}$ and $Cu_{.982}Fe_{.018}$, respectively. As is seen in these figures the Néel temperature of $Cu_{.974}Fe_{.026}$ is about 63 K and that of $Cu_{.982}Fe_{.018}$ is about 70 K. The intensity of the (110) reflection was measured between 90 K and 4.2 K. The magnetic peak intensity was obtained by subtracting (λ/2)-(220) intensity which was determined by the high temperature measurement. The temperature dependence of the magnetic (210) peak intensity of $Cu_{.974}Fe_{.026}$ was also observed and the observed Néel temperature coincides with that observed by (110). The magnetic (100) peak intensity for both samples was not observed within the statistical error. The spin structure concluded from the present experiment is a γ-Mn type. In contrast to the Abrahams' model where the spin axis inclines from [100] with an angle of 19°, the spin axis does not incline in the present case beyond ± 5° which is the limit of the experimental accuracy.

The accurate determination of the magnetic moment is now in progress.

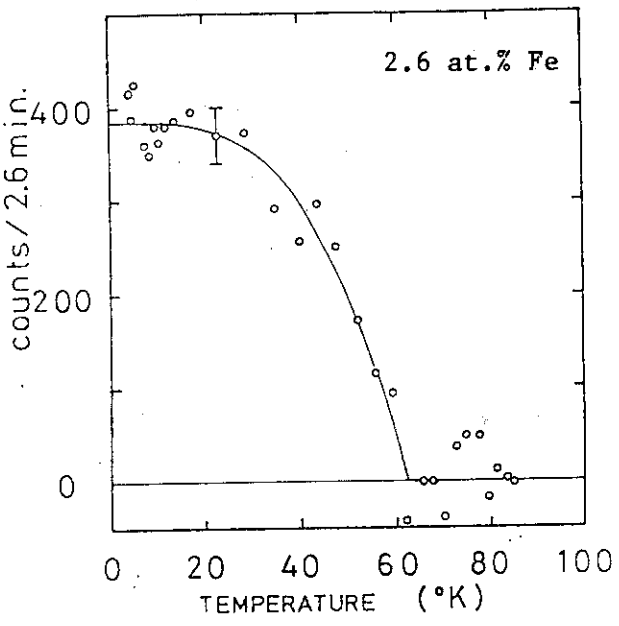

Fig. 1.
The temperature dependence of the magnetic (110) peak intensity of $Cu_{.974}Fe_{.026}$.

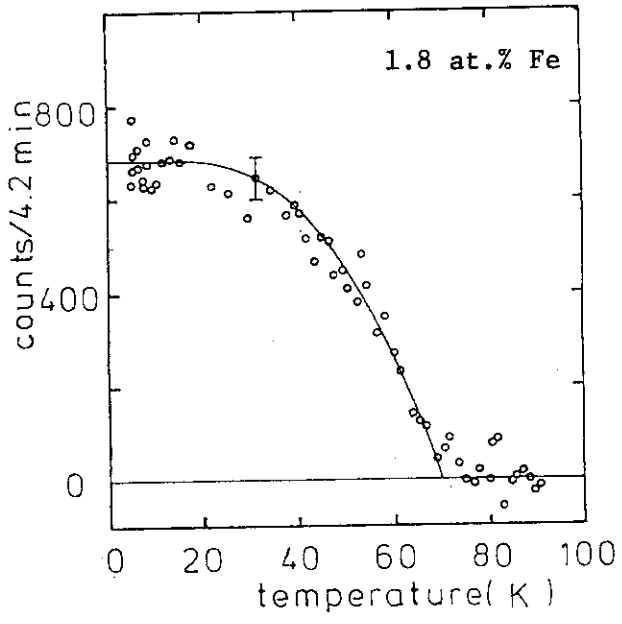

Fig. 2.
The temperature dependence of the magnetic (110) peak intensity of $Cu_{.982}Fe_{.018}$.

References

1) S. C. Abrahams, L. Guttman and J. S. Kasper ; Phys. Rev. 127 (1962) 2052
2) U. Gonser, C. J. Meecham, A. H. Muir and H. Wiedersich ; J. Appl. Phys. 34(1963) 2373
3) G. J. Johanson, M. B. Mcgirr and D. A. Wheeler ; Phys. Rev. B1(1970) 3208
4) private communication

III7 Polarized Neutron Diffraction Study of Weak Ferromagnetic Mn_3Sn

Shoichi Tomiyoshi and Yasuo Yamaguchi

The Research Institute for Iron, Steel and Other Metals, Tohoku University
Sendai 980

Mn_3Sn (hex. DO_{19} type) is an antiferromagnet (T_N=420 K) with a ferromagnetic remanence. In order to clarify the origin of the weak ferromagnetism we studied the spin structure and its dependence on the magnetic field direction by using polarized neutron diffraction.

The flipping ratio was measured for the h0ℓ reflections with a magnetic field H of 8 kOe applied parallel to [010] and for the hhℓ reflections with H∥[$\bar{1}$10]. The magnetic structure factor was obtained from the flipping ratio by assuming the absence of the spin-flip scattering. This assumption is assured from the facts that the flipping ratio of the 100 and 110 reflections have very large values and the observed magnetic form factor derived using above assumption agrees well with the calculated Mn^{2+} magnetic form factors. The magnetic structure was determined to be a triangular spin configuration and the magnetic moment to be 1.78 μ_B/Mn at room temperature. For a triangular spin configuration there must be a component of the magnetic moments perpendicular to the neutron spin polarization direction which contributes to the Bragg reflection as a spin-flip scattering, however, in the present case the spin-flip scattering was not observed, so that the orientation of the spin triangle was determined to be as to cancel the perpendicular components with each other due to the phase factors. The orientation of the spin triangle was found to vary for H∥[010] and H∥[$\bar{1}$10], but the spin plane was not determined from these measurements.

Next, the magnetic field direction dependence of the flipping ratio was measured for several reflections by rotating the crystal about the scattering vector under a magnetic field of 8 kOe applied perpendicular to the scattering vector. Fig. 1 shows the flipping ratio R of the 101 reflection measured as a function of the field direction. From the analysis of the flipping ratio data it was shown that the spin plane of the triangle coincides with the c-plane and the spin triangle rotates opposite to the rotation of the c-plane component of the magnetic field as shown in Fig. 2. If we assume that the easy magnetization axes are along [010] for Mn-A, [$\bar{1}\bar{1}$0] for Mn-B, and [100] for Mn-C, i.e., nearest neighbour Sn atom

direction, then a spin triangle which has the magnetic moment directions along its own easy axes will be stable against the spin triangle shown in Fig. 2, in which the magnetic moment directions do not accord with its own easy axes simultaneously. On the other hand, in this crystal structure we must consider the contribution of the Dzyaloshinski-Moriya interaction $E_{DM} = \vec{d}\cdot(\vec{S}_A\times\vec{S}_B+\vec{S}_B\times\vec{S}_C+\vec{S}_C\times\vec{S}_A)$. Here, $\vec{d}$-vector is along the c-axis. This term favors the spin triangle shown in Fig. 2 against another triangle mentioned above and compensates an increase of the crystalline field anisotropy energy, so stabilizes former. In the model shown in Fig. 2 the magnetic moments deviated from the easy axes are pulled slightly toward its own easy axes, so the equilateral triangle deforms and the weak ferromagnetic moment appears opposite to the rotation of the triangle in consistent with the experimental results. Full paper will be appeared in J. Phys. Soc. Jpn.

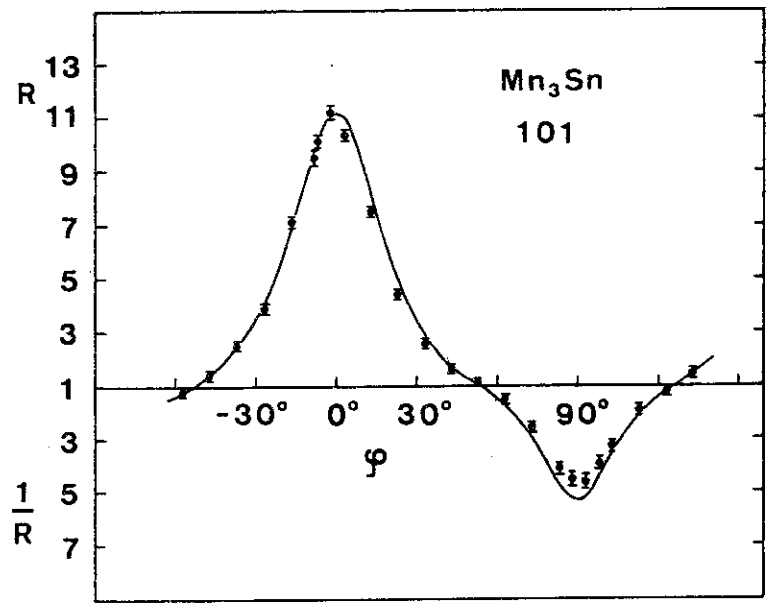

Fig. 1. Flipping ratio of 101 reflection as a function of the magnetic field direction. The flipping ratio is plotted by R for R≥1 and 1/R for R≤1. φ=0° corresponds to H∥[010]. Smooth curve is calculated for the model shown in Fig. 2.

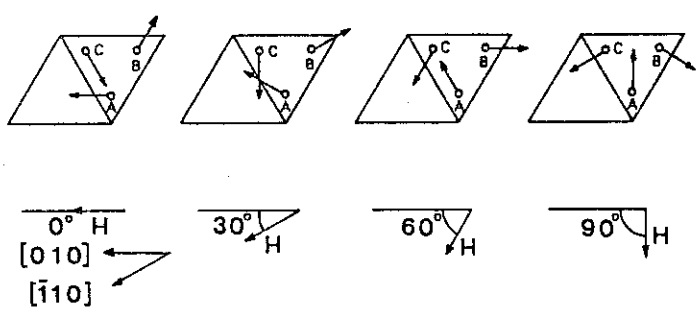

Fig. 2. Triangular spin configuration compatible with the experimental results. The spin triangle rotates depending on the c-plane component of the magnetic field. The magnetic moments in a half of the unit cell are labelled as A,B,C.

III8 Pressure effect on SDW in Cr 0.5 at % Ge

Jun'ichiro Mizuki* and Yasuo Endoh

Department of Physics, Tohoku University, *Nuclear Reactor Division, McMaster University, Hamilton, Ontario, L8S 4K1,Canada

Recently much interest has been directed to the perturbation of the spin density wave (SDW) by the non transition metal impurities. In particular much experimental efforts have been devoted to the SDW of Cr alloys containing elements of 4th group in the periodic table such as Si, Ge and Sn. Although many interesting aspects have been exposed which in some cases are quite similar impurity effects on SDW to that of alloying with 3d transition metal impurities.

Cr Ge is a typical example where the magnetic behaviors are interpreted well as if Ge atoms donate electrons to the Cr band like a Mn impurity[1,2]. As already discussed extensively the effect of Si impurities on the SDW is quite similar to those of Fe in many respects[3]. Since applying pressure is a very nice perturbation which is equivalent to the decrease of effective numbers in electrons to atom ratio without the subtle alloying effects, the pressure dependence of the magnetic phase diagram was studied in Cr Ge. Our primary concern was whether the complicated phase diagram found in Cr 1.4 at % Si would be visible in this case of Cr 0.5 at % Ge. At ambient pressure the phase diagrams of Cr Ge and Cr Si resemble each other.

A single crystal of Cr 0.5 at % Ge was loaned by Prof. Kunitomi and measurements were carried out on TUNS spectrometer installed at JRR2. The high pressure neutron diffraction technique was essentially identical to that described in the previous papers.[4]

The magnetic phase diagram is shown in Fig. 1 where both pressure-temperature and concentration-temperature diagrams are presented. The transition temperature from paramagnetic to CSDW states decreases while that from CSDW to ISDW increases with the increase of pressure such that the CSDW phase disappears above about 3 kbar. This behavior is quite similar to that found in Cr 0.5 at % Mn although the CSDW still exists at 6 kbar. The relationship between diagrams with respect to pressure and

with regard to concentration can be understood on the standpoint of the simple postulate that the increase in pressure gives rise to the decrease in electrons to atom ratio.

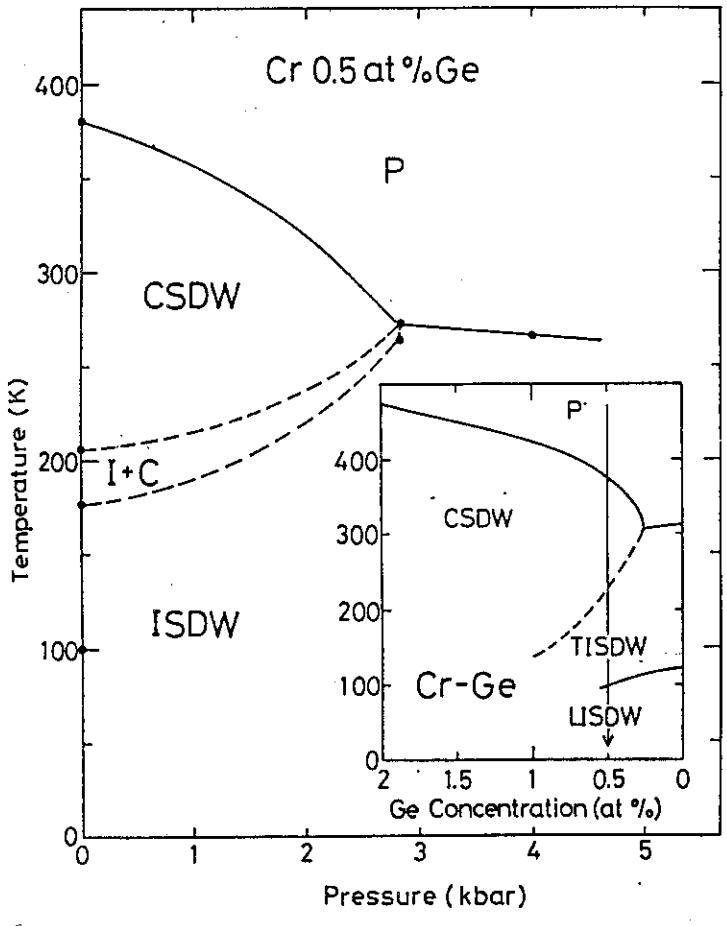

Fig. 1. Magnetic phase diagram of Cr 0.5 at % Ge with respect to pressure. Insert is illustrated in concentration coordinate for the sake of comparison.

This empirical correspondence interpretes immediately the following result of the shift of the SDW wave vector Q with respect to pressure. The pressure dependence of Q in the ISDW phase is illustrated in Fig. 2 together with the results of Cr 0.5 at % Mn. At ambient pressure at 206 K, Q changes abruptly from 1 in units of $2\pi/a$ to a smaller value with the first order, and further decreases upon reducing temperature. When pressure increases Q shifts towards smaller values. Though the direct comparison is not easy, the rate of Q shift with pressure change apparently is very close in all the case of pure Cr, Cr-0.5 at % Ge and Cr-0.5 at % Mn.

These behaviors make a considerable contrast against either the results of Cr 1.4 at % Si or those of Cr 1.4 at % Al. Both results are shown in Fig. 3 and Fig. 4.

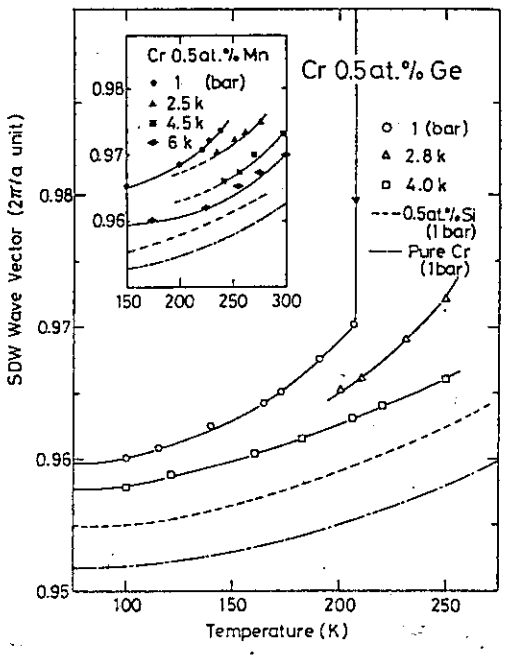

Fig. 2. SDW wave vector Q shift in Cr 0.5 at % Ge with respect to temperature at various pressure. Cr 0.5 at % Mn case is shown in an insert figure.

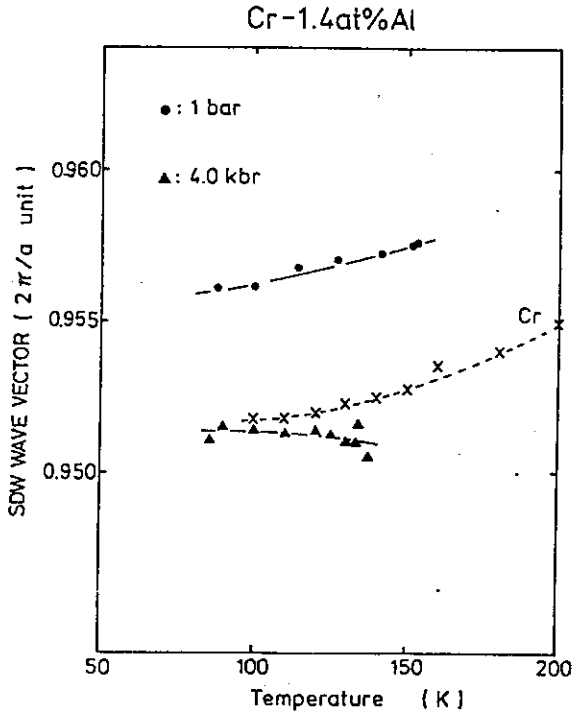

Fig. 3. Temperature dependence of Q in Cr 1.4 at % Al.

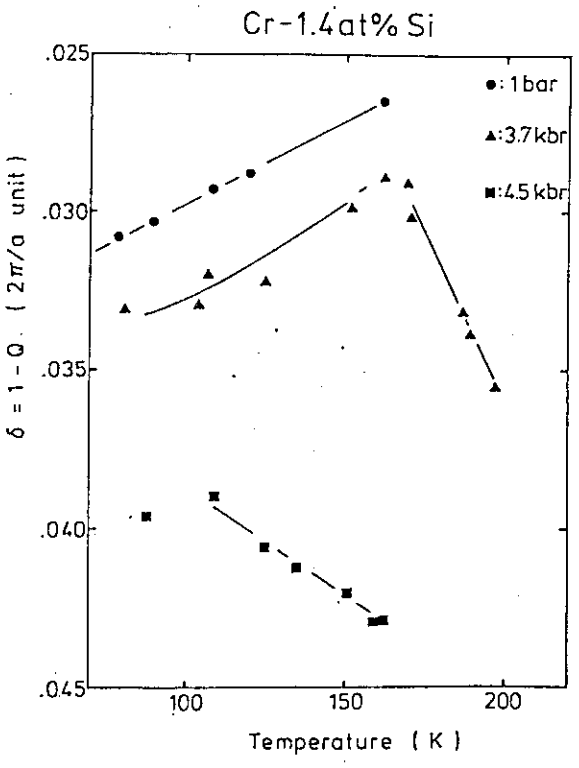

Fig. 4. Temperature dependence of Q in Cr 1.4 at % Si.

In conclusion, we emphasize that the magnetic phase diagram in particular at the pressure coordinate of Cr 0.5 at % Ge is quite different from that of Cr 1.4 at % Si, whereas their magnetic phase diagrams at ambient pressure are similar to each other. Thus the present results not only show the magnetic characteristic of Cr Ge, which has similar feature of Cr Mn, but confirm the unusual feature of Cr Si. This point should be very important to understand the mechanism of the first order transition in Cr Si as well as Cr Fe.

References

1) Iida, S. Kawarazaki and N. Kunitomi: J. Phys. Soc. Jpn. 50 (1981) 3612.
2) J. Mizuki, Y. Endoh and Y. Ihsikawa: submitted to J. Phys. Soc. Jpn.
3) Y. Endoh, J. Mizuki and Y. Ishikawa: submitted to J. Phys. Soc. Jpn.
4) J. Mizuki and Y. Endoh: J. Phys. Soc. Jpn. 50 (1981) 914.

III9 Randomly mixed antiferromagnets with competing anisotropies

John M. Newsam, Yasuo Endoh, Yoshikazu Ishikawa,
Humihiko Takei*, Yasuhiko Syono* and Atsuko Ito**

Department of Physics, Tohoku University, *Institute for Iron Steels and Other Metals, Tohoku University, **Department of Physics, Ochanomizu University

The mixed ilmenite system $Co_{1-x}Fe_xTiO_3$ has been investigated by neutron scattering. The end members of this series, $CoTiO_3$ and $FeTiO_3$, have identical structures but orthogonal easy axes in the antiferromagnetically ordered phase. For crystals containing randomly mixed components with such competing spin anisotropies, simple molecular field (MF) theory predicts that the two second order magnetic phase transition lines in the T-x diagram will approach a tetracritical point tangentially to each other. In other words, the orthogonal spin components are decoupled and by choosing an appropriate composition, x, two discrete transitions should be encountered on cooling. The first transition indicates ordering of the predominant component and the second transition then corresponds to a mixed ordering phase.

Recent renormalisation group theory results, however, indicate that the random field reduces the dimensionality by order 2 and that the transitions are not genuinely second order. Another recent interpretation also suggests the existence of higher order interactions which, although small, smear the transitions such that they are no longer decoupled.

The $Co_{1-x}Fe_xTiO_3$ system provides a useful test case for investigating the magnetic properties of mixed crystals with competing anisotropies. We have made neutron diffraction measurements on powder samples to determine the magnitude and orientation of the local magnetic moments and those data are now being analysed by the Rietveld method. We are also carrying out extensive neutron scattering measurements on single crystal of various compositions. Although data analysis is still at an early stage, we have observed some interesting features. The overall picture is consistent with the results of simple MF theory, but the magnetic ordering in the mixed ordering, lower temperature, phase appears to be imperfect. The peak

profiles of the magnetic Bragg reflections show pronounced temperature dependence and we have also observed substantial diffuse scattering in the vicinity of the magnetic Bragg reflections which varies in intensity with temperature. These features might possibly be understood in terms of the random field hypothesis.

References

A. Ito, K. Someya, H. Ikeda, Y. Shono and H. Takei, Solid State Commun. in press.

III10 Two-Dimensional Character of Spin Correlation in Stoichiometric YFe_2O_4

Satoru FUNAHASHI*, Jun AKIMITSU**, Kiiti SIRATORI***
Noboru KIMIZUKA****, Midori TANAKA*****and Hideshi FUJISHITA******
*Physics Division, Japan Atomic Energy Research Institute, **Faculty of Science and Engineering, Aoyamagakuin University, ***Faculty of Science, Osaka University, ****Institute for Researches in Inorganic Materials, *****Faculty of Science, Ochanomizu University, ******Institute for Solid State Physics, University of Tokyo.

YFe_2O_4, a hexagonal layered crystal, was reported to exhibit two-dimensional long range spin ordering below about 220K, when oxygen is deficient by 0.04 or further in the formula unit. Spins order within a c-plane without correlation along the c-axis. Thus, "Bragg lines" are observed at (1/3,1/3,ℓ),etc.[1] When it is stoichiometric, however, two-step first order transition appears and the spin ordering is considered to be three-dimensional.[2,3] Lattice distortion and discontinuous increase of electrical conductivity are accompanied by the transition. Unfortunately, a large stoichiometric single crystal is not available at present and a detailed study of the low temperature phase is not possible.

In the present study, neutron diffraction was performed on stoichiometric polycrystals to elucidate the fundamental characteristics of the spin correlation. Critical diffuse scattering was measured between 230K and 260K at around (1/3,1/3,0). Calculated 2θ angle of (1/3,1/3,0) assuming room temperature lattice parameters is about 25.8° for the wavelength used(λ=2.351 Å, 14.8meV in energy). Profile of the observed scattering shows a characteristic of the two-dimensional lattice[4] as shown in Fig.1. The line shape is similar to that of the non-stoichiometric powder below T_N. Fig.2 shows integrated intensities at $25.8° \leq 2\theta \leq 27.4°$ (I_1) and $24.8° \leq 2\theta \leq 25.4°$ (I_2). The first region includes the broad critical scattering and the second includes the sharp peak which appears below T_N. These results indicate that the spin correlation in the stoichiometric YFe_2O_4 is essentially two-dimensional and that the three-dimensional ordering appears through the spin lattice interaction and the lattice distortion.

Two additional diffraction lines were observed in the low temperature phase of the stoichiometric samples at angles corresponding to the lattice spacings d=12.0Å and 19.3Å. These lines are magnetic in origin because any traces were not detected with X-ray diffraction at low temperature. Both of them were absent in the non-stoichiometric specimen. Back ground increased

in that case but there was no sign of the two-dimensional character.

Experiments on the diffuse scattering was initiated by a suggestion of Dr. G.Shirane.

References 1) J.Akimitsu et al., Solid State Commun. 32(1979)1065.
2) Y.Nakagawa et al., J. Phys. Soc. Jpn. 47(1979)1369.
3) J.Akimitsu et al., read at ICM'79 at München, 1979.
4) B.E.Warren, Phys. Rev. 59(1941)693.

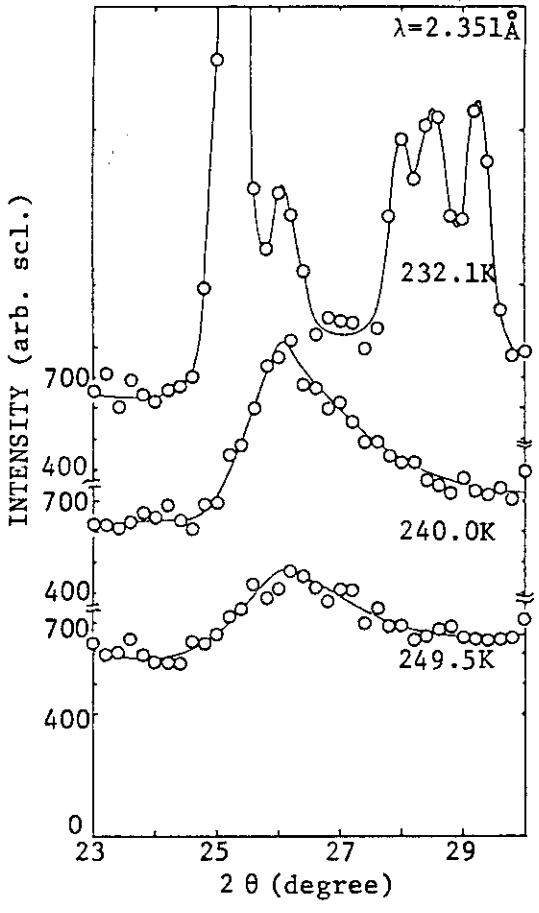

Fig.1. Profile of the θ-2θ scanning of the stoichiometric YFe_2O_4 around (1/3,1/3,0) near the critical temperature(∿235K).

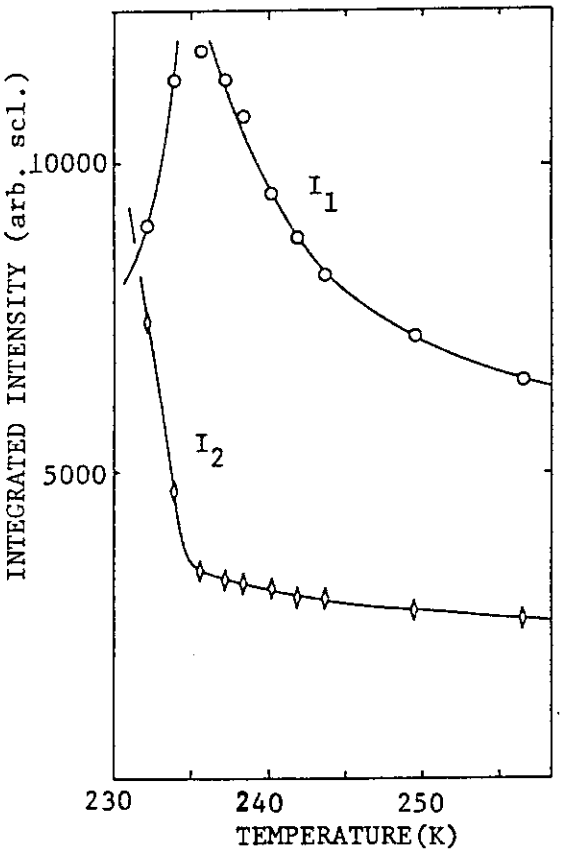

Fig.2. Integrated intensities at $25.8° \leq 2\theta \leq 27.4°$ (I_1) and at $24.8° \leq 2\theta \leq 25.4°$ (I_2) near the critical temperature.

III11 Magnetic and Neutron Diffraction Study of $SrCoO_{3-x}$

Hitoshi Oda*, Yasuo Yamaguchi, Hiroshi Watanabe and Humihiko Takei

The Research Institute for Iron, Steel and Other Metals, Tohoku University, Sendai Japan

$SrCoO_3$ is a ferromagnetic oxide with the perovskite-type crystal structure [1]. It contains Co^{4+} and has low electrical resistivity $\rho \simeq 10^{-1}$ $-10^{-3}\Omega$cm.

For the study of the magnetic scattering intensity, polarized neutron diffraction measurements were made of the sample of $SrCoO_{3-x}$ with x = 0.03. A depolarization correction ($d_s P_0$, where d_s = depolarization and P_0 = polarizability of monochromated neutrons) of 0.96±0.02 was applied to the data. The extinction effect, contamination due to $\lambda/2$ scattering, and multiple scattering were all negligibly small.

Fig. 1 shows the magnetic form factor curve. It is seen that the form factors for the reflections with more than two Miller indices are even and above the spherical symmetry curve (dotted line), while those for the reflections with more than two Miller indices are odd and below the spherical symmetry curve. The asphericity shown here cannot be due to that of the 3d wave function because it should occur only at higher scattering angles than we have scanned. But it evidences the presence of unpaired electrons on the oxygen atom. The values of magnetic moments of μ_d = (1.18 ±0.02)μ_B and $3\mu_p$ (oxygen) = (0.34±0.05)μ_B are obtained by least square fitting to the observed values.

The fact that the oxygen ion has a finite moment which is parallel to the cobalt moment is considered to be due to covalency. Through a survey of the series of oxides $SrMO_3$ (M = V, Cr, Mn, Fe and Co) it is considered that the $\pi^*(\uparrow)$ band is completely filled at M = Mn, and so $SrMnO_3$ is an insulator [2]. Since in $SrCoO_3$ the Co moment is close to but slightly higher than the low spin value of $1\mu_B$, both $\pi^*(\downarrow)$ and $\sigma^*(\uparrow)$ bands are partially filled. The electrons in the $\sigma^*(\uparrow)$ band may thus play the role of making the substance ferromagnetic and conductive.

References

[1] H. Watanabe: J. Phys. Soc. Jap. 12 (1957) 515; H. Watanabe and T. Takeda : Ferrites, Proc. Int. Conf. (Univ. Tokyo Press. Tokyo, 1971) p. 588;

T. Takeda and H. Watanabe: J. Phys. Soc. Jap. 33 (1972) 973.
[2] T. Takeda and S. Ohara: J. Phys. Soc. Jap. 37 (1974) 275.

Present address; * Advanced Research Center, Victor Company of Japan Ltd., Yokohama 221.

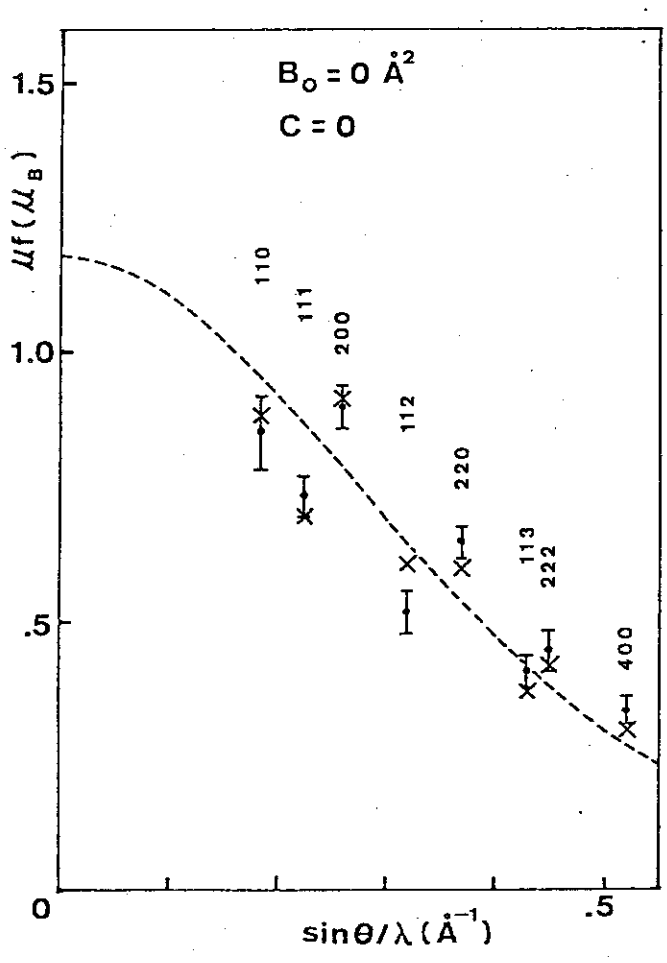

Fig. 1. Form factor curve for $SrCoO_{2.97}$. I = Experimental points. × = Calculated values by assuming $\mu_{Co} = 1.18\ \mu_B$ and $\mu_O = 0.39\ \mu_B$. ----- Form factor curve for spherically symmetric μ_{Co}^{4+}.

III12 Magnetic Polarization of Oxygen Ions in $SrFeO_3$

Hiroshi Watanabe, Hitoshi Oda,* Eiji Nakamura,**
Yasuo Yamaguchi and Humihiko Takei

The Research Institute for Iron, Steel and Other Metals, Tohoku University
Sendai 980,

The perovskite type oxides ABO_3 with alkaline earth and 3d transition elements (A=Ca, Sr; B=V, Cr, Mn, Fe, Co) are a family of interesting materials from the point of view of the correlation between the magnetic properties and the electrical conductivity. These oxides contain 4^+ ions of 3d transition elements and show metallic conductivity except for Mn compounds. $SrFeO_3$, which is a typical example of this family, is an antiferromagnet (T_N=134K) with a spiral spin structure [1] which is originated from the long range nature of the magnetic interaction, and this fact is probably associated with the metallic conductivity of this oxide. For $T>T_N$, the magnetic susceptibility of $SrFeO_3$ has been found not to obey the Curie-Weiss law and its magnitude is as large as 3×10^{-4} emu/g.[1,2]

We have made neutron diffraction measurements at 4.2K in order to study the electronic structure of $SrFeO_3$, and also made magnetization and polarized neutron diffraction measurements for $T>T_N$ in order to clarify the origin of the strange behaviour of the magnetic susceptibility.

We have made precise neutron diffraction measurements a single crystal of $SrFeO_{2.90}$ at 4.2K and 77K. From the least squares fitting of calculated nuclear intensities to the observed ones, the oxygen deficient parameter δ of $SrFeO_{3-\delta}$ and the Debye temperature H_D were obtained as δ=0.10±0.04 and H_D=740±110K.

The magnetic form factor of the iron ion as measured for [111] magnetic domain is shown in Fig. 1. There are some deviations of the experimental points from the spherical form factor curve calculated for a free ion of Fe^{4+}. We considered two causes of these deviations, one being the asphericity of the spatial distribution of 3d orbitals and the other the magnetic polarization of the oxygen ions. The latter was thought to be the main source of the deviations because the former takes very small values in the low angle region of $\sin\theta/\lambda<0.4$ ($\mathring{A}^{-1}$).

Magnitudes of the magnetic moments were obtained as μ_{Fe}=2.21±0.07 μ_B

and μ_0=0.10±0.03 μ_B by means of the least squares fitting of the calculated and observed values of the magnetic structure factors.

The magnetic susceptibility of $SrFeO_3$ has been known not to obey the Curie-Weiss law. In order to clarify this problem, we measured the temperature dependence of magnetization vs. magnetic field curves on five samples with different preparing conditions. We found some ferromagnetic impurities mixed in the samples, and the amounts of these impurities were found to depend on the heat treatment and the condition of preservation of the samples. The magnetic susceptibility of $SrFeO_3$ free from the ferromagnetic impurities has been found to obey the Curie-Weiss law, and the effective Bohr magneton number, μ_{eff}, is still found as large as 5 μ_B per formula. This μ_{eff} value is about twice larger than the value calculated from the magnetic moment for the ordered phase.

In order to study the origin of the large value of μ_{eff}, we have measured the spatial distribution of the magnetic susceptibility through a precise measurement of the induced magnetic moment as interference terms with nuclear scattering by using polarized neutron diffraction (PND) technique.

The experimental results at 140K and 180K under a magnetic field of 9.7 kOe are shown in Fig. 2 as the magnetic form factor of the induced moment around the iron ion site. This result indicates that the large magnetic susceptibility comes mainly from the iron ion site.

Although the experimental errors are considerably large, the deviations of the experimental points from the spherical form factor curve of Fe^{4+} ion were observed as seen in Fig. 2, and these deviations are well explained by introducing the induced moments at the oxygen ion sites from almost the same calculation as mentioned above. The induced magnetic moments are obtained to be 0.0608±0.0003 μ_B for an iron ion and 0.0026±0.0003 μ_B for an oxygen ion at 140K under the magnetic field of 9.7 kOe. This fact means that the magnitude of the localized magnetic moment of an iron ion is as large as 4.9 μ_B in the paramagnetic phase. Therefore, the large value of μ_{eff} for $SrFeO_3$ is found to come from the large value of μ_{eff} of the iron ion.

The magnitude of the magnetic moment of an iron ion in $SrFeO_{2.90}$ is measured to be 2.21±0.07 μ_B which is about 10% larger than the value for the low spin state of Fe^{4+} (t_{2g}^4, 2 μ_B). This fact shows that the iron ion takes an intermediate state between high and low spin states. Therefore, 3d-electrons of the iron ion partially occupy e_g orbital, and also occupy

σ-bonding orbital with 2p orbital of the oxygen ion, furthermore the electronic state of this oxide should be understood in the framework of the band model as mentioned in the previous report.[1)]

In the paramagnetic region, the iron ion has the magnetic moment of 4.9 μ_B. This value is more than twice the value of the ordered state. One of the explanations for the temperature dependence of the value of the magnetic moment is high spin-low spin transition of iron ion taking place at or near the Néel temperature.

References

[1] T. Takeda, Y. Yamaguchi and H. Watanabe: J. Phys. Soc. Jpn. 33 (1972) 967.

[2] H. Oda, Y. Yamaguchi, H. Takei and H. Watanabe: J. Physique 38 (1977) C1-121.

Present address; *Advanced Research Center, Victor Company of Japan Ltd., Yokohama 221. **Magnetic Materials Research Laboratory, Shin-Etsu Chemical Industry Co. Ltd., Takefu, Fukui 915.

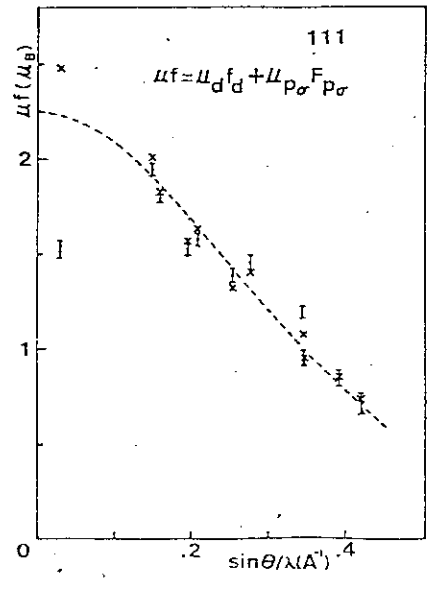

Fig. 1. Form factors for $SrFeO_{2.90}$. I = Experimental points. × = Calculated values (μ_{Fe}=2.21 μ_B and $\mu_{p\sigma}$=0.13 μ_B). The broken line is form factor for spherical Fe^{4+}.

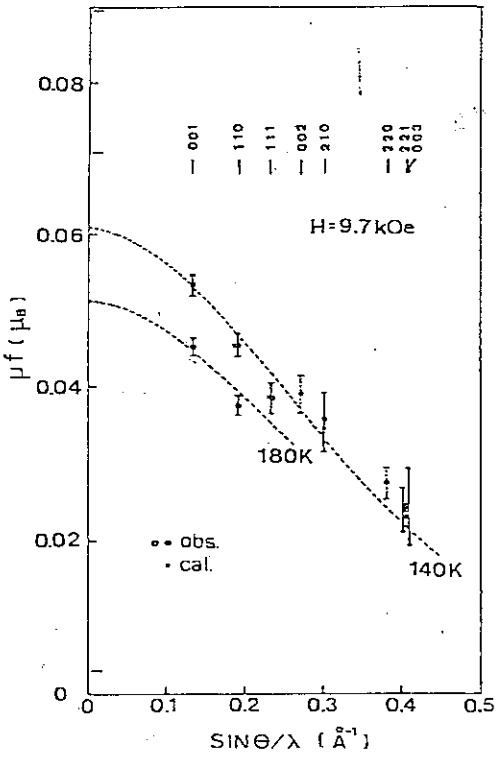

Fig. 2. Form factor curves of the induced magnetic moments for $SrFeO_{2.90}$ for $T>T_N$. Calculated values are obtained by assuming μ_{Fe} =0.0608 μ_B and μ_O=0.0028 μ_B.

III13 Electric Conductivity and 3d-electron Distribution in $CuCr_2Se_{4-x}Br_x$

Yasuo Yamaguchi, Yasutake Ohishi*, Masayoshi Ohashi,
Osamu Yamashita** and Hiroshi Watanabe

The Research Institute for Iron, Steel and Other Metals, Tohoku University
Sendai 980,

$CuCr_2Se_4$, which is a chalcogenide spinel, is a ferromagnet and shows metallic conductivity (ρ $10^{-5}\Omega\cdot$cm at 4.2K).[1] Polarized neutron diffraction (PND) study on this material[2] has shown that the ionic configuration is approximately $Cu^{+}Cr_2^{3.5+}Se_4^{2-}$ and the magnetic form factor of Cr agrees well with the calculated free ion form factor for Cr^{+}, in other words the radial distribution of 3d-electrons of Cr is more spread by about 20% compared with that of the calculated value for the free ion $Cr^{3.5+}$.

It is interesting to know why 3d-electron is so spread in $CuCr_2Se_4$. Is it a manifestation of the electron correlation or a general property seen among these chromium compounds?

In the present report, we deal with the $CuCr_2Se_{4-x}Br_x$ ($0.0\leq x\leq 1.0$) system. The electric conductivity decreases with increasing x value, and the substance becomes semiconductive for x=1.0.[1] The Curie temperature also decreases with increasing x.[1,2] The magnetization per formula increases linearly with increasing x from 4.76 μ_B for x=0.0 up to 5.67 μ_B for x=1.0.[2]

We have made PND experiments on a single crystal of $CuCr_2Se_{4-x}Br_x$ with x=0.5, in order to study the band structure of this system, and also to know the relation between the spatial distribution of 3d-electrons and the electric conductivity.

Precise measurements of the magnetic structure factors were made by using PND technique as the interference terms with the nuclear structure factors. The experimental results are shown in Fig. 1 in the form of the magnetic form factor. The magnetic form factor of Cr ion is shown with heavy circles in Fig. 1, and the solid curve drawn through these experimental points is the spheriecal part of this magnetic form factor whose angular dependence agrees well with the theoretical calculation for the free ion of Cr^{2+},[3] in contrast with that of Cr^{+} in the case of x=0.0.

There are two different origins for the deviations of the experimental

points from the spherical form factor, one is the magnetic polarization of anions as seen in the low angle reflections, and the other is the asphericity of 3d-orbitals for the high angle reflections. The asphericity of the magnetic form factor indicates that 80±5% of the 3d-electrons of Cr are in t_{2g} orbitals.

The extrapolation of the spherical form factor to $\sin\theta/\lambda=0.0$ gives the magnitude of the magnetic moment of the Cr ion as $\mu_{Cr}=2.77\pm0.07\ \mu_B$.

Magnetic polarization of Cu ion was measured for (220) and (660) reflections, and it has been found that the magnetic moment of the Cu ion is carried by 3d-electrons. The magnitude of the magnetic moment of Cu ion was obtained by extrapolating the magnetic form factor to $\sin\theta/\lambda=0.0$ as $\mu_{Cu}=-0.07\pm0.01\ \mu_B$.

From the concentration dependence of the magnetization and the magnetic susceptibility measurements for $CuCr_2Se_{4-x}Br_x$ system,[2] it is generally believed that the 3d-electrons of Cr in $CuCr_2Se_4$ occupy only the up spin band, so that the magnitude of the magnetic moment of Cr in μ_B unit indicates directly the number of 3d-electrons.[2] From the present experimental results, number of 3d-electrons of Cr has been known to increase from $n_{3d}=2.64\pm0.04$ for x=0.0 to $n_{3d}=2.77\pm0.07$ for x=0.5. The increasing of the 3d-electron number causes the increasing of the Coulomb repulsive energy among 3d-electrons, so that the radial distribution of 3d-electrons of Cr is expected to be more spread for x=0.5 than x=0.0. The experimental results on the radial distribution of 3d-electrons are opposite to the prediction, since the shape of the magnetic form factor agrees well with the theoretical calculation for the free ion of Cr^+ in the case of x=0.0, and that of Cr^{2+} in the case of x=0.5. The latter is contracted in real space by about 8% than the former. The contraction of 3d-electron distribution for x=0.5 is thought to come from the inrease of the correlation energy, since the electric conductivity is less than that for x=0.0.

References

1) k. Miyatani, K. Minematsu, Y. Wada, F. Okamoto, K. Kato and P.K. Baltzer : J. Phys. & Chem. Solids 32 (1971) 1429.

2) O. Yamashita, Y. Yamaguchi, I. Nakatani, H. Watanabe and K. Masumoto: J. Phys. Soc. Jpn. 46 (1979) 1145.

3) R.E. Watson and A.J. Freeman: Acta Crystallogr. 14 (1961) 27.

Present address; * Ibaraki Electric Communication Lab., NTT, Tokai, Ibaraki.
** Sumitomo Special Metals Co., Ltd., Shimamoto, Osaka.

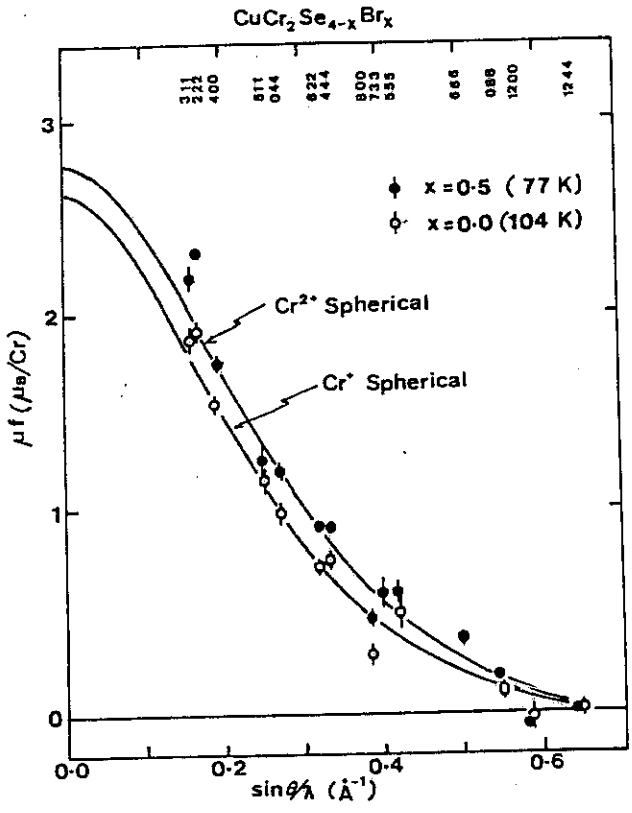

Fig. 1. Magnetic form factor of Cr for $CuCr_2Se_{4-x}Br_x$. Present results for x=0.5 are are compared with the previous results for x=0.0. Solid curves show the spherical form factors calculated for the free ion of Cr^{2+} (upper) and Cr^{+} (lower) multiplied by μ_{Cr}=2.77 and 2.64 μ_B, respectively. The deviations from the spherical form factor come from the asphericity of 3d-orbitals for high angle reflections and from the anion polarization for low angle reflections.

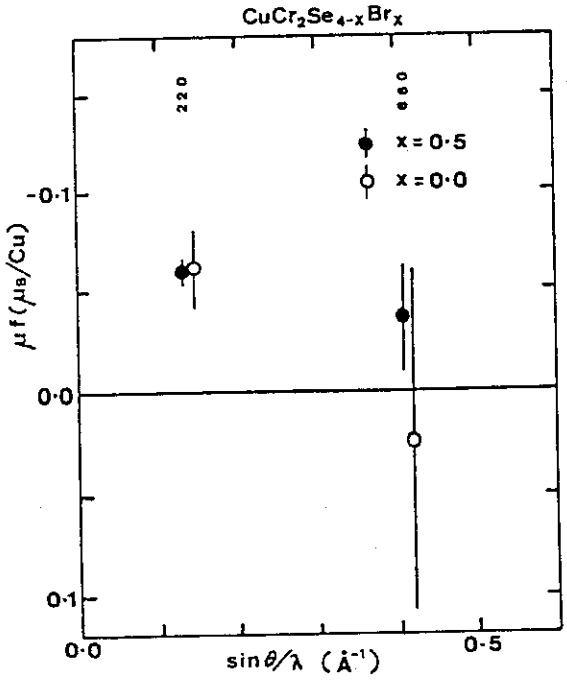

Fig. 2. Magnetic form factor of Cu for $CuCr_2Se_{4-x}Br_x$. Present results for x=0.5 (heavy circles with error bars) are compared with the previous results (open circles with error bars) for x=0.0.

III14 Helical Spin Ordering in Hexagonal Ferrite $(Ba_{1-x}Sr_x)_2Zn_2Fe_{12}O_{22}$ (x=0 - 1.0)

Nobuyuki Momozawa*, Yasuo Yamaguchi**,
Humihiko Takei** and Masaru Mita*

*Department of Physics,Faculty of Science and Technology,Science University of Tokyo,Noda,chiba. **The Research Institute for Iron,Steel and Other Metals, Tohoku University, Sendai.

In the solid solution $(Ba_{1-x}Sr_x)_2Zn_2Fe_{12}O_{22}$ (x=0-1.0),the influence of Sr concentration X,temperature T and magnetic field H on the heli-magnetic turn angle ψ_o were investigated by the use of "TOG" and also "POLTO".

(A). It is known that spins lie in the crystallographic c-plane and form themselves into the helical spin ordering propagating along the c-axis[1,2]. So in order to determine the ψ_o,the c-axis was directed parallel to the scattering vector. The diffraction peaks of the (00ℓ) planes are indexed as ℓ=3n (n:integer) for nuclear scattering peaks and ℓ=3(n±δ) for magnetic scattering ones (satellites), in which δ is the proper non-integer number smaller than 0.5 . The ψ_o,=δ×180/o.5 degree,was determined on each X (Fig.1).

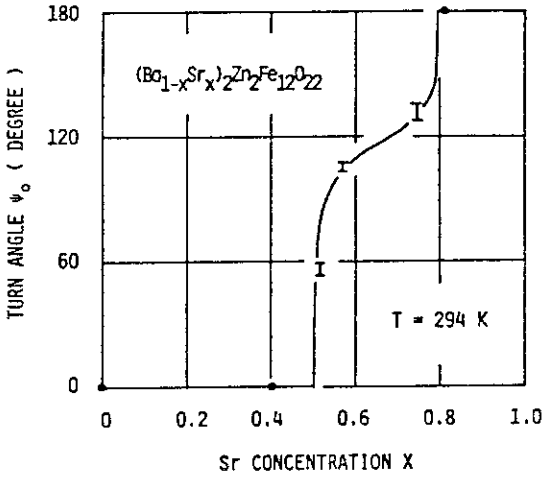

Fig.1 variation of ψ_o vs. X

As is seen from the figure, spin structure varies progressively ferro, helix and antiferro with increase of X. Total spin numbers in the saturated state, measured in our laboratory , are not affected by the replacement of Ba^{++} ion by Sr^{++} ion. It is because of both being non-magnetic ions. The varies of spin structure in these types may be expected owing to modification of exchange interaction between spins by localized lattice distortion and symmetry breaking with change of X.

(B). Temperature dependence of ψ_o for the fixed X=0.74 were measured in the region of 77K-340K($\simeq T_N$).The ψ_o is 85° at 77K and increases stepwisely with increase of T, accompanying by the sudden change of slope in the lattice constant C vs. T curve, and comes to 180° just below T_N. Especially the ψ_o holds an angle 90° in the wide temperature range (103K-195K).

(C). The deformation of helix due to a magnetic field H parallel to the screwing plane (c-plane) were investigated with the use of poralized neutron beams. The following three cases were employed in the experiment (Table 1).

Tab.1

T=77 K	X=0.74	ψ_o=85°
294	0.52	58
294	0.74	130

The magnetization curves vs. H show that the helix changes stepwisely into three spin states with H; slightly deformed helix, fan-like and ferro[1]. The fan-like state is realized in the field approximately higher than $H_F/10$, where the H_F sets on the ferro state. It differs from predicated value $H_F/2$ of the theory[3]. The results from investigating diffraction pattern of (00ℓ) planes shows that the three spin states are described with a common fashion regardless of T and ψ_o at H=0 for above cases in table 1. The fashion is the following: In the weaker field than $H_F/10$, the ferro component (ψ_o=0) induced by H overlaps on the nuclear scattering peaks in the diffraction pattern, and satellites move towards the position where ψ_o=90° with increase of H until they end in that position. This state corresponds to the slightly deformed helix state. For further increase of H, the peak corresponding to ψ_o=180° newly appears, that is to say, there coexist three ψ_o's; ψ_o=0°, 90° and 180°. this state corresponds to the fan-like state. The intensity of the peaks for ψ_o=90° and 180° decreases with increase of H and vanishes in the ferro state ($H>H_F$). The coexistence of ψ_o's may be unique in the presence of magnetic field.

References;

1). U.Enz, J. Appl. Phys., Suppl. to 32 (1961), 22s

2). V.A.Sizov, R,A,Sizov and I.I.Yamzin, Sov. Phys.-JETP, 26 (1968),736

3). T.Nagamiya, K.Nagata and Y.Kitano, Prog. Theor. Phys. 27 (1962), 1253

III15 Magnetic Correlations in a Competing Interaction System $0.88FeTiO_3$-$0.12Fe_2O_3$ with Spin Glass Behaviors

Yoshikazu Ishikawa, Masatoshi Arai, Masahumi Kohgi,
Norio Saito and Fumihiko Takei*

Physics Department, *Institute for Iron, Steel and Other Metals, Tohoku University, Sendai 980

The paper reports the results of neutron scattering studies on a single crystal of $0.88FeTiO_3$-$0.12Fe_2O_3$. The sample has been found to exhibit the spin glass behaviors below 50K. $FeTiO_3$, ilmenite, with the $R\bar{3}$ symmetry (the hexagonal crystal with alternating Fe^{2+} and Ti^{4+} layers) becomes antiferromagnetic below 68K along the c axis by the negative Fe^{2+}-Fe^{2+} ions interactions via the Ti^{4+} layer (the n.n.n. interactions). When a small amount of Fe_2O_3 is added to $FeTiO_3$, Fe^{3+} ions entering randomly in the Ti^{4+} layers tend to align the moment of neighboring Fe^{2+} ions parallel by the strong Fe^{3+}-Fe^{2+} interactions (the n.n. interactions), resulting in developing the short range ferrimagnetic order (superparamagnetic cluster) below 150K. The sample exhibits the spin glass transition below 50K by competition of the n.n. and n.n.n. interactions.

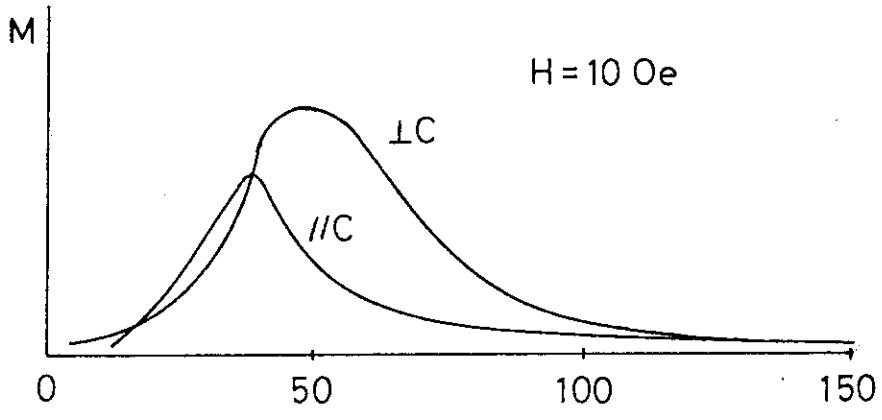

Fig. 1. Static susceptibilities of $0.88FeTiO_3$-$0.12Fe_2O_3$ measured in a weak field of 10 oe applied along the (axis $\chi_{//c}$10) and perpendicular to it $\chi_{\perp c}$(o).

A single crystal of $0.88FeTiO_3$-$0.12Fe_2O_3$ was prepared by floating zone method under a controlled oxygen atmosphere. Fig. 1 shows the static susceptibilities measured along the c axis ($\chi_{||}(0)$) and perpendicular to it ($\chi_{\perp}(0)$) in a weak field of 10 Oe. The susceptibility is quite anisotropic; $\chi_{||}(0)$ has a sharp peak at 37K, while $\chi_{\perp}(0)$ shows a broad hump around 50K.

The neutron scattering studies were carried out using a cylindrical single crystal 8mm in diameter and 30mm in height. The crystal was mounted on the triple axis spectrometer of Tohoku University (TUNS) installed at JRR-2 with the rotation axis perpendicular to both of c* and a* axes. The magnetic short range order was studied around four different reciprocal lattice points (0,0,3), (1,0,1), (0,0,1.5) and (1,0,-0.5) as shown in Fig. 2. The scattering around (0,0,3) and (1,0,1) detects the ferrimagnetic short range order by the n.n. interactions, while that around (0,0,1.5) and (1,0,-0.5) shows the ilmenite type antiferromagnetic order.

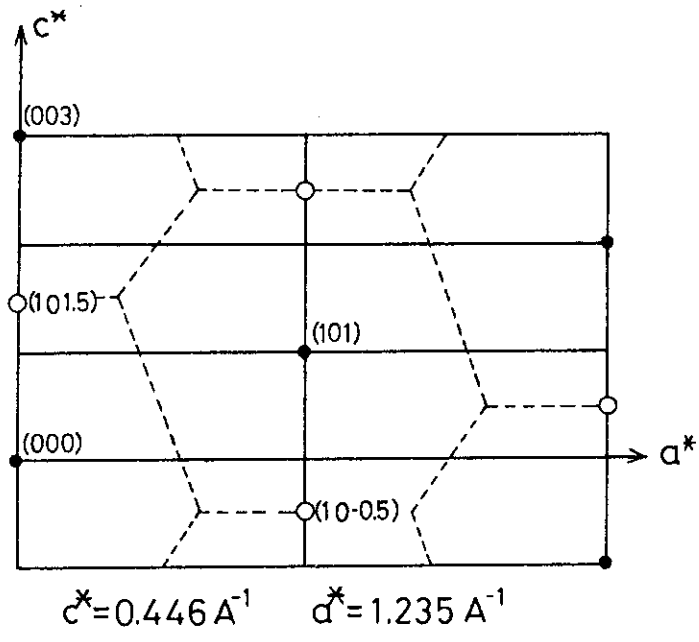

Fig. 2. Reciprocal lattice of ilmenite ● nuclear points, o antiferromagnetic points.

The intensities of scattering are related to the parallel and perpendicular susceptibilities as

$I(0,0,3) \propto 2T\chi_{\perp}^{F}(Q)$,

$I(1,0,1) \propto T(1.11\ \chi_{\perp}^{F}(Q) + 0.88\ \chi_{||}^{F}(Q))$,

$I(0,0,1.5) \propto 2T\chi_{\perp}^{A}(Q)$,

$I(1,0,\bar{0}.5) \propto T(1.03\chi_{\perp}^{A}(Q) + 0.97\ \chi_{||}^{A}(Q))$,

where χ^F and χ^A represent the susceptibilities corresponding to the ferrimagnetic and antiferromagnetic orders respectively. Four important susceptibilities $\chi_{||}^{F}$, $\chi_{\perp}^{F}$, $\chi_{||}^{A}$ and $\chi_{\perp}^{A}$ can, therefore, be separately

obtained from four different scattering measurements.

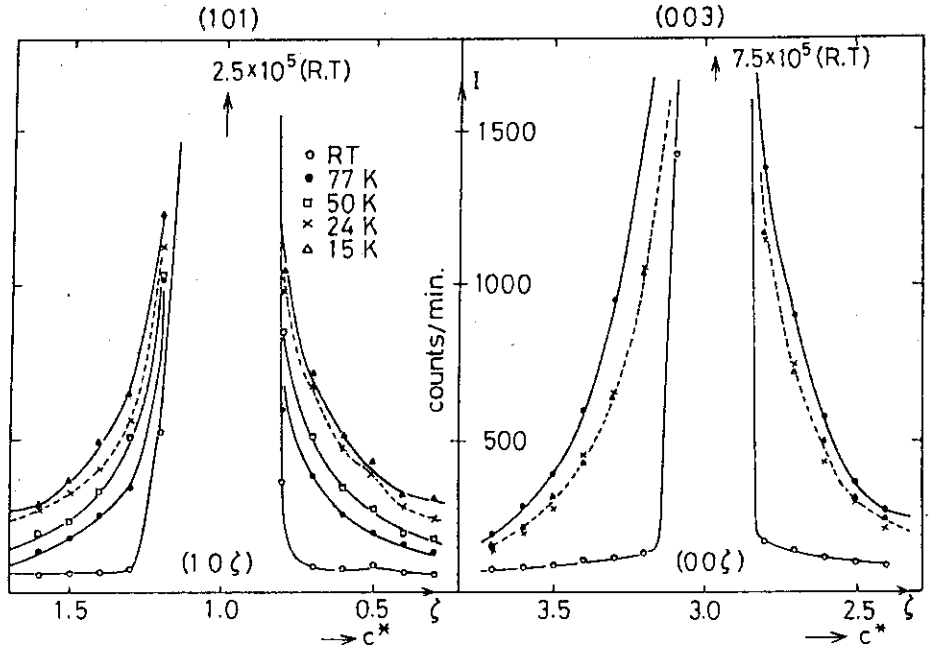

Fig. 3. Ferrimagnetic scattering developed around the nuclear points.

Fig. 3 shows the diffuse scattering along the c*axis developed around (0,0,3) and (1,0,1). Note that the 0,0,3 scattering has the different temperature dependence from the 1,0,1 scattering. Although, because of contamination of the nuclear Bragg peak, the measurements with TUNS are limited to a rather large q range ($q \geq 0.09 \mathring{A}^{-1}$), the profile for lower q values ($q \geq 0.0086 \mathring{A}$) could be explored by measurement of the scattering around (0,0,0) with the small angle scattering machine at KENS (KENS-SAN). The results suggest that the ferrimagnetic cluster size at 45K is about 125Å in the c axis.

In contrasted with the scattering from the ferrimagnetic order, the antiferromagnetic scattering appears only around (1,0,-0.5) as seen in Fig. 4, suggesting that the antiferromagnetic correlation axists only for the c axis components of spins. The linewidth (FWHM) Γ corrected for the instrumental resolution is 0.02 $\mathring{A}^{-1}$ at 10K, the correlation length of the antiferromagnetic order being about 300Å at 10K. The antiferromagnetic order disappears at 50K as shown in the inset to Fig. 4.

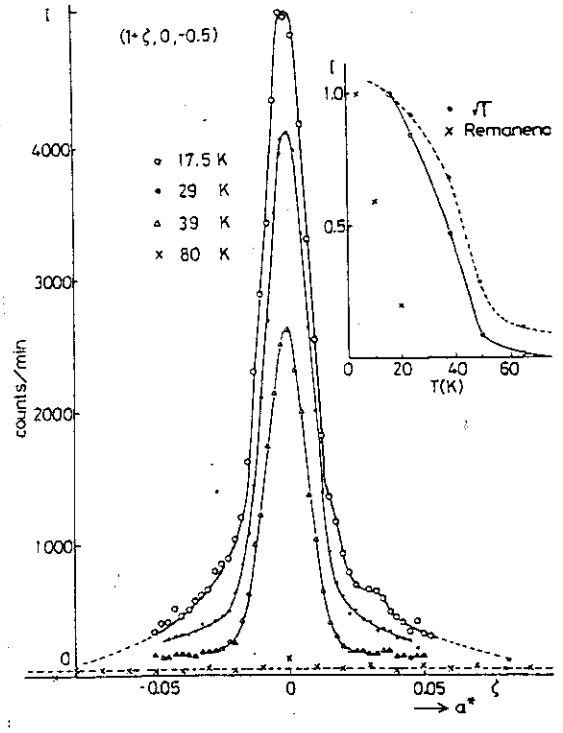

Fig. 4. Antiferromagnetic scattering developed around (1,0,-0.5). The peak intensity is plotted against temperature in the inset.

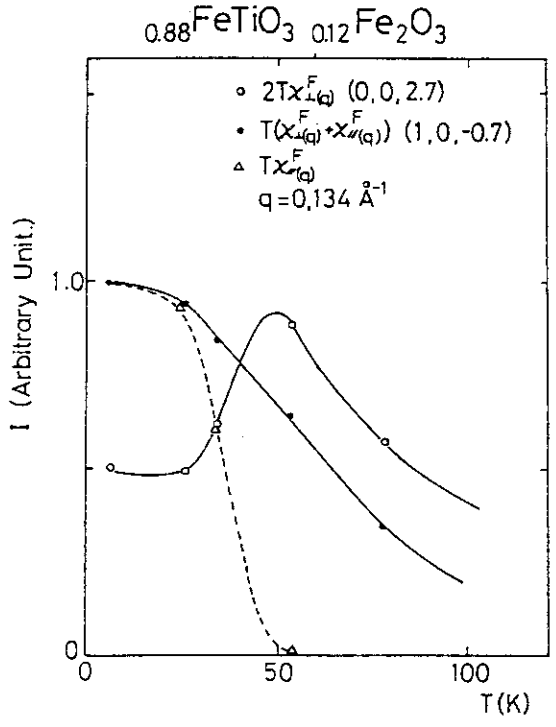

Fig. 5. Temperature dependences of ferrimagnetic scattering. $\chi_{\perp}^{F}(q)$ and $\chi_{11}^{F}(q)$ are separated from I(0,0,2.7) and (1,0,-0.7).

The temperature dependences of the ferrimagnetic correlation at a given wave vector q=0.134Å^{-1} are displayed in Fig. 5 for separated χ_{11}^{F} and $\chi_{\perp}^{F}$. Note that $\chi_{\perp}^{F}(q)$ has the maximum at 50K, independent of q, while $\chi_{11}^{F}(q)$ depends strongly on q; $\chi_{11}^{F}(q)$ at q=0.13Å starts to increase below 50°K in parallel with $\chi_{11}^{A}(q)$, but $\chi_{11}^{F}(q)$ for smaller q values has a peak at lower temperature (38K) as is the case with $\chi_{11}^{F}(o)$.

In summary, the ferrimagnetic short range order developed below 150K starts to be modified by the onset of the ilmenite type antiferromagnetic order at $T=T_N^*$, the c axis components apears below T_N^* which align in long period spiral with the pitch of 50Å by suppressing the ferrimagnetic correlations for smaller wave vectors. The temperature where $\chi_{11}^{F}(o)$, has the peak is not the critical temperature as far as the magnetic order is concerned.

III16 Magnetic Structure of $Cr_{1/3}NbS_2$

Tomonao Miyadai*, Katsuya Kikuchi* and Hiromitsu Kondo**

* Department of Physics, Faculty of Science, Hokkaido University,

** Faculty of Education, Saitama University.

$Cr_{1/3}NbS_2$ is an intercalate of 2H-type NbS_2 with a layer structure and is reported as a metallic ferromagnet [1]. This compound belongs to the space group D_6^6-$P6_322$, having no inversion symmetry. The sequence of the layers containing the individual constituent elements is Nb-S-Cr-S-Nb- along c-axis. Cr can be replaced by other 3d-transition metals from Mn to Ni. The magnetism of $M_{1/3}NbS_2$ changes from ferromagnetism to antiferromagnetism as M goes from Cr to Ni. M-atoms form an h.c.p. lattice. Cr is considered to be in the trivalent state and to have a localized moment (about 3 μ_B/Cr) [1-3]. $Cr_{1/3}NbS_2$ is an easy-plane type ferromagnet and its T_c is 127 K. The magnetization curve along the hard c-axis is an ordinary curve, but the curve in c-plane exhibits a metamagnetic behavior with a small critical field of about 1.4 kOe (roughly independent of temperature). This latter fact suggests the existence of a helical structure.

The purpose of this note is to examine whether this compound is a helimagnet or not. The result was negative but leaving a possibility for a long-period helical structure.

Neutron diffraction measurements were made on a powder sample at about 5 K and room temperature(RT), by means of the diffractometer of ISSP installed at JRR-2 ($\lambda = 2.44$ A; (002) of PG monochrometer).

Nine reflections between $2\theta = 15°$ and 60° were collected. The obtained results are given in Table I, in which the relative intensity normalized to (11·1) is indicated. (Cr atoms do not contribute to (11·1) reflection.) Either antiferromagnetic reflection or satellite could not be detected within the experimental sensitivity and the half width of the observed reflections. (e.g. the width for (00·2) is about 0.7° at $2\theta = 23°$.)

In Table I, the calculated intensities are also given. In the calculation of nuclear reflections, the following parameters were used: b(S) = 2.85×10^{-13} cm, b(Nb) = 7.11×10^{-13} cm, b(Cr) = 3.532×10^{-13} cm; x(S) = 0.670, y(S) = 0.020, z(S) = 0.128, z(Nb) = 0.992. In the calculation

of the magnetic part, the form factor for Cr^{3+} ion was taken from Watson and Freeman [4]. The intensity for magnetic reflections was calculated for the ferromagnetic spin arrangment with spins lying in c-plane. The spin direction in c-plane cannot be determined in the present case. The observed magnetic reflections were obtained by subtracting the intensity at RT from that at 5 K. As seen in Table I, we have a satisfactory agreement between the observed and the calculated intensities of the magnetic part, considering the experimental errors in the present measurement. We obtained a reliability factor of $R = 0.05$. For the model in which the spins incline out of c-plane, R takes larger values than 0.05. However, there still remains a possibility that $Cr_{1/3}NbS_2$ has a helical spin structure with a period longer than 20 sheets along c-axis, if the half width of (00·2) reflection is considered.

Recently, Moriya accounted for the metamagnetic behavior of this compound on the basis of a helical spin structure which is attributed to the antisymmetric exchange interaction [5]. He suggested, from the analysis, a very long period of about 480 Å, which is consistent with our observation mentioned above.

The present authors would like to express their sincere thanks to Prof. K. Hirakawa for allowing them to use the diffractometer.

Table I

hk.l	I_{obs} R.T.	I_{obs} 5 K	I^N_{cal}	I^M_{cal}	I^M_{obs}
11.1	100	100	100	0	0
00.2	190	225	208.6	40.2	35
10.1	20	55	21.0	53.3	35
01.2	10	30	5.8	14.8	20
10.3	5	30	3.7	27.6	25
00.4	10	20	10.4	7.0	10
11.0	135	150	137.5	8.9	15
$\binom{10.4}{11.2}$	270	285	278.4	21.0	15

References

1) F. Hulliger and E. Pobitschka: J. Solid State Chem., 1(1970) 117.

2) R.H. Friend, A.R. Beal and A.D. Yoffe: Phil. Mag., 35 (1977) 1269.

3) S.S.P. Parkin and R.H. Friend: Phil. Mag., 41 (1980) 65.

4) R.E. Watson and A.J. Freeman: Acta Cryst., 14 (1961) 27.

5) T. Moriya and T. Miyadai: Tech. Rep. ISSP, Ser.A No.1185 (Dec. 1981), submitted to Solid State Commun.

III17 Magnetic Properties of $Mg_{1-p}Mn_pTe_2$ near p=0.5

Tomonao Miyadai, Osamu Okada and Katsuya Kikuchi

Department of Physics, Faculty of Science,
Hokkaido University.

$Mg_{1-p}Mn_pTe_2$ crystallizes in the pyrite structure in the whole range of p and the metal sites form an fcc lattice. Mn is in the divalent state with a localized moment of 5 μ_B. Since $MnTe_2$ is an antiferromagnet (T_N=87 K) with the 1'st kind of AF ordering in fcc lattice, $Mg_{1-p}Mn_pTe_2$ is a diluted system of an fcc antiferromagnet. Magnetic study shows that T_N falls rapidly near p=0.5 (the critical concentration), and that for 0.3<p<0.5 there is a peak in χ-T curve [1].

In this work, we tried to make clear the behavior near p=0.5 from view point of the magnetic ordering. The report including magnetic study on this system has already been published in ref.(2).

Neutron diffraction measurements were performed by meas of the diffractometer of ISSP at JRR-2. (λ=1.80 Å; (002) of PG). The used samples have p=0.53($>p_c$), 0.45 and 0.35 ($<p_c$), and were all in powder form. The measurements were made at 2.5 K, 4.2 K and RT. The magnetic part of reflections was separated by subtracting the data at RT from those at 4.2 K or 2.5 K. Fig.1 shows the diffraction pattern for p=0.53 at 4.2 K. We observe clearly two antiferromagnetic reflections (100) and (110), which correspond to the AF ordering of the 1'st kind. From these two reflections and nuclear (111) reflection, we obtained 1.5_4 μ_B for the average magnetic moment per metal site. If all the manganese moments in the sample ordered antiferromagnetically, we could have 5p=2.65 μ_B. Thus about 40 % of the manganese ions do not contribute to the long range order. Instead, they (all or a part) seem to contribute to

short range order(a diffusive-like broad peak is seen around (100) peak.). For p=0.45 and 0.35, we observed much weaker (100) peak at 4.2 K. Its intensity remains almost the same at 2.5 K. In these samples, only 30 % of Mn ions contribute to the long range order.

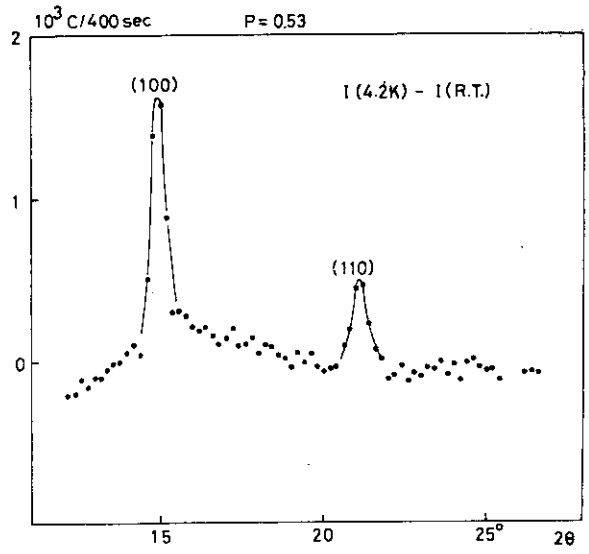

Fig. 1. Diffraction patterns of the magnetic part for $p = 0.53$. It is separated by subtracting the data at RT from those at 4.2 K. [2]

In Table I are given the observed average moment per metal site μ (in μ_B), and also the fraction f of Mn ions, which contribute to the long range order.

Table I

p	0.53	0.45	0.35
μ (μ_B)	1.5_4	0.7_6	0.5
f	0.6	0.3	0.3

In conclusion, although we observed the AF ordering at both sides of p_c, the fraction which contribute to the long range order is much smaller for $p<p_c$ than for $p>p_c$.

The present authors would like to express their sincere thanks to Prof. K. Hirakawa for allowing them to use the diffractometer.

References

1) O. Okada: J. Phys. Soc. Japan, 48 (1980) 391.
2) O. Okada, T. Miyadai and K. Kikuchi: J. Mag. Mag. Mat. 22 (1981) 306.

III18 Neutron Scattering Study of Phase Transition in Two-Dimensional Planar Ferromagnet K_2CuF_4

Kinshiro Hirakawa, Hideki Yoshizawa and Koji Ubukoshi

Institute for Solid State Physics, University of Tokyu, Roppongi, Minato-ku, Tokyo

In the previous paper, Hirakawa and Ubukosh[1] suggested from their magnetization measurements that K_2CuF_4 undergoes a phase transition basically interpreted as a Kosterlitz-Thouless transition with T_{KT} = 5.5 K. The weak 3D interaction modifies the transition point to the actual Curie point of 6.25 K. In this paper, we report a detailed neutron quasi-elastic scattering study performed to check the above conjecture. Measurements were made on a big excellent crystal (3 cc with the mosaic spread of ~3') and the critical parameters such as κ, ξ and η were determined directly by measuring the 2D correlation functions. For instance, κ or ξ is shown as a function of temperature in Fig.1. The apparent κ is q_c dependent at temperatures lower than 6.6 K showing the crossover from 2D XY to 3D XY in agreement with the magnetic study. In the figure, the full line is the Kosterlitz theory with T_{KT} = 5.5 K. Observed points are not only consistent with the curve but also the absolute value is consistent with the parameters in the spin Hamiltonian giving the correct values of crossover temperature. In Fig.2 the temperature dependence of the η is shown. In the 2D XY crossover regime η falls on the value of approximately 1/4. In Fig. 3, the effect of the magnetic field (symmetry breaking field) for the crossover from 3D XY to 2D XY is shown. This is a fundamental idea of the analysys of the magnetization curve and from this experiment a direct proof of the crossover is given i.e. at T_c with application of only 100 Oe, the q_c dependent 3D correlation changes to a q_c independent 2D correlation. Finally, the temperature dependence of the diffuse scattering due to spin wave scattering is exhibited in Fig.4. The linear T dependence indicates unrenormalized magnon frequencies up

very vicinity of T_c. The intensity suddenly goes up and typical feature of critical scattering appears. This sudden rise of the intensity suggests a sudden decrease of the stiffness constant . This might be a cause of so-called universal jump in the KT transition. All of the neutron scattering measurements were made using ISSP ND-1 in JRR-2.

1) K.Hirakawa and K. Ubukoshi: J. Phys. Soc. Japan 50(1981) 1909
2) K. Hirakawa: The 27 th MMM meeting, Atlanta (1981)

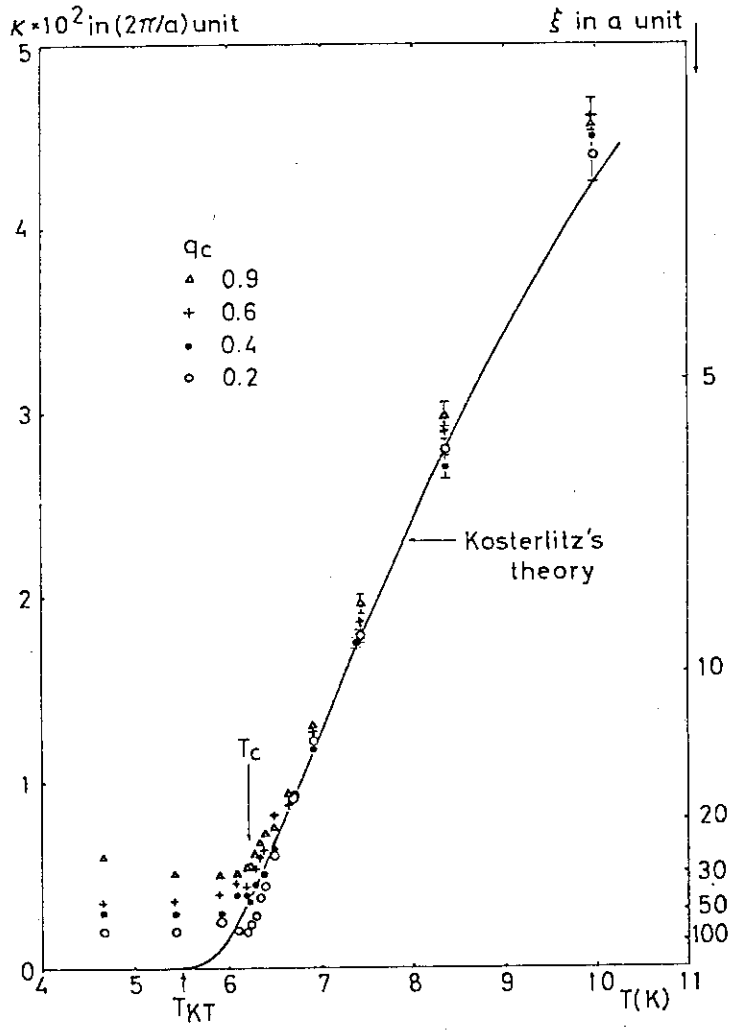

Fig. 1

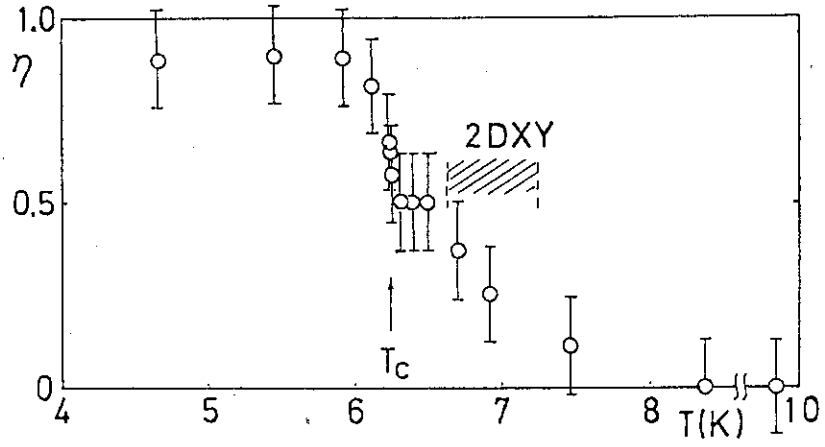

Fig. 2

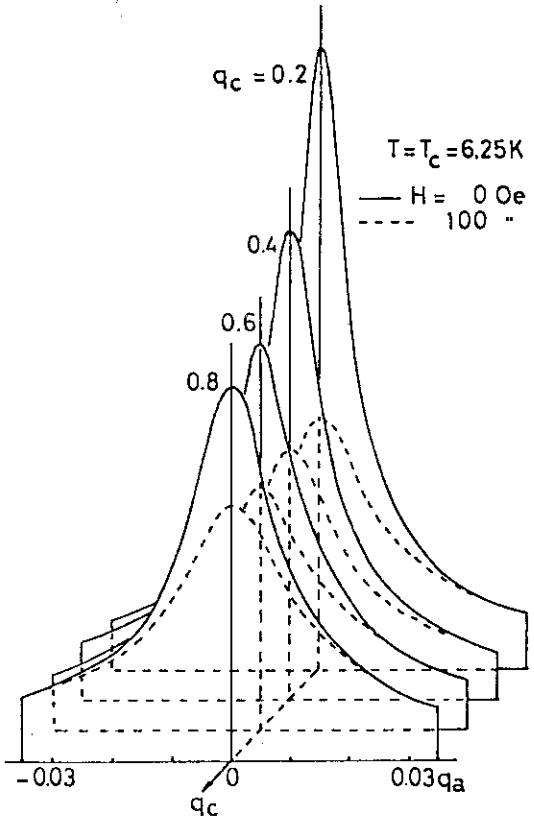

Fig. 3

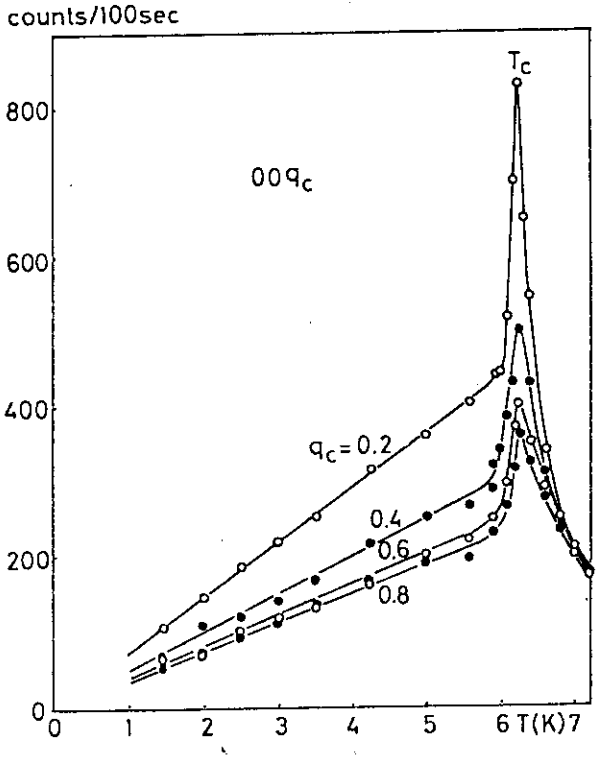

Fig. 4

III19 Neutron Scattering Study of One-Dimensional Heisenberg Antiferromagnet $CsVCl_3$

Kinshiro Hirakawa, Hideki Yoshizawa and Koji Ubukoshi

Institute for Solid State Physics, University of Tokyo, Roppongi, Minato-ku, Tokyo

Present address: Brookhaven National Laboratory, Upton, NY. USA

Niel et al[1] have found that $CsVCl_3$ has $CsNiCl_3$ structure with a = 7.228 Å and c = 6.030 Å. They found that the susceptibility has a broad maximum at about 400 K and it decreases with lowering temperature until $\sim$10 K , where it starts increasing with further lowering temperature. They thus suggested that it is one of the typical 1D Heisenberg antiferromagnet with S = 3/2. Recently, Steiner et al[2] have made neutron scattering measurement and found quasi-elastic scattering peak at T = 10, 51 and 100 K suggesting 1D correlations. But, they have found no evidence of 3D ordering down to 10 K.

In order to see the magnetic properties more in detail, we performed neutron scattering measurements on the single crystal grown by us. The crystal of about 2 cc had a rather wider mosaic spread of 20'. Measurements were made by the ISSP ND-1 spectrometer in JRR-2. For the quasi-elastic scattering study, incident neutrons of 41 meV were used. For the Bragg scattering measurements, 13.7 meV neutrons were used. Fig.1 shows the observed quasi-elastic scattering demonstrating the existence of the reciprocal plane for one-dimensional chain. But the intensity is unexpectedly weak. As the quasi-elastic condition is poorly satisfied even for the use of 41 meV incident neutrons, no exact correlation function could be estimated but qualitatively, the width is broaden when the temperature is elevated to room temperature supporting the magnetic study. At $T < T_N$ = 13.3 K , which we found, a Bragg peak appears at (1/3,1/3,1), (2/3,2/3,1) etc. This suggests a magnetic structure shown in Fig.2. The temperature dependence of the Bargg scattering intensity is shown in Fig.3. Unexpectedly, the intensity reaches maximum at around 4 K and after that it decreases with further decreasing temperature. This decrease can be seen even down to 0.3 K. The Maximum intensity corresponds to about 40% of the full saturation moment. The authors suggest that the small moment and anomalous temperature change is related to a quantum effect accompanied by a frustration effect. Further detailed study is now in progress.

1) M. Niel, C.Cross, G.Le. Flem, M.Pouchard and P. Hagenmuller: Proc. of the Int. Conf. on Magnetism , ed. by P.F.de Chatel and J.J.M.France, North-Holland (1976)702

2) M. Steiner, J.M.Dance and M.Niel: Berichte aus der Arbeitsgrupe Neutronenstreuung, Hahn-Meitner Inst. B.332(1980)17

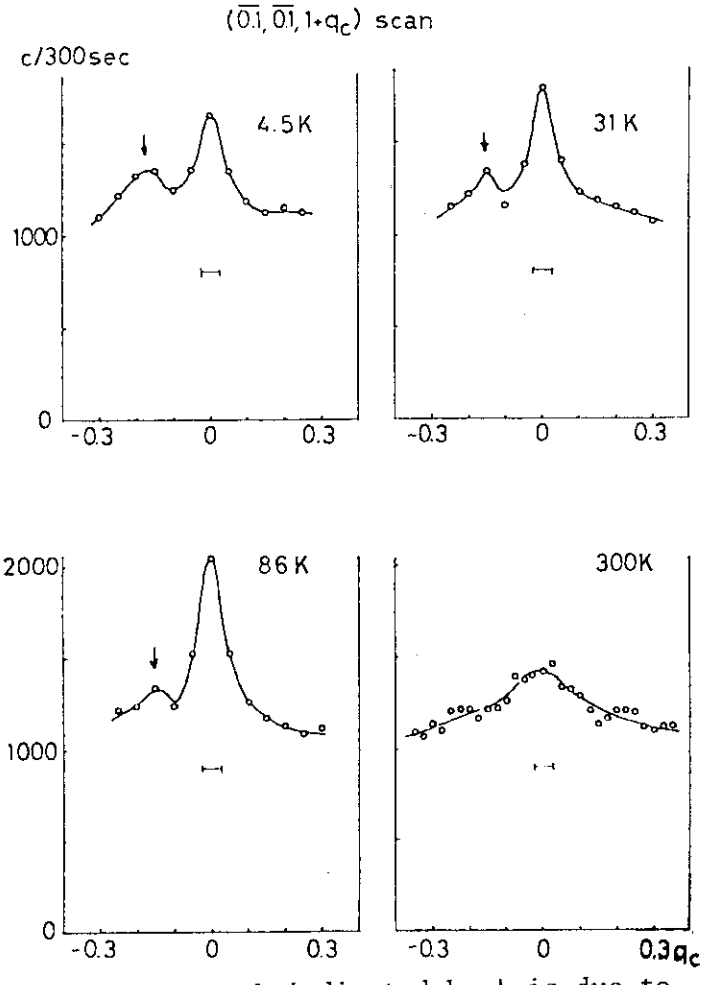

Fig.1. The peak indicated by ↓ is due to the Al holder.

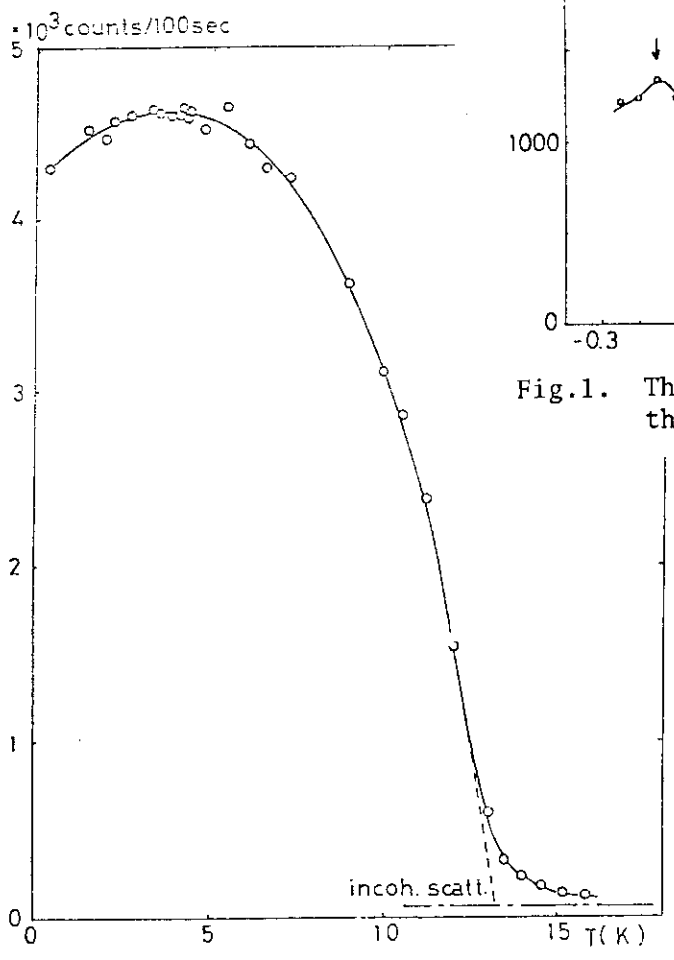

Fig.3.

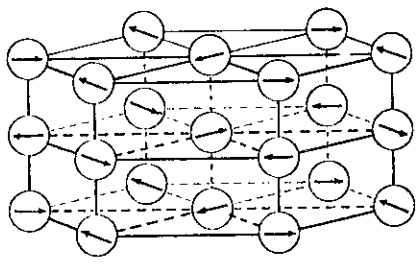

Fig.2.

III20 Incommensurate Magnetic Phase Transitions in the Triangular XY-like Antiferromagnet $RbFeCl_3$*

Nobuo Wada, Koji Ubukoshi* and Kinshiro Hirakawa*

Department of Physics, Faculty of Science, Hokkaido University

*Institute for Solid State Physics, University of Tokyo, Tokyo

The frustration in triangular lattice antiferromagnet is a topic of current theoretical and experimental interest. $RbFeCl_3$ with a hexagonal lattice consists of quasi-1D XY-like chains with strong ferromagnetic interactions. These chains are coupled with a weak interchain antiferromagnetic couling of about $J' = 0.5$ K.[1] The ground state is thought to be equivalent to a 2D lattice with classical spins which are coupled by an antiferromagnetic interaction with XY-like symmetry, the c-plane being an easy plane. In fact Davison et al[2] have shown that the moment lying in the c-plane are coupled at 120° to each other at 1.86 K. On the otherhand, Haseda et al[3] have shown that the transitions occur at $T_{N1} = 1.95$ K, $T_{N2} = 2.25$ K and $T_{N3} = 2.6$ K through their heat capacity measurement.

This work started in order to clearify above complicated transition by neutron scattering measurements. A single crystal of about 1 cc with the mosaic spread of ~5' was used setting the [001] axis vertically using ISSP ND-1 spectrometer installed in JRR-2. The results obtained are as follows;

$T < T_{N1}$

The magnetic peaks were observed at (1/3,1/3,0), (2/3,2/3,0), etc supporting the triangular spin arrangement (120 each other) proposed by Davison et al (Fig.1). On elevating temperature a discontinuous drop of intensity is observed at 1.95 K suggesting the 1st order transition in agreement with the heat capacity measurement[3].

$T_{N1} < T < T_{N2}$

At 1.95 K, the Bragg point splits into three peaks, one is at $(1/3-\delta_x, 1/3-\delta_x, 0)$ which is denoted by #1 type, δ_x being 0.008. Corresponding this, the (2/3,2/3,0) peak moves to $(2/3+\delta_x, 2/3+\delta_x, 0)$. The other peaks appears at $\pm\delta_y$ from the position of #1 peak in the direction normal to the x ([110]) axis. These peaks are denoted by #2.

They are shown in Fig.2 and 3. In this temperature range , only the central #1 peak decrease its intensity with increasing temperature and at T_{N2} = 2.32 K, it disappears.

At $T > T_{N2}$,

The #2 peaks loose the intensity gradually and at the same time the peak widths are broaden with increasing temperature as shown in Fig.4. No clear T_{N3} could be found.

Further details are now in progress.

As a conclusion , we suggest that such a very long period modification of the spin structure might be caused by the dipolar interactions. Recently Shiba has proposed a theory which can interpret quite well our observed data[4]. We are grateful to Professor Shiba for very stimulating discussions.

1) H. Yoshizawa, W. Kozukue and K. Hirakawa; J. Phys. Soc. Japan 49 (1980)144

2) G.R.Davison,M.Eibshutz, D.E.Cox and V.J.Minkiewicz: A.I.P. Conf. Proc. 5(1971)436

3) T.Haseda, N. Wada, M. Hata and K. Amaya: Physica 108B(1981)841

4) H.Shiba: Tech. Rep. ISSP-SerA (1981)No.1184

* N. Wada, K.Ubukoshi and K.Hirakawa: Tech. Rep. ISSP Ser.A (1981)1180

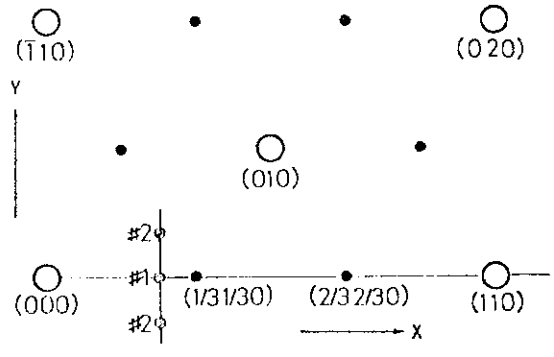

Fig. 1

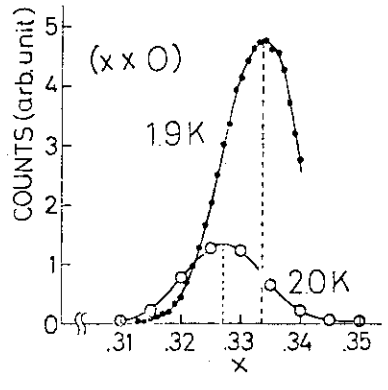

Fig. 2

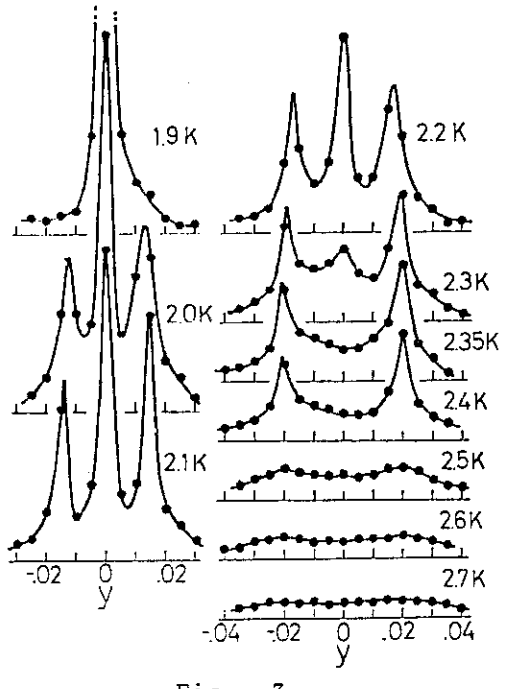

Fig. 3

III21 Neutron Scattering Study of One-Dimensional XY Antiferromagnet Cs_2CoCl_4

Kinshiro Hirakawa and Koji Ubukoshi

Institute for Solid State Physics, University of Tokyo, Roppongi, Minato-ku, Tokyo,

According to the heat capacity measurement by Algra et al[1], Cs_2CoCl_4 is one of the most promising candidates of realistic one-dimensional(1D) XY antiferromagnets. The crystal is orthorhombic K_2SO_4 (or Cs_2ZnCl_4) structure with a = 9.74Å, b = 7.39Å and c = 12.97Å. The magnetic specific heat has a maximum at 0.9 K, whereas T_N = 0.222K. From the analysis of their data, they suggested that the system can be well described by the S = 1/2, 1D XY antiferromagnet with $J_\perp$ = 1.35 K and $J_\perp/J_\parallel \sim 4$. From the consideration of the atomic arrangements, they suggested that the chain axis might be parallel to the b-axis.

In order to ascertain above conjectures, we performed neutron scattering experiments at JRR-2, Tokai. Big single crystal of about 5cc was made from the melt of the mixture of 2CsCl and $CoCl_2$. The sample was cut out from the ingot and set in a sorption type ^3He cryostat newly instoled. Fig 1 shows the crystal structure and the magnetic lattice is extracted from the figure and shown in the attatched figure. We performed several quasi elastic scans as shown by the arrows indicated in Fig.2 using the incident neutron energy of 13.7 meV at temperatures both 1.45 K and 0.3 K. As shown in an example in Fig.3, no peak structure could be observed at 1.45 K, but at 0.3 K we could find clear 1D-like intensity plates which pass through (0 0 0.5), (0 0 1.5), etc. We thus confirmed that Cs_2CoCl_4 is at least 1D antiferromagnet whose chain axis is parallel to the b-axis. Further detailed studies are now in progress at BNL in USA.

We wish to express our hearty thanks to Professor L.J. de Jongh who interested us to study this compound.

1) H.A.Algra, L.J. de Jongh, H.W. Blöte, W.J.Huiskamp and R.L. Carlin, Physica 82B(1976)239

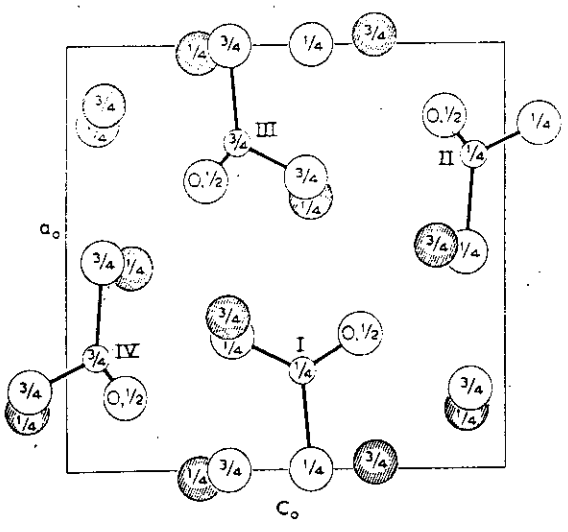

Fig. 1. Projection of the unit cell of Cs_2ZnCl_4 along the *b* axis. The Zn and Cl atoms are represented by the small and large open circles, respectively. Shaded circles denote the Cs atoms. Heights of the atoms above the plane are indicated.

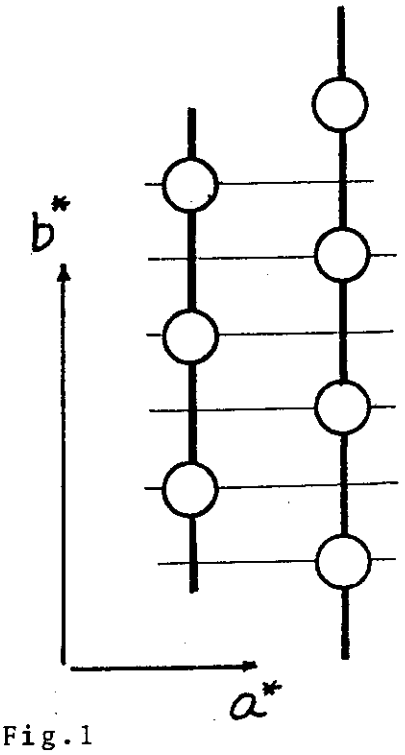

Fig.1

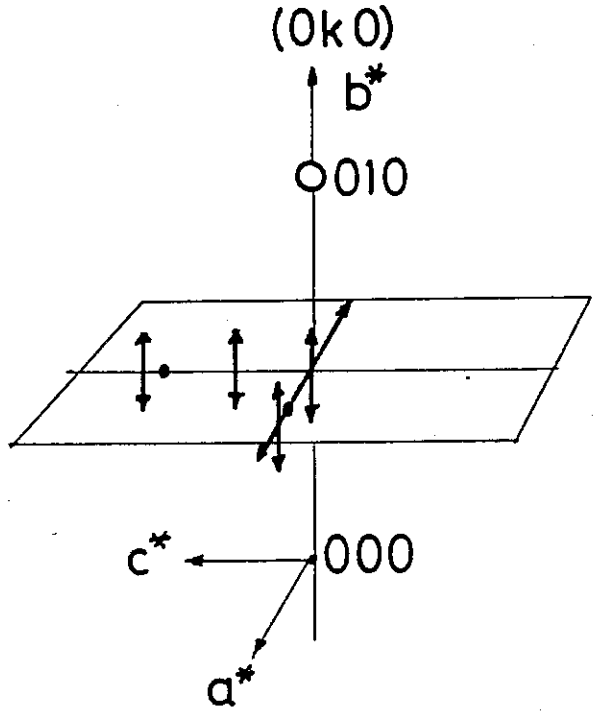

Fig.2

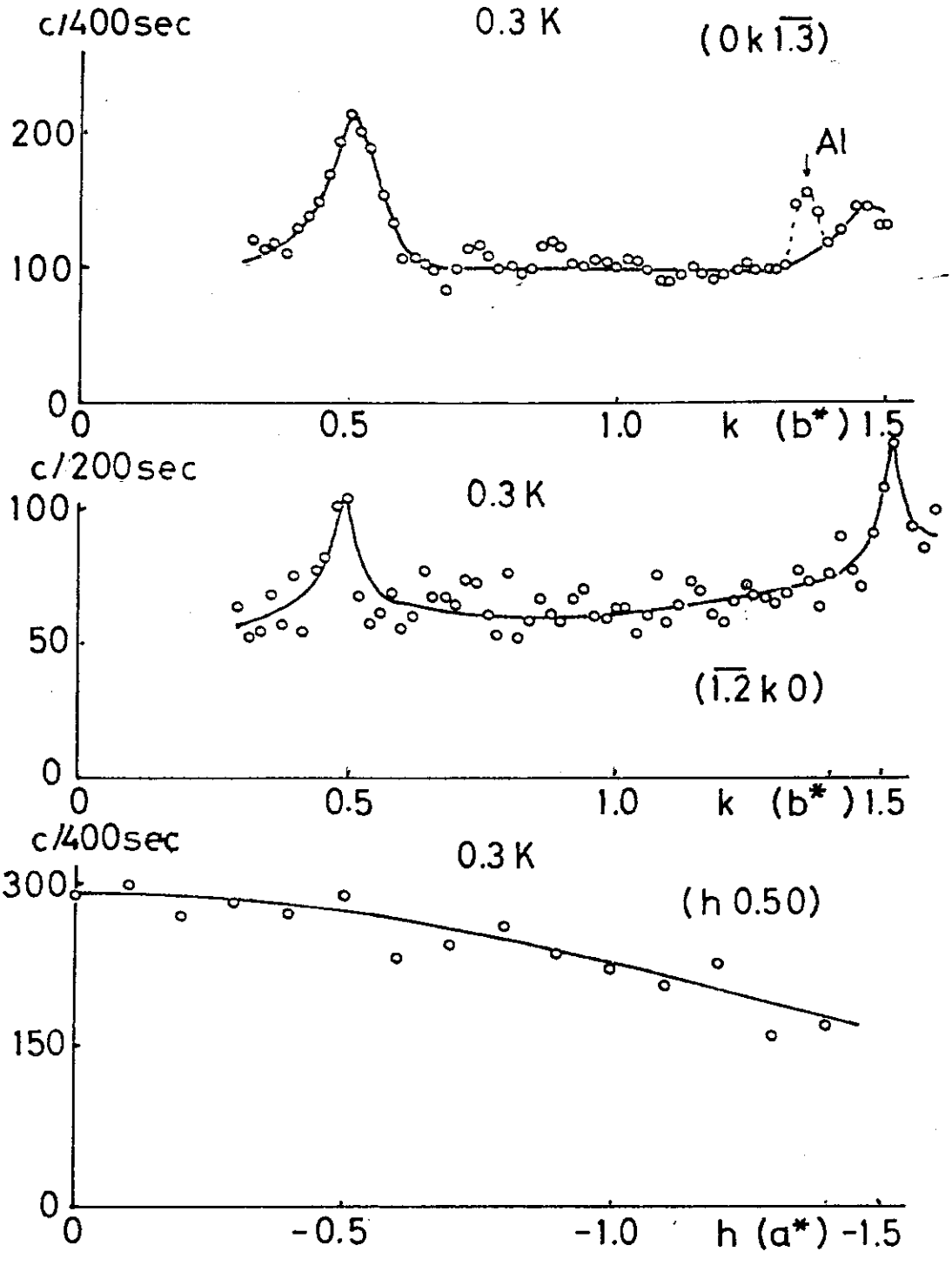
c/400sec
0.3 K
(0 k $\bar{1}$.3)
200
100
0
Al
0
0.5
1.0
k (b*) 1.5
c/200sec
0.3 K
100
50
0
($\bar{1}$.2 k 0)
0
0.5
1.0
k (b*) 1.5
c/400sec
0.3 K
300
150
0
(h 0.50)
0
-0.5
-1.0
h (a*) -1.5

Fig.3

III22 Sharp Phase Transition in Two-Dimensional Dilute Antiferromagnets $Rb_2Co_cMg_{1-c}F_4$

Hironobu Ikeda

Department of Physics, Ochanomizu University, Ohtsuka, Bunkyo-ku, Tokyo 112

Neutron elastic and quasi-elastic scattering have been measured in homogeneously-mixed two-dimensional dilute antiferromagnets $Rb_2Co_cMg_{1-c}F_4$. The result gives a first observation of sharp phase transition at the Neel temperature irrespective of magnetic concentration c even near the percolation threshold. The magnetic correlation length near the Neel temperature increases as the concentration of magnetic Co ions decreases.

III23 Phase Transition in Two-Dimensional Random Antiferromagnets $Rb_2Co_cNi_{1-c}F_4$

Hironobu Ikeda, Tomoko Abe and Ichiro Hatta*

Department of Physics, Ochanomizu University,Bunkyo-ku, Tokyo 112,
*Department of Applied Physics, Nagoya University,Chikusa-ku, Nagoya 464

Neutron scattering and specific heat capacity measurements were made on a two-dimensional randomly-mixed antiferromagnets $Rb_2Co_cNi_{1-c}F_4$. The experimental results show sharp phase transition which has not been ever found in the random magnetic systems. This gives an answer to a long-lived question whether or not a sharp phase transition occurs in a homogeneously random magnetic system. The critical exponents α, β, ν and γ of $Rb_2Co_cNi_{1-c}F_4$ is identical with those of two-dimensional Ising model.

III24 Mössbauer and Neutron Diffraction Studies of Competing Magnetic Orderings in Random Mixtures : $Co_{1-x}Fe_xTiO_3$

Atsuko Ito*, Setsu Morimoto*, Yoshiko Someya*, Hironobu Ikeda*
Yasuhiko Syono** and Humihiko Takei**

*Department of Physics, Faculty of Science, Ochanomizu University, **The Research Institute for Iron, Steel and Other Metals, Tohoku University.

A great deal of interest has recently been taken in random mixtures of two antiferromagnets with orthogonal spin anisotropies, because the mixtures are expected to show the characteristic phase transitions.

We investigated the mixture $Co_{1-x}Fe_xTiO_3$ by means of neutron diffraction and Mössbauer measurements. Information from neutron diffraction measurement and from Mössbauer measurement has been shown to be complementary to each other.[1] Therefore, application of both of the techniques to the same specimen is very useful for clarifying the properties of the mixture. In Fig.1 we show one of temperature variations of the scattering intensities of neutrons for $Co_{0.37}Fe_{0.63}TiO_3$ at the

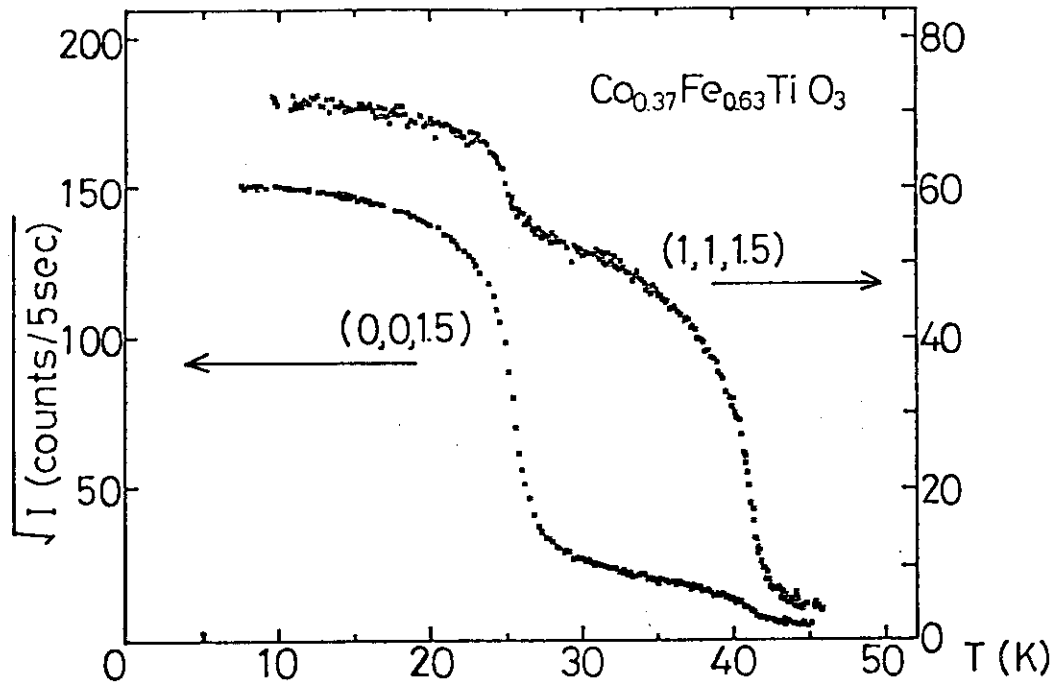

Fig.1 Temperature variation of the square root of the magnetic scattering intensities, $\sqrt{I}$.

(0,0,1.5) and (1,1,1.5) magnetic reciprocal-lattice positions.* The scattering at (1,1,1.5) appears at a temperature of 42 K and inceases rapidly. On the other hand, rapid increase of the scattering at (0,0,1.5) is seen when the temperature decreases down to 27 K, which is also reflected on the intensity at (1,1,1.5). These facts show that a long-range order of the spin component $S_{//}$ is established at 42 K, which means that the Néel temperature (T_N) of $Co_{1-x}Fe_xTiO_3$ is 42 K. On the other hand, a long-range order of the spin components $\vec{S}_{\perp}$ is considered to start at 27 K. We take this temperature as T_L which determines the lower boundary of the AF phase and below which the mixed ordering phase or the OAF phase is considered to be realized. The concentration (x) vs. temperature(T) phase diagram determined by the neutron diffraction study is shown in Fig.2, on which the T_N determined by the Mössbauer measurement is also shown.

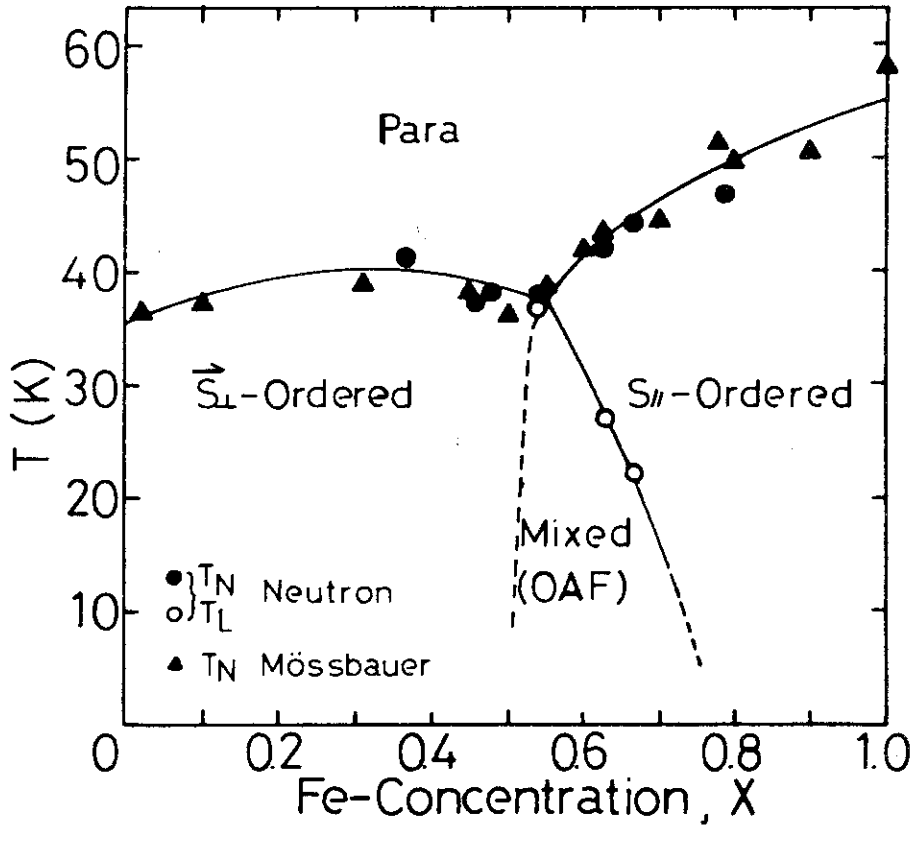

Fig.2 Concentration vs. transition temperature phase diagram of $Co_{1-x}Fe_xTiO_3$

Although according to the neutron diffraction experiment the lower transition temperature T_L is shown to exist (see Fig.1), any remarkable change of the Mössbauer spectra is not seen near T_L. The Mössbauer results show that the Fe spin is tilted even in the AF phase as well as in the OAF phase. This fact means that the orthogonal spin components are not completely decoupled with each other in the AF phase at least in a time scale of the Mössbauer measurement contrary to the theoretical predictions.[2] The details are reported in reference 3.

* The reflections are indexed in the chemical hexagonal cell.

References

1) A.Ito, Y.Someya and K.Katsumata : Solid State Commun. 36 (1980) 681

2) S.Fishman and A.Aharony : Phys.Rev. B18 (1978) 3507, and references therein. F.Matsubara and S.Inawashiro : J.Phys. Soc.Jpn. 42 (1977) 1529

3) A.Ito, S.Morimoto, Y.Someya, H.Ikeda, y.Syono and H.Takei : to be published in Solid State Commun.

III25 Mössbauer and Neutron Diffraction Studies of Competing Magnetic Orderings in Random Mixtures : $Ni_{1-x}Fe_xCl_2$

Atsuko Ito, Toyomi Tamaki, Yoshiko Someya and Hironobu Ikeda

Department of Physics, Faculty of Science, Ochanomizu University

Random mixtures of two antiferromagnets with competing spin anisotropies have received considerable attention because of their characteristic magnetic structures. On the concentration(x) vs. temperature(T) phase diagram, two smooth lines are crossed with each other at a point located in an intermediate concentration region ; accordingly there exist three ordered phases : the two AF phases and the OAF phase. The location of the OAF phase depends on a balance of the anisotropies of the two kinds of relevant magnetic ions.

We gave investigated the mixture $Ni_{1-x}Fe_xCl_2$ by means of neutron diffraction and Mössbauer techniques. In the mixture $Ni_{1-x}Fe_xCl_2$, the anisotropy of Ni ions ($\perp c$) is much weaker than that of Fe ions ($/\!/ c$). Therefore, the OAF phase is expected to appear at around a small value of x ; experimentally the OAF phase appears in a narrow range of concentration around x=0.05. In this case, the information from neutron diffraction study in the concentration region which we are interested in is almost completely concerned with the ordering of Ni spins. This is very helpful in order to investigate the behavior of one kind of magnetic ions separately. It should be noted here that, on the other hand, Mössbauer measurements give the information only from Fe spins, as well known.

One of the preliminary results of the neutron diffraction study is shown in Fig.1, which is obtained for the sample $Ni_{0.96}Fe_{0.04}Cl_2$. The scattering intensity at the (0,0,3) magnetic reciprocal-lataice position* represents the component of the sublattice magnetization $|M_\perp|^2$. As seen in the figure, the scattering intensity appears at 51 K showing the onset of a long-range order of the spin component of $\vec{S}_\perp$. We should emphasize here that, although the intensity increases rapidly at first, but it attains to the maximum around 37 K, and then

decreases gradually. This fact means that the spin component of $\vec{S}_{\perp}$ falls to decreasing below a certain temperature. On the other hand, the spin component of $S_{//}$ is observed to increase almost linearly down to 4.2 K without showing any saturation. This is considered to be closely related to the decrease of the component $\vec{S}_{\perp}$ at low temperatures. Taking into the temperature variations of the components $S_{//}$ and $\vec{S}_{\perp}$, it is certain that the increase of the component $S_{//}$ at low temperatures is attained at the expense of the decrease of the component $\vec{S}_{\perp}$. It is the first time that this kind of phenomenon is observed in the mixtures. Details are in preparation for publication.

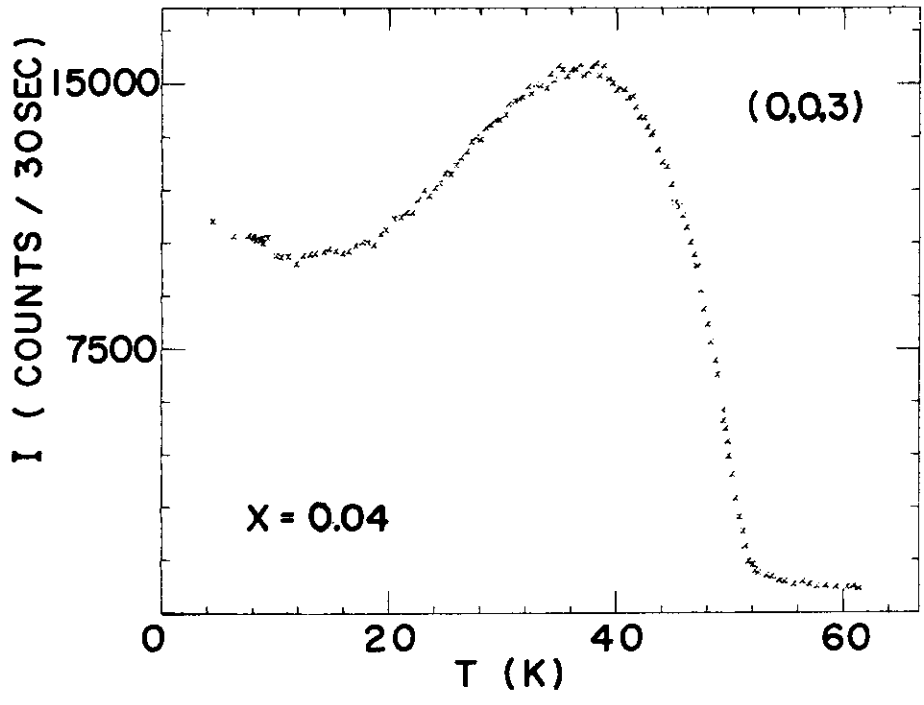

Fig. 1 Temperature variation of the magnetic scattering intensity, I

* The reflections are indexed in the double hexagonal cell in which the c-axis is twice of the chemical cell.

III26 Neutron Diffraction Experiment on $Fe_{(1-x)}Co_xCl_2$

Koichi Katsumata*, Tadahiro Tawaraya* and Hideki Yoshizawa**

*Research Institute of Applied Electricity, Hokkaido University, Sapporo 060, and **The Institute for Solid State Physics, The University of Tokyo, Roppongi, Minato-ku, Tokyo 106

Much theoretical and experimental studies have been done on randomly mixed magnets with competing spin anisotropies[1]. A new type of magnetically ordered phase, called a "mixed ordering phase" or an "oblique antiferromagnetic (OAF) phase" has been predicted theoretically to exist in the concentration versus transition temperature phase diagram. Experiments on $K_2Mn_{(1-x)}Fe_xF_4$(ref.2), $Fe_{(1-x)}Co_xCl_2\cdot 2H_2O$(ref.1), anhydrous $Fe_{(1-x)}Co_xCl_2$(ref.3) and on some other mixed crystals have indeed demonstrated the existence of the new phase, although the phase transition from the antiferromagnetic phase to the new phase is smeared in $Fe_{(1-x)}Co_xCl_2$(refs.3,4).
In the OAF phase, the directions of antiferromagnetically coupled spins are at an angle from the easy axes of the pure substances. We have made a neutron scattering measurement on a powdered sample of $Fe_{(1-x)}Co_xCl_2$, in order to obtain value of the tilting angle and magnitude of the sublattice moment in the new phase.

The experiment was carried out by using the ISSP spectrometer installed at JRR-3, JAERI, Tokai. The wavelength of the neutrons was 1.824A. The (111) reflection from a Ge-monochromator was used. The powdered sample used in the experiment was obtained by crushing a single crystal. The sizes of the grains were less than 500 μm.

In Fig.1 are shown the (003) and (10$\bar{1}$) magnetic reflections as well as the (006) nuclear one obtained in the x=0.315 sample.

In the following, we analyze the powder pattern, in the OAF model[5,6], to obtain value of the tilting angle and magnitude of the (mean) sublattice moment at T≃5.4K and x=0.315. We assume that the magnetic domains observed in the new phase

are arranged as in the case of pure $CoCl_2$, i.e., that there are three equivalent directions, which make the same angle ϕ with the c-axis, for the domains.

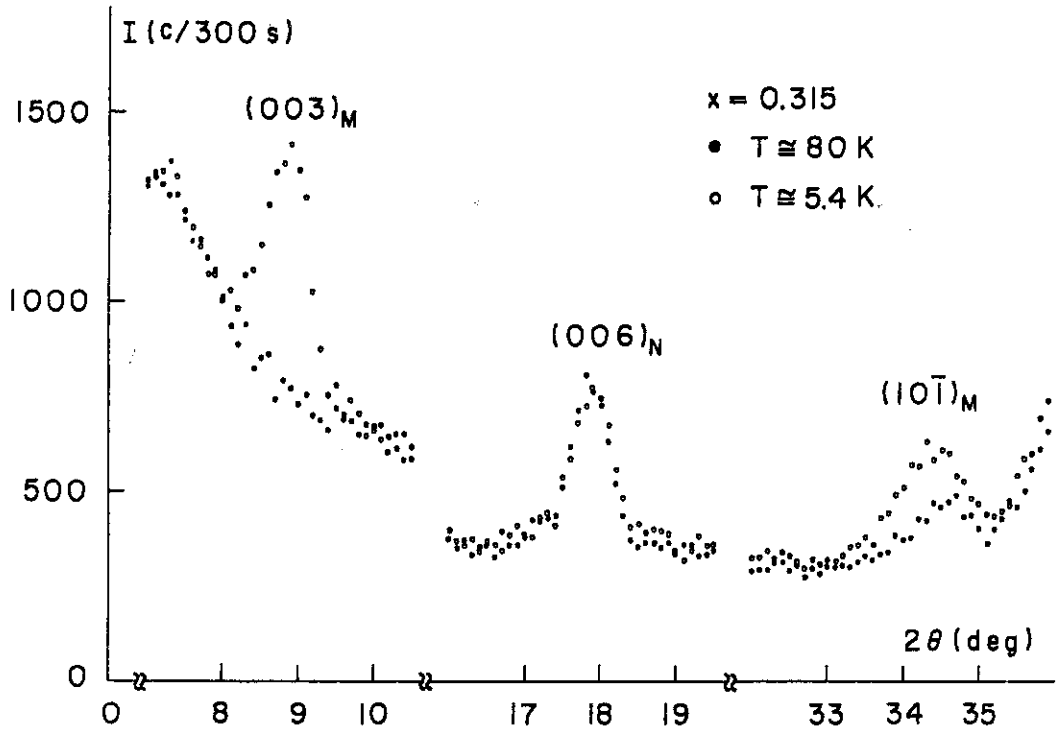

Fig.1. Powder diffraction patterns for the x=0.315 sample obtained in the OAF phase(T≃5.4K) and in the paramagnetic phase(T≃80K).

The calculated intensity ratio of the (003) reflection to the (10$\bar{1}$) one is,

$$I_{003}/I_{10\bar{1}}=\{|f(\theta_{003})|^2 J_{003}L(\theta_{003})\cdot\sin^2\phi\}/\{|f(\theta_{10\bar{1}})|^2 J_{10\bar{1}}L(\theta_{10\bar{1}}) \times(0.504\ \sin^2\phi + 0.992\ \cos^2\phi)\}, \quad (1)$$

where $f(\theta)$ is the magnetic form factor, J the multiplicity and $L(\theta)$ the Lorentz factor. In this analysis we have used the magnetic form factor of the mixture which is given by a sum of the magnetic form factors of Fe^{3+} and Co^{2+} with the respective

fractions multiplied. By comparing the observed ratio of $I_{003}/I_{10\bar{1}}=2.59$ with eq.(1), we have $\phi=33°\pm5°$. Then we obtain, from the intensity ratio of the (006) nuclear reflection to the (003) and (10$\bar{1}$) magnetic ones, magnitude of the (mean) sublattice moment to be, $\mu=4.4\pm0.5\mu_B$/atom. The magnitudes of the moments in the pure substances have been determined to be[7] $4.5\mu_B(//c)$ and $3.0\mu_B(\perp c)$ for $FeCl_2$ and $CoCl_2$, respectively. Although we cannot determine, in the present study, the magnitudes and the directions of Fe and Co spins separately, the values obtained above may be reasonable ones in the OAF model.

The authors wish to express their thanks to Prof.K.Hirakawa for his many helpful discussions and encouragements. Thanks are also due to Dr.Y.Tsunoda for his many helpful discussions and advices.

References

1) For details, see the references cited in, K.Katsumata, M.Kobayashi, T.Satō and Y.Miyako: Phys. Rev. B19(1979)2700.
2) L.Bevaart, E.Frikkee, J.V.Lebesque and L.J.de Jongh: Solid State Commun. 25(1978)539.
3) T.Tawaraya and K.Katsumata: Solid State Commun. 32(1979)337.
4) Po-zen Wong, P.M.Horn, R.J.Birgeneau, C.R.Safinya and G.Shirane: Phys. Rev. Lett. 45(1980)1974.
5) F.Matsubara and S.Inawashiro: J. Phys. Soc. Jpn. 42(1977) 1529.
6) T.Oguchi and T.Ishikawa: J. Phys. Soc. Jpn. 45(1978)1213.
7) M.K.Wilkinson, J.W.Cable, E.O.Wollan and W.C.Koehler: Phys. Rev. 113(1959)497.

III27 Neutron Scattering Experiment on $Rb_2Mn_{(1-x)}Cr_xCl_4$ Spin-glass

Koichi Katsumata*, Takashi Nire* and Hideki Yoshizawa**

*Research Institute of Applied Electricity, Hokkaido University, Sapporo 060, and **The Institute for Solid State Physics, The University of Tokyo, Roppongi, Minato-ku, Tokyo 106

There has been a growing interest in spin-glasses for the last decade. It seems now to be widely accepted that a competition between ferromagnetic and antiferromagnetic exchange interactions plays an essential role in determining spin-glass properties. As the competition occurs not only in the case of the long-range Ruderman-Kittel-Kasuya-Yosida interaction but in near-neighbor exchange interactions, we expect that a spin-glass state exists in insulators where the short-range interaction dominates. In spite of many theoretical efforts[1-4], there has been no experimental finding of a spin-glass in a randomly mixed insulating ferromagnet and antiferromagnet. We have found that a randomly mixed insulating ferromagnet (Rb_2CrCl_4) and antiferromagnet (Rb_2MnCl_4), exhibits spin-glass behavior[5]. The mixed crystals with the intermediate concentrations ($0.38 \leq x \leq 0.58$) show a cusp in the temperature dependence of the susceptibility. In order to examine further whether this compound is a spin-glass or not, we have performed a neutron diffraction experiment. If this mixture is a spin-glass, magnetic long-range orderings should be absent.

The neutron experiment was carried out on the triple-axis spectrometer of the ISSP which is installed at JRR-2, JAERI, Tokai. The monochromator was pyrolytic graphite and the wavelength of the neutrons was 2.44Å. The powdered sample used in the experiment was obtained by crushing single crystals. The sizes of the grains were less than 500μm.

Figure 1(a) shows clearly that there is no antiferromagnetic long-range order in the x=0.58 sample at T≃7K.
For comparison, we have plotted in Fig.1(b) the result for the

x=0.21 sample, which is antiferromagnetic below about 30K. The reflections in Fig.1 are indexed based on the K_2NiF_4-type magnetic unit cell. To check the absence of ferromagnetic long-range order, we also measured temperature dependence of the intensity of the (111) nuclear reflection in the x=0.58 sample ($T_{SG}\simeq 11K$).

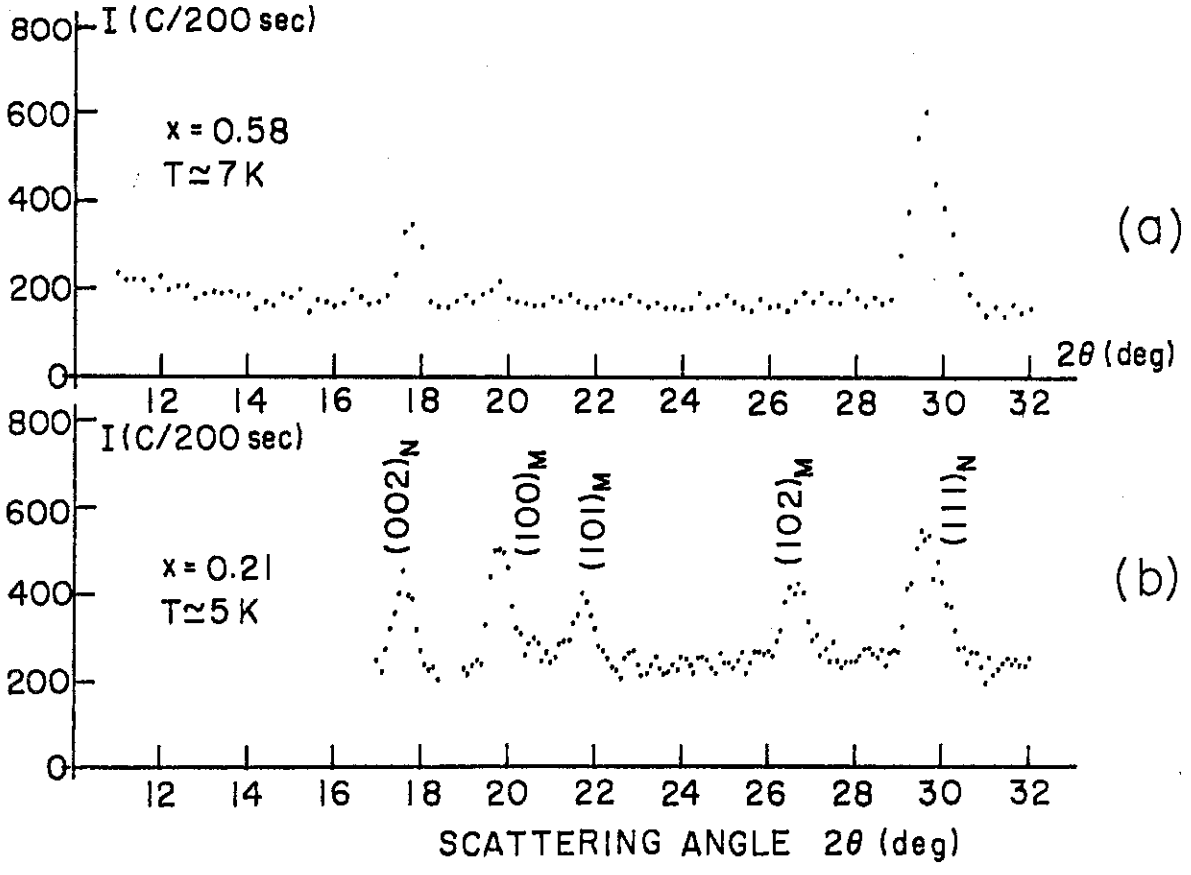

Fig.1. Neutron diffraction patterns for powdered $Rb_2Mn_{(1-x)}Cr_xCl_4$ (a) in the spin-glass and (b) in the antiferromagnetic states.

The intensity was temperature independent between 8K and 50K within the experimental scatter. Thus, the mixture with x=0.58 exhibits neither antiferromagnetic nor ferromagnetic long-range ordering below T_{SG}.

We have confirmed further that $Rb_2Mn_{(1-x)}Cr_xCl_4$ is a spin-glass, from electron spin resonance (ESR) experiment[5]. The frequency versus magnetic field relation of the resonance points in the x=0.38 and x=0.58 samples observed at T=4.2K is very similar to that observed in a metallic spin-glass CuMn[6,7].

From the susceptibility[5], neutron diffraction and ESR experiments, it becomes clear that a randomly mixed insulating ferromagnet and antiferromagnet, $Rb_2Mn_{(1-x)}Cr_xCl_4$ is a new type of spin-glass, the origin of which is different from those found in metals and in the diluted ferromagnet, $Eu_xSr_{(1-x)}S$(ref.8).

We would like to express our sincere thanks to Prof. K. Hirakawa for his many helpful discussions and encouragements.

References

1) F.Matsubara: Prog. Theor. Phys. 52(1974)1124.
2) M.V.Medvedev and E.L.Rumyantsev: Phys. Status Solidi B85 (1978)427.
3) T.Oguchi and Y.Ueno: J. Phys. Soc. Jpn. 46(1979)729.
4) S.Fishman and A.Aharony: Phys. Rev. B19(1979)3776;21(1980) 280.
5) K.Katsumata, T.Nire, M.Tanimoto and H.Yoshizawa: Phys. Rev. B24(1981)No.11.
6) J.Owen, M.E.Browne, V.Arp and A.F.Kip: J. Phys. Chem. Solids 2(1957)85.
7) K.Okuda and M.Date: J. Phys. Soc. Jpn. 27(1969)839.
8) H.Maletta and W.Felsch: Phys. Rev. B20(1979)1245.

IV1 Study of Forbidden Magnon Scattering in an Invar Alloy Fe_3Pt

Masahumi Kohgi*,Kiyoichiro Motoya**,Yoshikazu Ishikawa*

*Department of Physics,Tohoku University, **Institute for Solid State Physics,the University of Tokyo.

It has been shown that the decrease of the magnetization of the invar alloys,$Fe_{65}Ni_{35}$ and Fe_3Pt,with increasing temperature is much faster than the calculated by the spin wave theory using the spin wave stiffness constants obtained by neutron scattering. The spin wave excitations also exhit abnormally large damping[1]. One possible model to explain these anomalies is to postulate the presence of regions whose local magnetization axes slowly fluctuate around the bulk magnetization axis even at the low temperatures (this kind of model is originally proposed for the existence of well defined spin wave excitations near and above T_c in the metallic ferromagnets,Fe and Ni,by several authers[2]). If this picture is true,one can observe the forbidden neutron magnon scattering (magnon annihilation/creation scattering for neutrons polarized parallel/antiparallel to both of magnetization and scattering vector) [3]. In order to check this model,we performed magnon scattering experiments on Fe_3Pt using polarized neutrons.

The neutron scattering experiments were caried out on the polarized neutron spectrometer PANSI of ISSP at JRR2. The polarized neutrons were obtained by a Cu_2MnAl monochromater. The incident neutrons were selected to be 30 or 40 meV. The sample was a cylindrical single crystal (1 cm in diameter and 3 cm in length). In order to see the depolarization of neutrons by the sample,we measured the magnetic field dependence of the polarization of the direct beam transmitted through the sample at room temperature using a Cu_2MnAl analyzer. The magnetic field was applied perpendicular to the incident beam in the horizontal plane. The result is shown in Fig.1 by a solid line. As the flipping ratio without sample is about 15,the observed value is too small even at the highest magnetic field. This means that about 80% of the incident neutrons are depolarized by transmission at 11.4 Koe. This is probably because of the insufficiency of the saturation of the sample. We also measured the spin wave scattering from this sample by polarizing the neutrons parallel to the scattering vector. In Fig.1 is also plotted by open circles the ratio of the magnon annihilation scattering

intensity at Q=(0.94,0.94,0.94) and $\hbar\omega \sim -1.5$ meV at room temperature for the neutron spin flipper off (I_+) to that for flipper on (I_-),against applied magnetic field. It can be seen from the figure that the flipping ratio of the magnon scattering intensities coincide roughly with that of the transmitted neutrons. We also measured the temperature dependence of the flipping ratio of the magnon scattering at H = 11.4 Koe,and found that there is no appreciable change up to the Curie temperature (T_c=435K). Therefore we can conclude that the low flipping ratio of the magnon scattering observed in our experiments come from the depolarization of the incident neutrons and that the forbidden scattering might be small up to near the Curie temperature. The fraction of the forbidden scattering, $I_-/(I_+ + I_-)$,at room temperature is estimated to be less than about 0.1, if any,assuming that the incident neutrons has the same polarization as the transmitted beam just before scattering. Therefore the above model seems not to be realized in Fe_3Pt. The experiments in higher magnetic field will soon be performed.

References

1) S.Onodera,Y.Ishikawa and K.Tajima: J.Phys.Soc.Jpn.,50(1981)1513.
2) for example,V.E.Korenman,J.L.Murray and R.E.Prange: Phys.Rev.,B16(1977) 4032,4048,4058.
3) J.B.Sokoloff,C.H.Perry,R.D.Lowde,F.Soffge,V.Wagner and M.C.K.Willshire: J.Appl.Phys.,50(1979)1961.

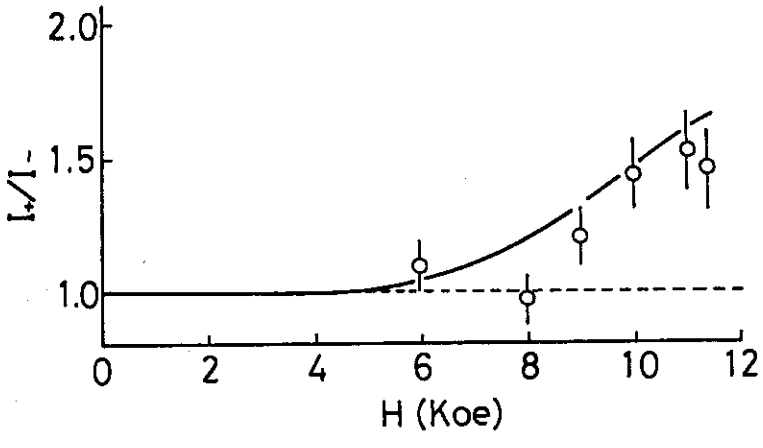

Fig.1. Magnetic field dependence of the flipping ratio of the direct beam transmitted through the sample (solid line) and of the magnon scattering at Q=(0.94,0.94,0.94) (open circles),at room temperature.

IV2 Spin Wave Stiffness Constant of Laves Phase Invar Compound $(Zr_{0.7}Nb_{0.3})Fe_2$

Shigehumi Onodera,* Yoshikazu Ishikawa,** Masayuki Shiga*** and Ze Xianyu**

*Sendai Radio Technical College, **Department of Physics, Tohoku University
***Department of Metal Science and Technology, Kyoto University

A few characteristic properties, which are common in invar alloys independent of atomic order, atomic disorder, crystalline and noncrystalline, have been found by inelastic neutron scattering and magnetization measurement.[1,2,3,4] One of these properties is that the spin wave stiffness constants(D_N) of various invar alloys determine by inelastic neutron scattering are larger than the spin wave stiffness constants(D_M) deduced from magnetization measurement. In other words, the temperature decrease of the magnetization of invar alloys cannot be explained only by the spin wave excitations. We must assume the exsistence of other magnetic excitations to explain the discrepancy between D_N and D_M. This characteristic property is very imprtant to understand the origin of invar effect, because the invar effect is induced by the special type of magnetic excitations which is accompanied by large positive volume magnetostriction. It is therefore quite interesting to know whether a qualitative relation exsists between 'the difference between D_N and D_M' and 'the large spontaneous volume magnetostriction' or not. In order to investigate this problem, it is necessary to measure the spin wave stiffness constants(D_N and D_M) and spontaneous volume magnetostriction of many invar alloys extensively.

$(Zr_{0.7}Nb_{0.3})Fe_2$ is a cubic Laves phase($MgCu_2$ type) compound which shows a large positive volume magnetostriction. It becomes ferromagnetic below 382°K(Curie temperature).[5] The polycrystalline sample was used for both of spin wave scattering experiment and magnetization measurement. The experiments of spin wave scattering were performed on a triple axis spectrometer of Tohoku University (TUNS) installed at JRR-2 in JAERI. The incident neutron energy was fixed to be 14.8 meV . Measurements corresponding to momentum transfer of $q=0.08A^{-1}$ and $0.1A^{-1}$ were made around the (0,0,0) reciprocal lattice point using the constant Q mode of operation. The horizontal collimation was 30"-10"-10"-30".

The observed scattering profiles at various temperatures are shown by open circles in Fig.1. At room temperature a well defined magnon groups could not be observed in the allowed energy range with E_i=14.8meV. However the magnon like hump appears at high tempertures where D_N becomes small as shown in lower spectra. The broken lines in this figure were calculated by convoluting the neutron scattering cross section of Lorentzian shape with the resolution function[6] of the specrometer, assuming the spin wave life time to be infinite. The spin wave stiffness constants(D_N) thus determined are shown in Fig.2 by closed squares. In the same figure ,the spin wave stiffness constants (D_M) estimated from magnetization measurements below 50°K as well as

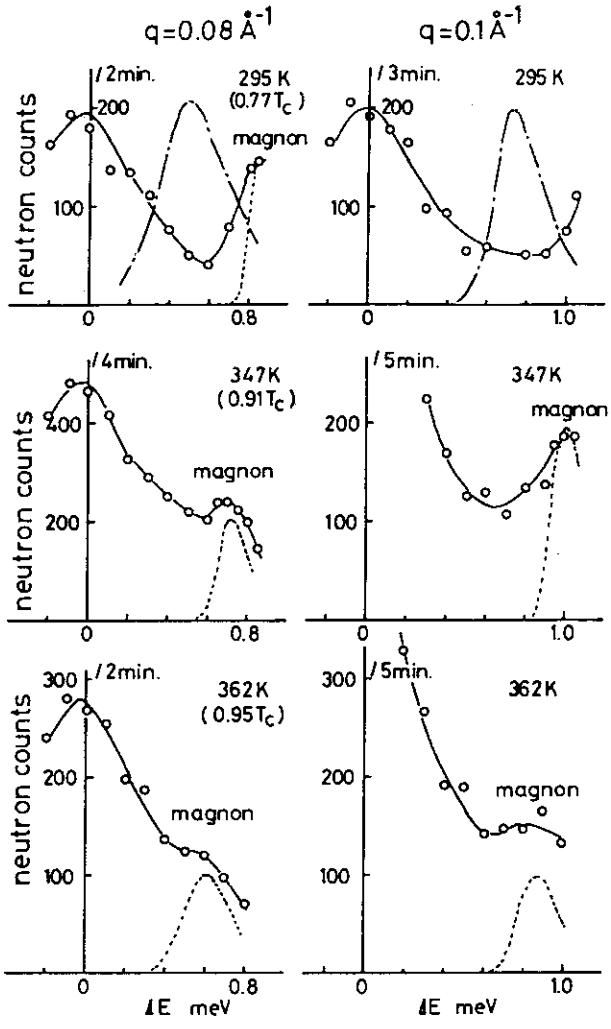

Fig.1. Spin wave spectra at various temperatures measured by constant Q mode of operation around (0,0,0). Circles are measured points. Broken lines are spin wave spectra with infinite life time calculated by taking into account the instrumental resolution. Solid lines are only for guide to eyes. Chain lines are spin wave spectra calculated assuming D_M to be 70 meVA^2.

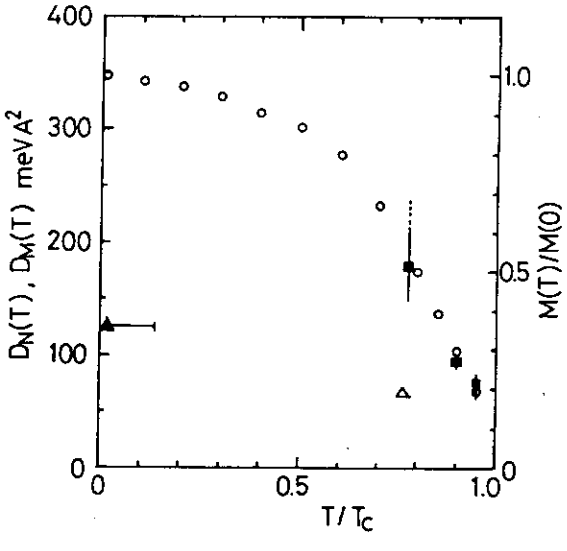

Fig.2. Spin wave stiffness constants (D_N,D_M) and magnetization of Laves phase $(Zr_{0.7}Nb_{0.3})Fe_2$. Open circles are magnetization. Closed squares show the spin wave stiffness constants(D_N) determined by neutron scattering. Closed triangle is spin wave stiffness constant deduced from magnetization measurement. Open triangle is D_M estimated by the temperature dependence of magnetization.

temperature dependence of magnetization of $(Zr_{0.7}Nb_{0.3})Fe_2$ are plotted by closed triangle and open circles respectively. In order to compare D_N with D_M, the value of D_N below 50°K was estimated by extraporating D_N at high temperature data by using the temperature dependence of magnetization M(T) to be 350 ± 50 mevA^2. This value is significantly greater than the value 125 meVA^2 deduced from the magnetization measurement. By using a similar procedure, the value of D_N at room temperature can be estimated to be 70 meVA^2. In Fig.1 is also displayed by chain lines the calculated magnon groups with D=70 meVA^2. The figure shows clearly the magnon of this compound cannot have such a low stiffness constant even if the experimental error as well as the approximate procedure for estimation of $D_M(T)$ are taken into account.

In conclusion $(Zr_{0.7}Nb_{0.3})Fe_2$ has the spin wave stiffness constant D_N ($=350\pm50$ meVA^2 at 0 °K) three times larger than D_M($=125\pm10$ meVA^2) deduced from the magnetization measurement. This characteristic is entirely the same as those found in all other Invar materials (Fe_3Pt, $Fe_{65}Ni_{35}$, amorphous-$Fe_{86}B_{14}$, etc.).

References

1) Y.Ishikawa, S.Onodera and K.Tajima:J.Magn. & Magn. Mater. 10(1979) 183
2) S.Onodera, Y.Ishikawa and K.Tajima:J. Phys. Soc. Jpn. 50(1981) 1513
3) Y.Ishikawa, K.Yamada and K.Tajima and K.Fukamichi:J.Phys. Soc. Jpn. 50(1981) 1958
4) Y.Ishikawa, Z.Xianyu, S.Onodera, S.Ishio and M.Takahashi:Fourth International Conference on Rapidly Quenched Metals (Sendai) August,1981
5) M,Shiga and Y.Nakamura:J. Phys. Soc. Jpn. 47(1979) 1446
6) M.T. Cooper and R. Nathans:Acta Cryst. 23(1967) 357

IV3 Spin Dynamics in the Amorphous Ferromagnetic Alloy $Fe_{70}Cr_{10}P_{13}C_7$ with no Invar Effect

Ze Xianyu, Yoshikazu Ishikawa and Shigehumi Onodera*

Physics Department, Tohoku University, Sendai 980, *Sendai Radio Technical College, Miyagi, 989-31

In a previous paper discussing the spin dynamics of the amorphous invar ferromagnetic alloy $Fe_{86}B_{14}$,[1] we reported that this alloy exhibits anomalous spin dynamics which have commonly been found in the crystalline invar alloys $Fe_{65}Ni_{35}$ and Fe_3Pt;[2] well defined magnon groups were observed by neutron inelastic scattering at small wave vector q with the quadratic dispersion relations $\hbar\omega_q=E+D_sq^2$, but the spin wave stiffness constant D_S is much larger than that derived from the magnetization measurements D_M. The magnon linewidth Γ shows the quadratic wave vector dependence and it depends slightly on temperature, in quite contrast to the Heisenberg system where a relation $\Gamma\propto q^4T^2$ holds. From these results we have suggested that the origin of the invar effect is common in these materials, irrespective of atomic arrangement.

In order to give a further experimental support to this suggestion, we have studied the spin dynamics of another amorphous ferromagnet $Fe_{70}Cr_{10}P_{13}C_7$ which does not show the invar effect. The specimen in a ribbon form was prepared by rapid quenching technique. The sample about 10g in weight was encased in an aluminum tube and neutron scattering experiments were performed on the triple axis spectrometer of Tohoku University (TUNS) installed at JRR-2, Tokai. The incident neutrons with an energy of 14.8meV were employed and the beam collimation was chosen to be B'-10'-10'-30'. Examples of observed magnon spectra measured with constant Q mode of operation were shown in Figs. 1 and 2. The former represents the wave vector dependence at 100K, while the latter shows the temperature dependence for $q=0.14\text{Å}^{-1}$. Solid lines are calculated by convoluting the resolution function of Cooper and Nathans with the magnon scattering cross section with Lorentzian shape. The linewidth Γ determined is indicated in each spectrum. The pronounced peak at center ($\hbar\omega=0$) is incoherent elastic scattering presumably due to the disordering of Fe and Cr atoms. The spin wave dispersions obey a quadratic relation

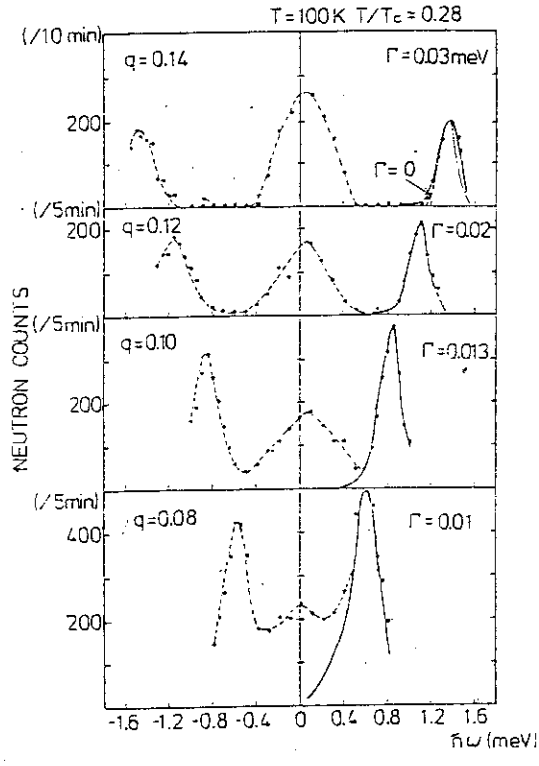

Fig. 1. Constant Q scans at several values of q at 100K. Background as well as incoherent elastic scattering were subtracted.

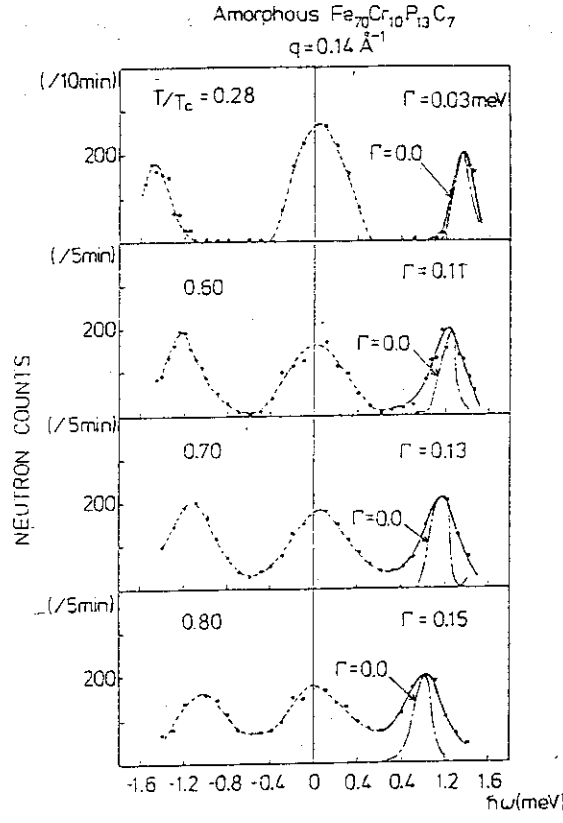

Fig. 2. Constant Q scans at $q=0.14\text{Å}^{-1}$ at several temperatures.

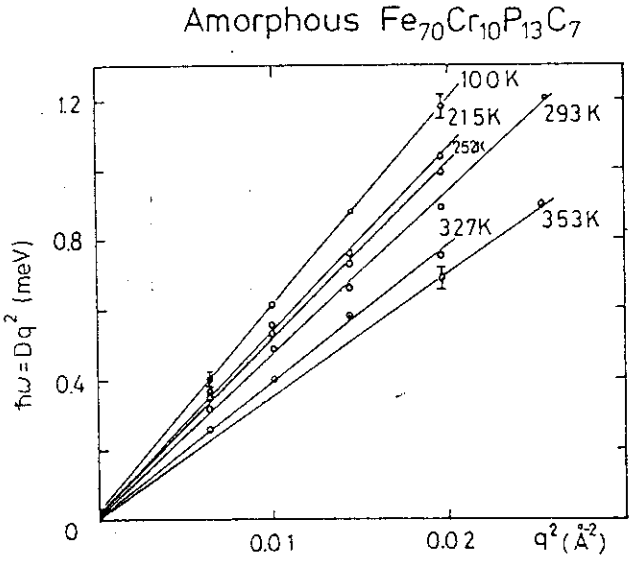

Fig. 3. Spin wave energies at different temperatures plotted against q^2.

$\hbar\omega_q = E(\tau) + D_s(\tau)q^2$ as displayed in Fig. 3 and the spin wave stiffness constants determined was found to vary with temperature T as $D_s(\tau) = D_s(0)(1+aT^{\frac{5}{2}})$. The $D_s(0)$ was determined to be $60\pm2\text{meV}\text{Å}^2$. In Fig. 4 the temperature dependence

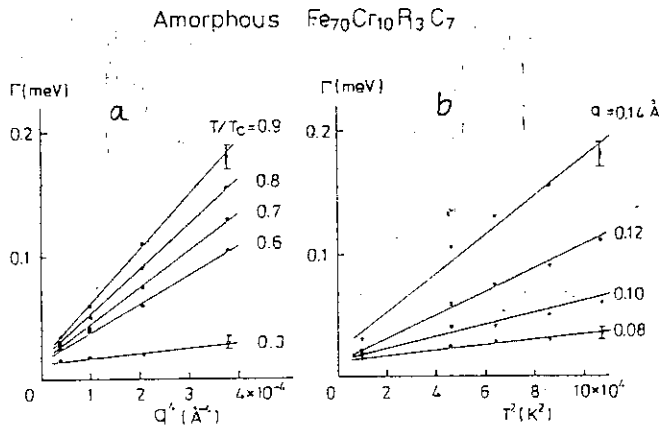

Fig. 4. (a) Spin wave linewidth Γ at different value pf T/T_c plotted against q^4. (b) Spin wave linewidth Γ at different wave vector q plotted against T^2.

of magnetization of the sample M(T) measured with a vibrating sample magnetometer was plotted against $T^{3/2}$. A linear relation holds at low temperatures as the spin wave theory predicted. The spin wave stiffness constant D_M derived from the slope of the $T^{3/2}$ dependence is 54.0meVÅ^2 which is rather close to D_S=60±2meVÅ^2. The chain line in the figure was calculated based on the spin wave theory with the magnon dispersions $\hbar\omega_q(T)$ experimentally determined. The agreement between the observation and calculation is reasonable, suggesting that the magnon excitation are the main origin of M(T). Futhermore we also found that the magnon linewidth Γ nearly obeys the relation $\Gamma \propto q^4 T^2$ as shown in Fig. 5, in sharp contrast to the amorphous invar alloy $Fe_{86}B_{14}$.

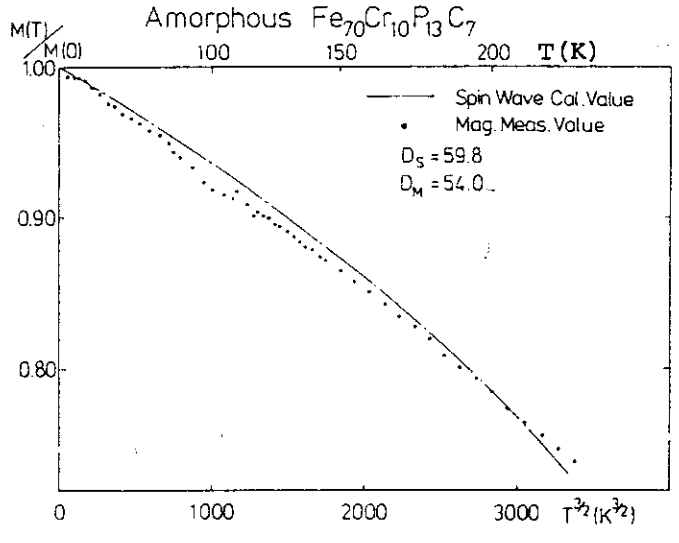

Fig. 5. Temperature dependence of magnetization plotted against $T^{3/2}$.

In conclusion we found that the amorphous ferromagnet $Fe_{70}Cr_{10}P_{13}C_7$ exhibits the normal spin dynamics which are expected for the Heisenberg system. This is consistent with the case for amorphous ferromagnets $(Fe_xNi_{1-x})_{75}P_{16}B_6Al_3$ which show no invar effect and normal spin dynamics.[3)]

Therefore we can conclude that the anomalous spin dynamics ($D_S \neq D_M$) often found in some amorphous ferromagnets are not due to the amorphous structure but to the invar properties.

References

1) Y. Ishikawa, K. Yamada, K. Tajima and K. Fukamichi: J. Phys. Soc. Jpn. 50(1981) 1958.

2) Y. Ishikawa, S. Onodera and K. Tajima: J. Magn. & Magn. Mater. 10(1979) 183; S. Onodera, Y. Ishikawa and K. Tajima: J. Phys. Soc. Jpn. 50(1981) 1513.

3) Y. Ishikawa. Z. Xianyu, S. Onodera, S. Ishio and M. Takahashi: Conf. Proc. of RQ4(August, 1981, Sendai) to be published.

IV4 Spin-Wave Dispersion Relations in Mn_2Sb Doped with Cr and Fe

Satoru FUNAHASHI

Physics Division, Japan Atomic Energy Research Institute

Exchange interaction between tetragonal layers of Mn_2Sb changes sensitively when a small part of Mn is replaced by some transition element. The most typical and best known case is $Mn_{2-x}Cr_xSb$ in which exchange inversion (ferrimagnetic-antiferromagnetic) transition occurs with $x \gtrsim 0.025$. We reported for the case of $x=0.05$ that the spin-wave dispersion relation along the c*-axis changes greatly with temperature and that the temperature dependence feature was well accounted for by the theory developed by Kittel and Jarrett on the basis of the exchange magnetostriction.[1] Later on, however, we found in $Mn_2Sb(x=0)$, which is ferrimagnetic through all temperature below T_c, that the interlayer ferromagnetic interaction increases below 200K with decreasing temperature. This result is contrary to the assumption taken in Kittel-Jarrett theory that the interlayer ferromagnetic exchange interaction decreases with the lattice contraction with cooling and, in the case of exchange inversion, it finally changes sign to become antiferromagnetic.

In order to obtain further knowledge of the exchange inversion, we measured spin waves of $Mn_{1.9}Fe_{0.1}Sb$ and $Mn_{1.97}Cr_{0.03}Sb$. In the latter sample, an intermediate phase appears between the antiferro and the ferrimagnetic phases while the former sample becomes no more antiferromagnetic than x=0.

Fig.1 shows the spin-wave dispersion curves for q//c* of $Mn_{1.9}Fe_{0.1}Sb$ and $Mn_{1.97}Cr_{0.03}Sb$. In both cases, the spin-wave frequency increases below 200K. We assume a simplified model as used before that hard ferromagnetic layers are stacked along the c-axis. Effective exchange interactions between the first neighbor layers J_1 and the second neighbor layers J_2 were obtained in the form of product with S, the effective spin of a layer. Fig.2 shows J_1S and J_2S of these samples together with those of former results of other compositions.[2] Through all region of the temperature, J_2S is not greater than one half of J_1S and the temperature dependence is weak. On the other hand, J_1S increases below 200K so long as the sample stays ferrimagnetic below that temperature. It should be noted that in $Mn_{1.97}Cr_{0.03}Sb$, the intermediate phase appears below about 150K, nevertheless J_1S increases below 200K. These results indicate that the exchange inversion in $Mn_{2-x}Cr_xSb$ is not to be explained by the exchange magnetostriction. Contrary to the low temperature behavior described so far, J_1S at higher temperature has a striking composition dependence as shown in Fig.3. The onset of the exchange inversion tran-

sition at lower temperature is reflected on the magnitude of J_1S at high temperature. Concerning the increase of J_1S below 200K, any anomaly or change of physical property at 200K have not been reported up to present other than our results.

References 1) S.Funahashi and N.Kazama, J.Phys.Soc.Jpn. 41(1976)811.
2) S.Funahashi and Y.Hamaguchi, J.Mag.Mag.Mat. 15-18(1980)353.

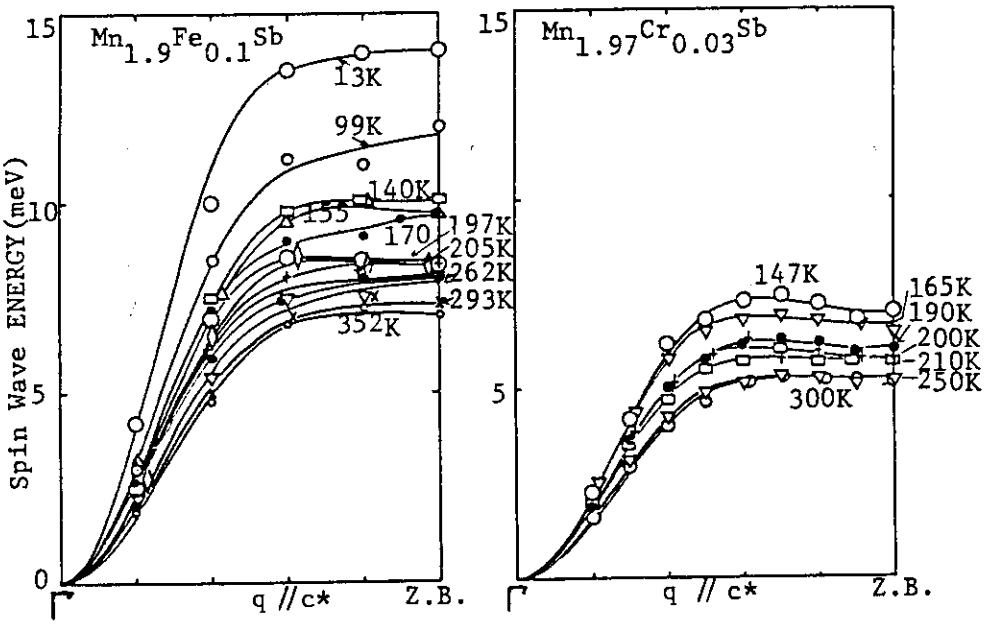

Fig.1 Temperature dependence of spin-wave dispersion curves of $Mn_{1.9}Fe_{0.1}Sb$ and $Mn_{1.97}Cr_{0.03}Sb$ in ferrimagnetic phase.

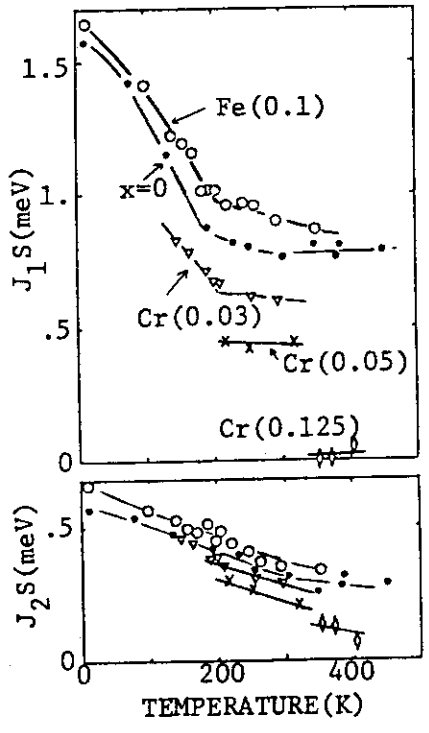

Fig.2. Temperature dependence of first and second neighbor interlayer interaction with various impurity compositions.

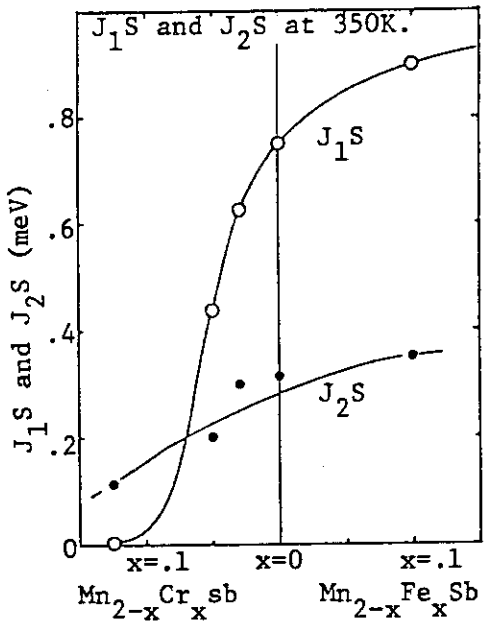

Fig.3 Doping composition dependence of J_1S and J_2S at high temperature (350K).

IV5 Magnetic excitation in Fe_2P

S. Komura, K. Tajima*, H. Fujii, Y. Ishikawa* and T. Okamoto
Faculty of Integrated Arts and Sciences, Hiroshima University, Hiroshima
*Department of Physics, Fauclty of Sciences, Tohoku University, Sendai

Fe_2P is a ferromagnet which shows first order transition at Tc = 209 K. It has a large magnetic anisotropy with the easy axis along the c-axis. The crystal structure is C22 which belong to the hexagonal structure having two crystallographically different Fe sites, Fe_I and Fe_{II}. When 3 % of Fe in Fe_2P is replaced by Mn, it becomes an antiferromagnet with long wave-length structure.

1. Spin wave excitation.

In order to clarify the mechanism of the first order transition in Fe_2P and the properties to become an antiferromagnet by small substitution of Mn in place of Fe in Fe_2P, we have measured the dispersion relations of phonons and spin waves in Fe_2P at various temperatures. Fig. 1 shows the results of the measurement of phonon and magnon energy for the propagation vector q along the [10.0] = a*-axis and [001] = c*-axis. The results for q along the [110] = b*-axis are almost same as the a*-axis.

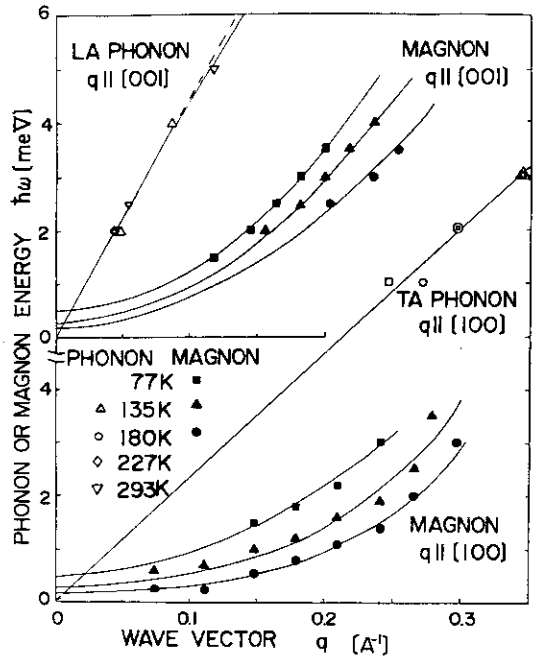

Fig. 1 Dispersion relations of phonons and spin waves.

Although the dispersion relation of phonons is independent of temperature, that of magnons is strongly dependent on temperature especially for q along the a*-axis. The energy of magnons for q along the a*- and b*-axes decreases more than that for q along the c*-axis with increasing temperature, exhibiting a phenomenon of the so-called "softening".

Such experimental facts suggest that with increasing temperature the one-dimensional ferromagnetic chains are almost unaffected while the two-dimensional ferromagnetic orders in the c*-plane are strongly affected below Tc and result in collapse of the three-dimensional orders above Tc.

We believe that the magnetic interaction in the c*-plane favours antiferromagnetic spin arrangement and that it is the strong ferromagnetic interaction along the c*-axis which is responsible for appearance of the bulk ferromagnetism. Since such idea suggests that some transformation of magnetic structure might happen at around Tc, we made the following measurements of magnetic scattering.

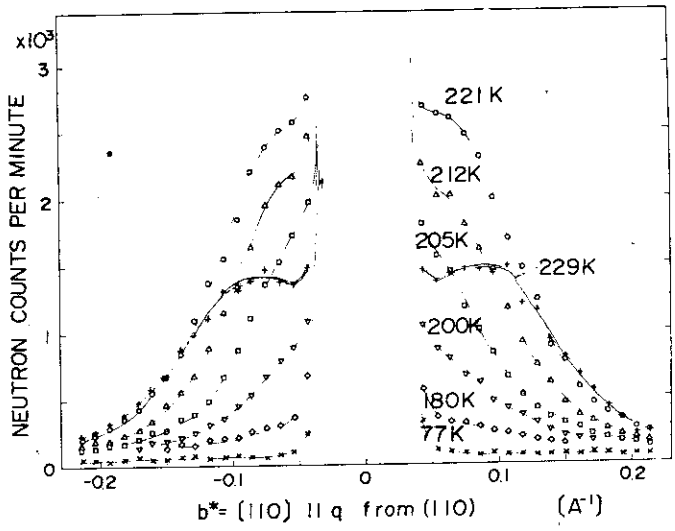

Fig. 2 Dependence on q ∥ b* of magnetic scattering at different temperatures.

2. Elastic magnetic scattering

As temperature is raised from low temperature up to near Tc, we observed magnetic scattering without energy transfer ($\Delta E = 0$) for $q = 0.05 \sim 0.2$ A^{-1} along the a*- and b*- axes near the ferromagnetic Bragg peak (110). Fig. 2 shows the q-dependence of the magnetic scattering along the b*-axis at seven different temperatures. The magnetic scattering is strongly dependent on temperature; it grows with temperature, reaches maximum near Tc and decreases rapidly above Tc. It is interesting to note that it looks like having a maximum near $q = 0.08$ A^{-1} at 229 K which is above Tc. Fig. 3 shows the temperature dependence of the magnetic scattering for three different values of q along the b*-axis. In addition the temperature dependence of the ferromagnetic Bragg peak (110) is shown in the same figure. Our energy analysis of the magnetic scattering revealed as is shown in Fig. 4 that it is elastic scattering which distributes around $\Delta E = 0$ with no more width than that of instrumental resolution (0.6～0.8 meV) and that such features remain unchanged for different values of q. Such results are entirely the same for q along both the a*- and b*-axes but could not be observed for q along the c*-axis.

Such experimental facts indicate that near but below Tc the ferromagnetic order in c*-plane is going to collapse due to the simultaneous appearance of long wave-length structures having various values of the propagation vector q along the a*- or b*-axis within the basal plane, while the ferromagnetic

order along the c*-axis is almost unaffected. In conclusion we believe that as we raise the temperature from T < Tc, long wave-length structures with relatively small values of q(< 0.05 A^{-1}) distributing around q = 0 A^{-1} appear at first within the c*-plane, gradually increasing the values of q and finally above Tc long wave-length structures with relatively large values of q(0.05 ~ 0.13 A^{-1}) distributing around q = 0.08 A^{-1} appear. This seems to be the origin of the first order transition in Fe_2P.

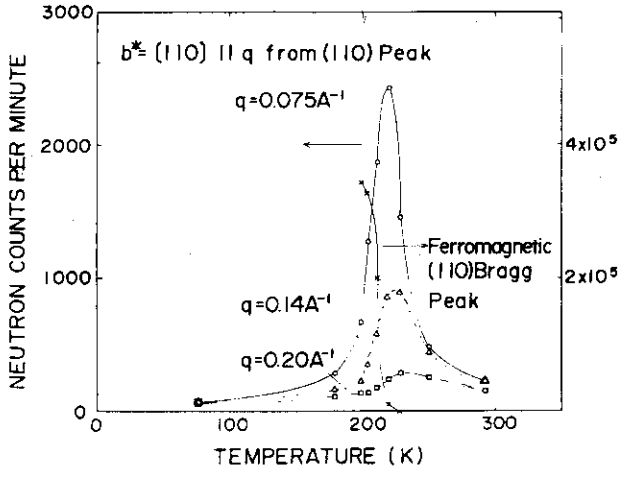

Fig. 3 Dependence on temperature of magnetic scattering for different q ∥ b*.

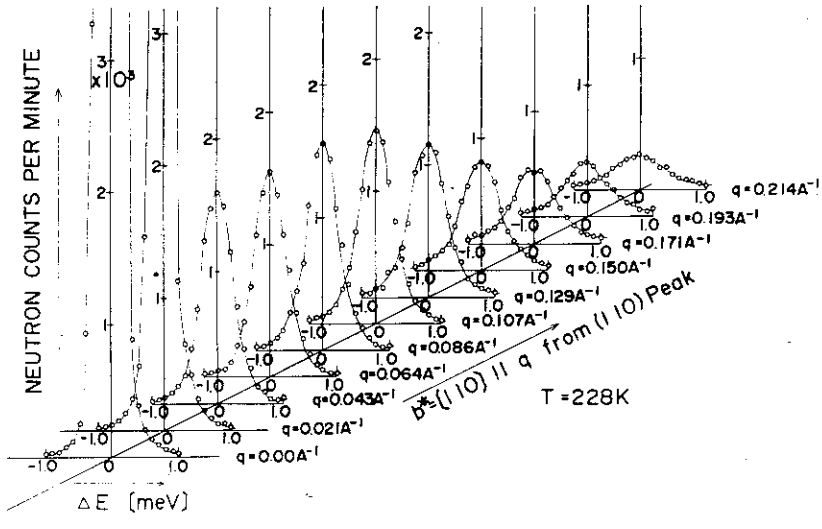

Fig. 4 Distribution of Δ E of magnetic scattering for different q ∥ b* at 228 K.

IV6 Neutron Scattering Study of Magnetic Excitations in Pseudo-One-Dimensional Singlet Ground State Ferromagnets $CsFeCl_3$ and $RbFeCl_3$

Hideki Yoshizawa, Wakae Kozukue and Kinshiro Hirakawa

Institute for Solid State Physics, University of Tokyo, Roppongi, Minato-ku, Tokyo

The magnetic excitation spectra in the pseudo-one-dimensional planar ferromagnets $CsFeCl_3$ and $RbFeCl_3$ were observed using inelastic scattering technique. The observed excitation spectrum of $CsFeCl_3$ has a gap at the magnetic zone center, while that of $RbFeCl_3$ has no gap with a feature of XY-system as shown in Fig.1. This prominent difference can be understood from the fact that they are singlet-ground state system. The observed spectra were analysed by means of the following Hamiltonian,

$$\mathcal{H} = \sum_i DS_{iz}^2 - \sum_{\langle ij \rangle} 2J_\perp (S_{ix}S_{jx}+S_{iy}S_{jy}) + 2J_\parallel S_{iz}S_{jz}) + \sum_{\langle im \rangle} \{2J'_\perp (S_{ix}S_{mx} + S_{iy}S_{my}) + 2J'_\parallel S_{iz}S_{mz}) \quad , \qquad (1)$$

$$\varepsilon = J'_\perp / J_\perp$$

and the numerical values listed in Table 1 could be obtained. Though $RbFeCl_3$ has a 3D LRO due to an exchange induced moment, $CsFeCl_3$ shows no sign of the LRO within the temperature range we measured. Moreover, from a view point of the temperature dependence, it is noticeable that the excitation spectrum of $RbFeCl_3$ shows the feature of XY system even in the paramagnetic phase. The one-dimensionality is evaluated to be about 0.05 for $CsFeCl_3$ and 0.1 for $RbFeCl_3$ showing that they have unexpectedly poor one-dimensionality.

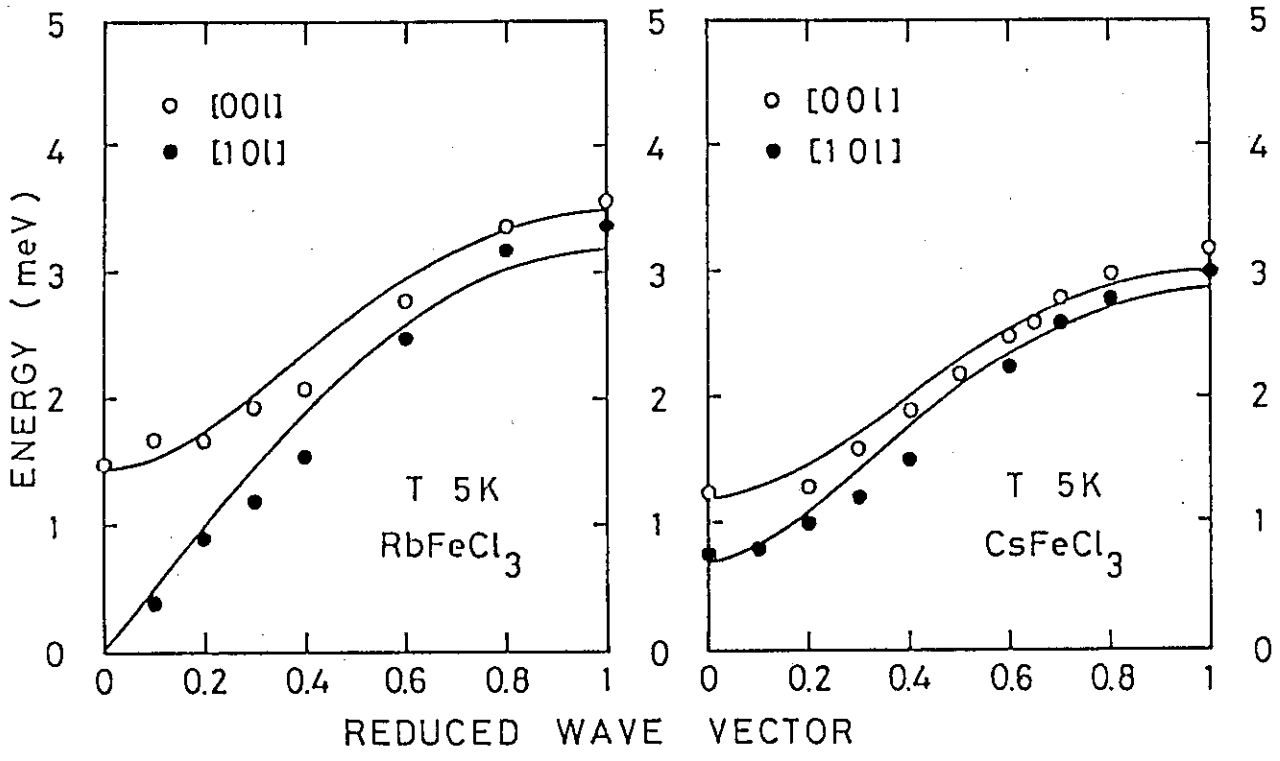

Fig. 1

Table 1. The Hamiltonian parameters

Reference	Model	$RbFeCl_3$ (meV)				
		$J_\perp$	$J'_\perp$	$J_\parallel$	D	ε
(8)	Pair model	1.36	/	0.62	1.49	/
(1)	CEF	0.34	/	0.006	1.02	/
Present work	CEF	0.519	0.047	0.371	0.699	0.091
Present work	Exciton	0.271	0.025	/	2.43	0.091
Present work	3 sublattice	0.488	0.068	0.458	1.70	0.139

$CsFeCl_3$ (meV)				
$J_\perp$	$J'_\perp$	$J_\parallel$	D	ε
0.62	/	0.31	1.61	/
/	/	/	/	/
0.325	0.018	0.0002	1.23	0.055
0.227	0.012	/	2.18	0.052
/	/	/	/	/

IV7 Neutron Scattering Study of Spin Waves in One-Dimensional Antiferromagnet $KCuF_3$

S.K.Satija, J.D.Axe, G.Shirane, H.Yoshizawa* and K. Hirakawa*

Brookhaven National Laboratory, Upton, NY, 11973
*Institute for Solid State Physics, University of Tokyo, Roppongi. Minato-ku, Tokyo

More than 10 years ago Hirakawa et al[1] pointed out that $KCuF_3$ is a good one-dimensional antiferromagnet through their magnetic study though it has a perovskite structure. The 1D property comes out from the special alignment of the 3d orbital wave functions caused by a cooperative Jahn-Teller effect. The overlap is strong along the c-axis, but very weak along the a-axes. This experiment[2] intends to make direct demonstration of the one-dimensionality through the measurements of spin wave dispersion curves. A single crystal of about 2 cc was prepared and the low excitation spin wave spectra including the two modes of excitation was mainly studied by means of ISSP ND-1 spectrometer installed in JRR-2. The higher energy excitations were studied at BNL in collaboration with Shirane's group. Fig.1 shows the dispersion curve observed along the (00ζ) and (ζ01) axes in which the solid line shows the theoretical curve analysed assuming the Hamiltonian in the form

$$\mathcal{H} = 2\sum_{lm}(J_c\vec{S}_l\cdot\vec{S}_m + D_{lm}S_l^zS_m^z) - 2\sum_{ll'}J_a\vec{S}_l\cdot\vec{S}_{l'} - 2\sum_{mm'}J_a\vec{S}_m\cdot\vec{S}_{m'} \quad (1)$$

The parameter obtained is J_c = 203 K and J_a/J_c = 0.01 , which is in very good agreement with the value of 190 K derived from the magnetic study[1] by using the Bonner and Fisher theory. Thus, $KCuF_3$ is the second example of quantum spin system. Drastic asymmetry of the spin wave spectra suggesting the excitation continum has also been observed. For the (ζ01) branch, two modes could be observed, one is the in-

plane oscillation mode and another the out of plane mode as can be predicted through the theory. This is shown in Fig.2.

1) K. Hirakawa and Y. Kurogi; Progr. Theor. Phys. 46S (1970)147

2) S.K.Satija, J.D.Axe, G.Shirane, H. Yoshizawa and K. Hirakawa; Phys. Rev. B21(1980)2001

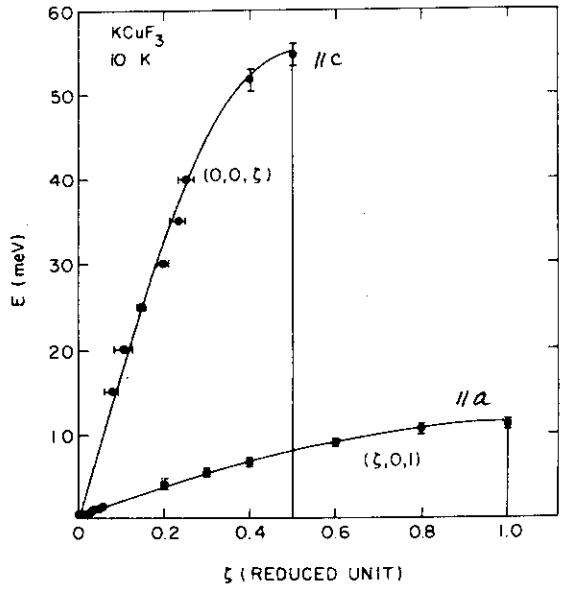

Fig. 1

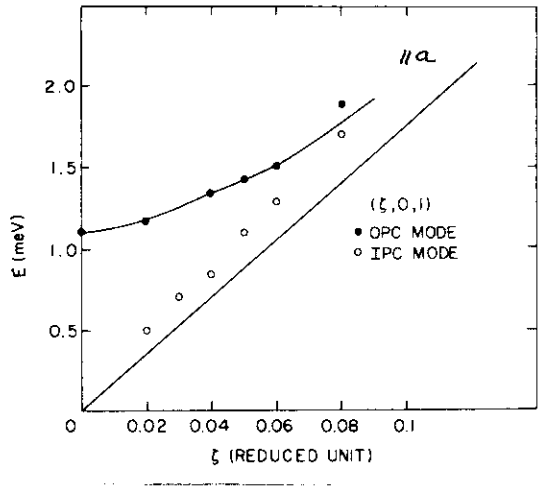

Fig. 2

IV8 Excitations in Two-Dimensional Random Antiferromagnets $Rb_2Co_cNi_{1-c}F_4$

Hironobu Ikeda, Yoshiko Someya, Yasuo Endoh*, Yasuhisa Noda** and Fumiaki Shibata

Department of Physics, Ochanomizu University, *Department of Physics, Tohoku University, **Sendai Radiotechnical College

Magnetic excitations in two-dimensional random antiferromagnets $Rb_2Co_cNi_{1-c}F_4$ (c=0.5 and 0.7) were studied by inelastic neutron scattering. Two well-defined bands of excitations with localized nature were observed. The over-all dispersion was calculated within Green-function formalism. The results show that the empirical relation in interactions between different magnetic atoms, $J_{CoNi} = (J_{CoCo}J_{NiNi})^{1/2}$, is not correct in these substances and J_{CoNi} has an enhanced Ising character.

V1 Structural Study of Liquid Pb-Te System

S. Takeda*, K. Iida*, H. Okazaki**, K. Honma**, Y. Tsuchiya†, S. Tamaki† and Y. Waseda††

*College of Bio-Medical Technology, Niigata University, **College of general education, Niigata University, †Department of Physics, Faculty of Science, Niigata University, ††Research Institute of Mineral Dressing and Metallurgy, Tohoku University.

From the susceptibility measurements[1] and other transport data[2,3], the liquid PbTe is considered to have a chemical complex similar to the solid one. To get a direct structural information about liquid Pb-Te alloys, we have measured the interference functions of liquid Pb-Te system, using the neutron diffraction method.

The observed total structure factors S(Q) and corresponding total pair distribution function g(r)'s of liquid Pb-Te system are shown in figure 1 and 2 together with those of pure Pb and Te for reference[4]. From the profiles of oscilation of total distribution functions, we can easily find a clear distinction in both Pb-rich and Te rich alloys.

Three partial structure factors $S_{ij}(Q)$'s of Pb-rich alloys are obtained from the total structure factors of 2o, 4o and 5o at% Te and results are shown in the figure 3 together with the X-ray intensity pattern of solid PbTe for comparison. As shown in the figure, the peak positions of each partial structure factor have good correspondence with the solid X-ray intensity pattern and the partial structure factor of unlike-atom pairs $S_{Pb-Te}(Q)$ tends to be unity as Q decreases to zero and has a sharp minimum of negative value at $Q = 2.2\ \mathring{A}^{-1}$ where the first peak of the partial structure factor of like-atom pairs can be seen. These characteristic profiles of the partial structure factors suggest that the atomic configurations of liquid PbTe resemble those of molten salts[5]. Small bars indicate the uncertainty at each Q. Corresponding partial pair distribution functions, $g_{ij}(r)$, are shown in figure 4.

The partial structure factors in Te-rich alloys are obtained from the total structure factors of 5o, 6o and 8o at% Te and ahown in figure 5. Corresponding pair distribution function of $g_{ij}(r)$'s are shown in figure 6 and small bars also due to the uncertainty.

From the partial pair distribution functions and coordination numbers,

the basic structure of liquid Pb-Te is considered to be a deformed NaCl structure in Pb-rich and the alloys in Te-rich side have essentially the liquid Te structure.

The above conclusion is supported by a more sophisticated consideration such as chemical bond. Detailes of these discussions will be published elsewhere.

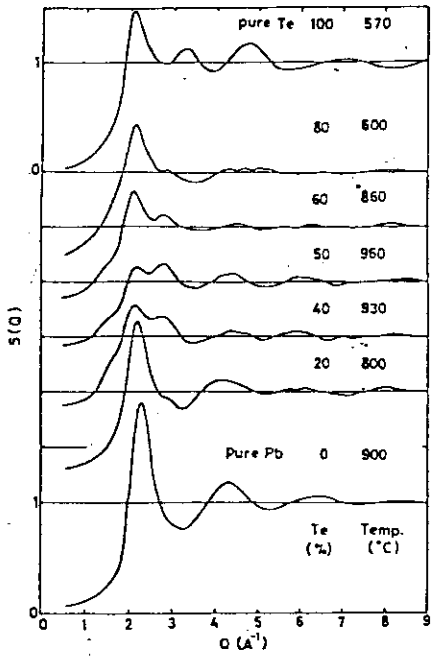

Fig. 1 Concentration dependence of the total structure factor S(Q).

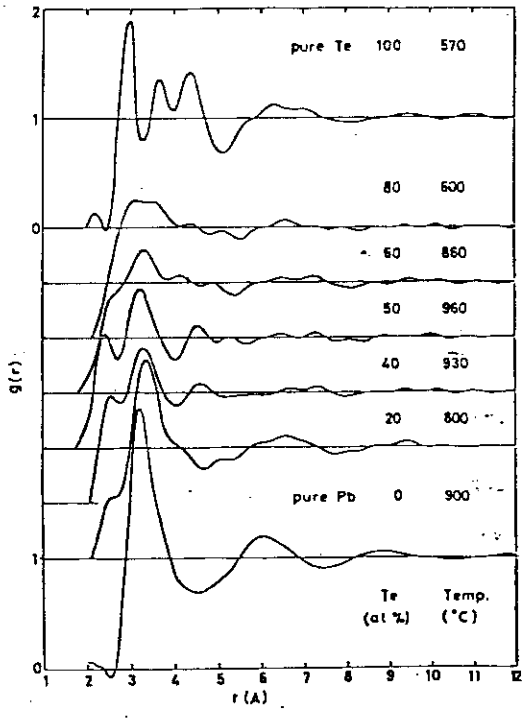

Fig. 2 Concentration dependence of the pair distribution function g(r).

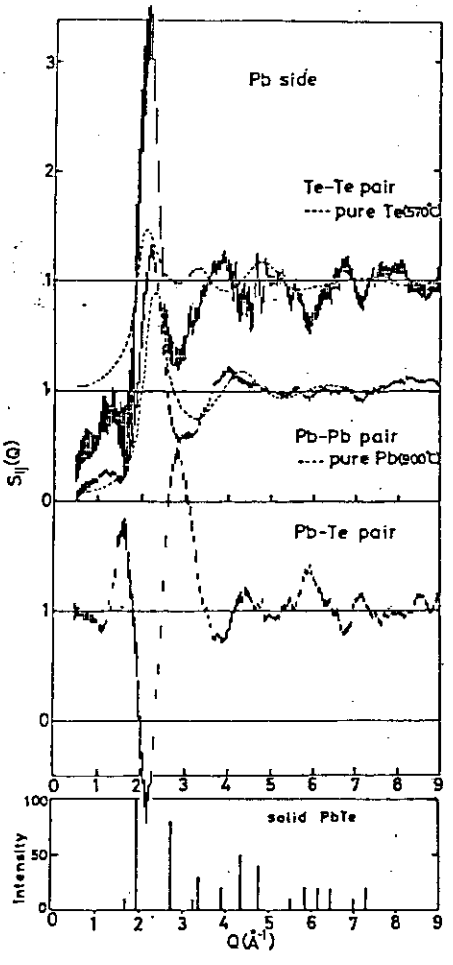

Fig. 3 Partial structure factors in Pb-rich alloy.

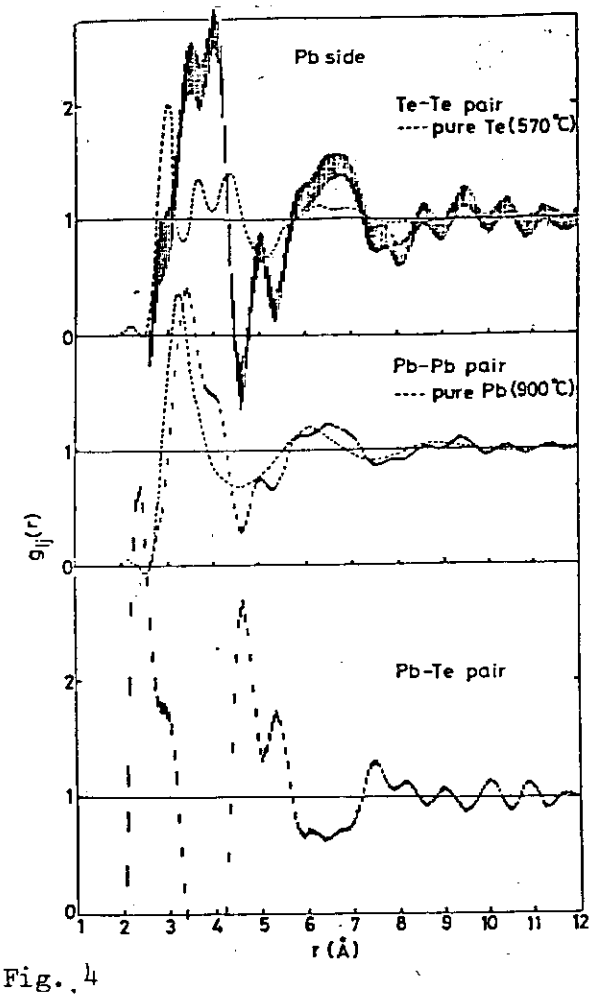

Fig. 4
Partial pair distribution function in Pb-rich alloys.

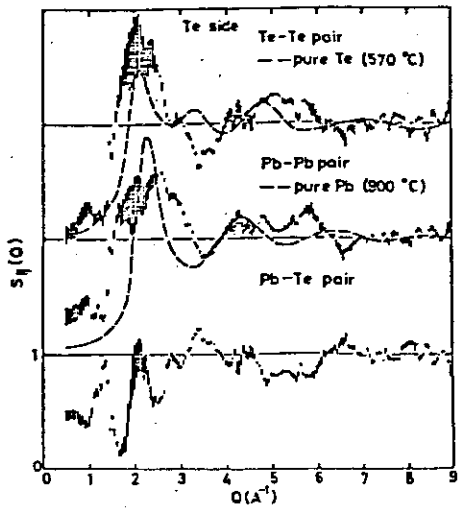

Fig. 5
Partial structure factors in Te-rich alloys.

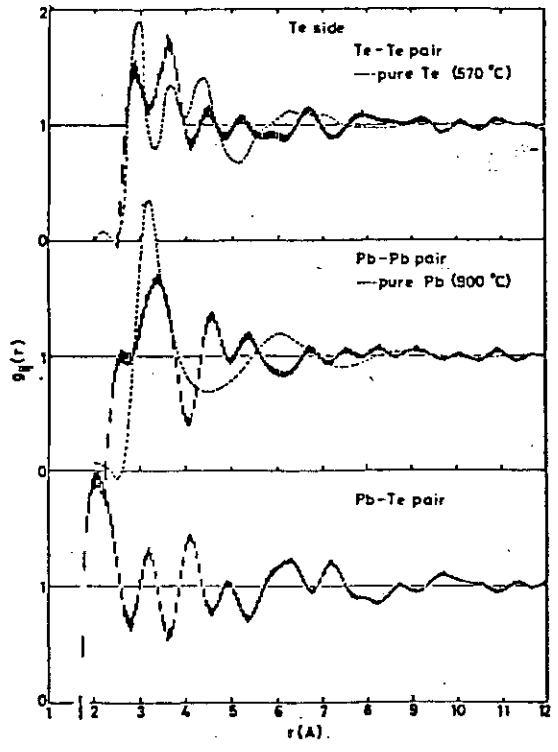

Fig. 6
Partial pair distribution function in Te-rich alloys.

References

1) Takeda S, Tsuchiya Y and Tamaki S 1978, J. Phys. Soc. Japan, 45, 479
2) Glazov VM, Chizhevskaya SN and Glagoleva NN 1969, "Liquid Semiconductors", Academic Press, New York
3) Valiant JC and Faber TE 1974, Phil. Mag. 26, 571
4) Waseda Y 1980, "The Structure of Non-Crystalline Materials", Macgraw-Hill, International Book Company

V2 Neutron Diffraction Study on Liquid Mg-Bi Alloys.

Koji Honma* and Keiichi Iida

*College of General Education,Niigata University,
College of Bio-Medical Technology,Niigata University.

It is known that Mg-Bi alloys show anomalous electric conductivity at the mole fraction of 3:2(atomic concentration of Mg:x=0.4).[1)-3)] We have tried neutron diffraction study to investigate its origin.

Neutron diffraction measurements were carried out, using ISSP-NDII diffratometer at JRR-3 reactor. Ge single crystal monochromator was used, and wave length 1.79 and 0.93 Å were got from (111) and (311) plane reflections. The alloys were contained in pure iron tubes(inside diameter:14mmϕ, outside diameter;15mmϕ,height:110mm) and set inside a vacuum high temperature furnace as shown in Fig.1. This furnace have been produced by us newly for liquid metals. The parto which neutron beam passes through was made of aluminium. Inert gas was introduced into the furnace up to about 2/3 atm. and heated. Temperature was controlled by PID controller within $\pm$2°C and temperature ditribution over specimens was within $\pm$10°C. Measurements were performed at this time in Bi-rich side;x=o.1.0.3,0.5 and 0.6. Temperatures were held at 450,700,700,and 850°C,respectively.

After correction due to iron cell absorption,background counting etc. ,structure factors were obtained. Some examples are shown in Fig.2,together with those of pure Mg and Bi by other authors[4),5)]. Contrary to our expectations,the structure factor anomaly is not clearly recognised at x=0.4,i.e., it is not observed for the main peak to split into some sub-peaks such as Cu-Sn,MgSb,etc. The structure factors of x=o.5 and 0.4 are resemble to each other. It is likely that total structure factors shift smoothly as the concentration is altered. Therefore,it seems at present that the rigid sphere model is favorable for the structure of Mg-Bi system,although wider range of composition should be examined in the near future. So that,it may be that the origin of the anomaly in the transport properties should be asked for in some other place.

We obtained the partial structure factor S_{12},corresponding to Mg-Bi correlation function,assuming that total structure factor consists of S_{11}, the structure factor of pure Mg,S_{22},that of Bi,and S_{12}. The total structure factor,S(s)is written as

$$S(s) = (x^2 \sigma_1 S_{11} + 2 x(1-x)\sqrt{\sigma_1 \sigma_2}\, S_{12} + (1-x)^2 \sigma_2 S_{22}) / \langle f \rangle^2$$

,where $\langle f \rangle = x\sqrt{\sigma} + (1-x)\sqrt{\sigma_2}$, σ_i being the coherent cross section of

stomic species,i. And s is 2 sin θ/λ. S_{12} for x=0.5 is shown in Fig.2. The position of the main peak of S_{12} is at s=0.47 $Å^{-1}$. So that, it seems that the interatomic distance between unlike atoms in the liquid alloy state is considerably smaller than 3.3 Å, the sum of each atomic radius in pure metals.

References

1) N.F.Mott and E.A.Davis,Electronic Processes in Non-Crystalline Materials, Clarendon Press(1971).
2) B.R.Ilschner and C.Wagner,Acta Met.,6(1958),712.
3) R.P.Ferrier and D.J.Herrell,Phil.Mag.,19(1969),853.
4) D.M.North,J.E,Enderby and P.A.Egelstaff,J.Phys.C,1(1968),1075.
5) H.Krebs,V.B.Lazarev and L.Winkler,Z.anorg.allgem.chem.,352(1967),277

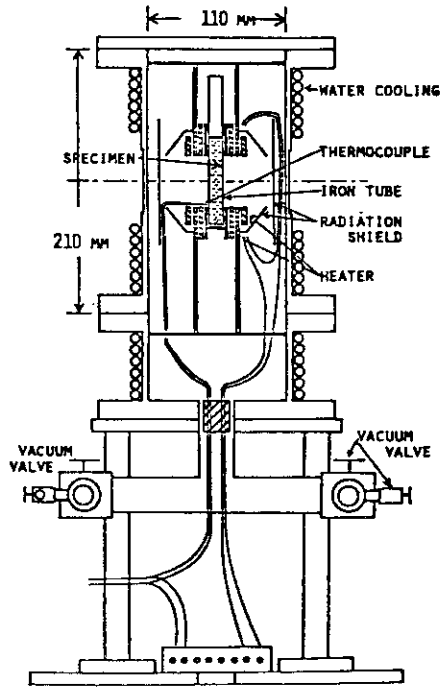

Fig. 1 Furnace.

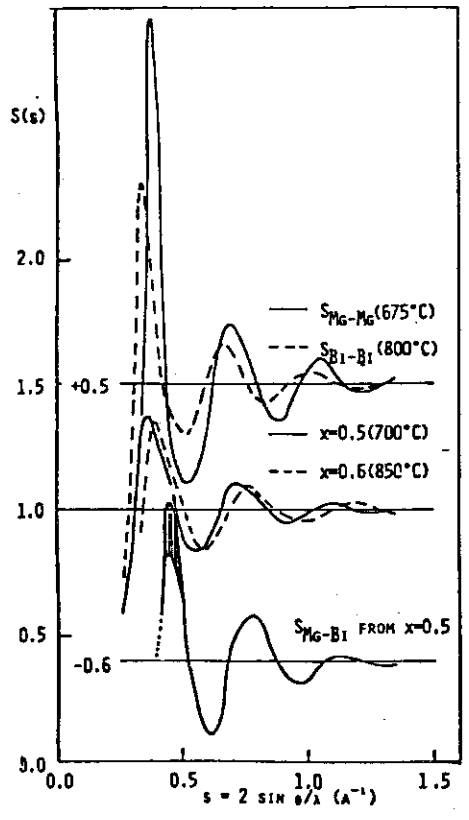

Fig. 2 Structure factors.

V3 X-Ray and Neutron Diffraction of Amorphous and Liquid $TlAsSe_2$

Tsuneo Satow, Katsumi Hoshino and Osamu Uemura

Department of Chemistry, Faculty of Science, Yamagata University

The liquid state of pure Se and its binary compounds as well as the crystalline states has been extensively studied because of their semiconducting properties. Several of these substances contain either polymeric chains or ring molecules as the basic structural unit even in the liquid state[1]. These materials have rather a large viscosity just above the melting point, and then become to be glasses easily by any cooling process. Therefore, it is possible to investigate the structure between amorphous and liquid phases which are both non-crystalline states and to compare the atomic arrangement between both phases. A ternary selenide $TlAsSe_2$ is considered to have a spiral chain structure in which As and Se atoms bind alternately, although the exact structural analysis for the crystal has not yet been made. Considering a strong covalent bonding between As and Se atoms in the chain, it can be expected that the chain structure remains undestroyed at least in the short range distance when melting. This report describes the result of respective distribution functions of amorphous and liquid $TlAsSe_2$ determined by X-ray and neutron diffraction methods.

Details of both the X-ray diffraction measurement for amorphous sample and the neutron diffraction measurement for liquid sample have been mentioned respectively in the previous paper [2,3].

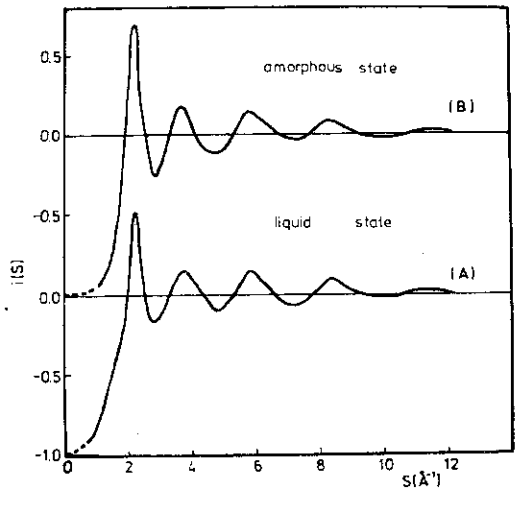

Fig. 1 The interference functions, i(s), for amorphous and liquid $TlAsSe_2$.

Fig. 1 shows interference functions i(s) for the amorphous and liquid $TlAsSe_2$. A whole functional form of both curves is almost equivalent in respect to both height and position of each peak despite different states and different diffraction methods. The values of s for the peaks given in the amorphous $TlAsSe_2$ are 2.22, 3.76, 5.86 and 8.40 $Å^{-1}$, respectively. Fig. 2 describes atomic radial distribution functions, $4\pi r^2 \rho_o g(r)$.

The detailed structure of crystalline $TlAsSe_2$ has not yet been established so far as we are aware. However, it

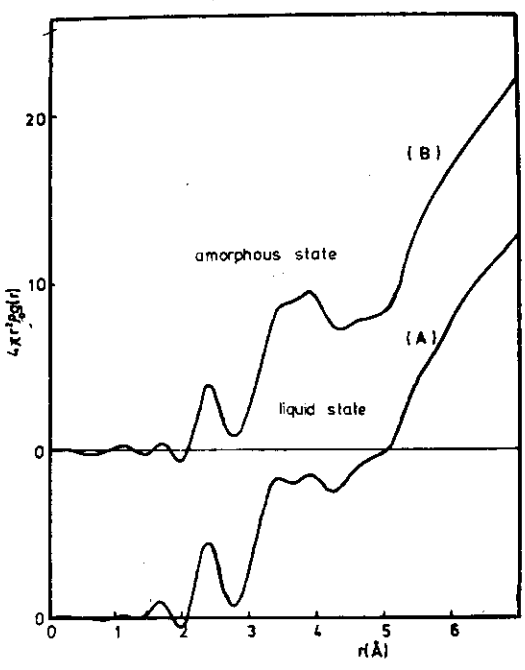

Fig. 2 The atomic radial distribution functions $4\pi r^2 \rho_o g(r)$, for amorphous and liquid $TlAsSe_2$.

Table 1 The structural parameters of both amorphous and liquid $TlAsSe_2$.

Sample	r_1 (Å)	n
a-$TlAsSe_2$	2.40	1.74
l-$TlAsSe_2$	2.40	1.61

seems resonable that it is assumed to take $TlAsS_2$ type structure, firstly because Se and S together belong to the same group in the periodic table and secondly because chemical properties of $TlAsSe_2$ are much similar to those of $TlAsS_2$. The crystal of $TlAsS_2$ is characteristic to contain spiral AsS_2 chain as illustrated below,

$$-\underset{\underset{S(1)}{|}}{As(1)} - S(4) - \underset{\underset{S(2)}{|}}{As(2)} - S(3) - \quad [4]$$

Covalent bondings between As and S atoms in spiral chains are very strong and Tl atoms are located without the spirals. Then, the average coordination number per atom takes a considerably small value below two. When it is assumed that $TlAsSe_2$ has similar spiral chains, the bond distances between As and Se atoms in the spirals distribute in the range from 2.18 to 2.50 Å (the average distance is about 2.37 Å).

Since the shape of the nearest neighbour shell in the radial distribution curves in Fig. 2 is an ideal Gaussian, the interatomic distance r_1 and the coordination number n for amorphous and liquid $TlAsSe_2$ can be clearly evaluated. These results are listed up in Table 1. Both values in Table 1 correspond well to the expected ones when the chain structure is assumed. A steep minimum just after the first peak in both curves in Fig. 2 also indicates a strong bonding between As and Se atoms in the spirals. Consequently, we can pointed out that the spiral chains consisting of As and Se atoms are present in both amorphous and liquid structures of $TlAsSe_2$.

[1] M. Misawa and K. Suzuki, Trans. JIM 18 (1977) 427.

[2] O. Uemura and T. Satow, phys. stat. sol.(a) 40 (1977) 303.

[3] T. Satow, O. Uemura, S. Akaike and S. Tamaki, J. Non-Cryst. Solids 29 (1978) 215.

[4] A. Zemann and J. Zemann, Acta Cryst. 12 (1959) 1002.

V4 A new Method to measure the Full-Width at Half Maximum of Quasielastic Neutron Scattering Spectrum

Takashi Sakuma*, Kaoru Shibata** and Sadao Hoshino**

* Department of Physics, Faculty of Science, Ibaraki University and
**Institute for Solid State Physics, The University of Tokyo.

Quasielastic neutron scattering experiment is one of the powerful techniques to study the structures and dynamical properties of solution. Measurements of the quasielastic neutron scattering spectrum have been performed by the constant-Q mode of operation with one energy resolution (Fig. 1 (a)). A diffusion constant and a rest time of an atom in solution have been obtained by analyzing Q ($= 4\pi\sin\theta/\lambda$) dependence of the full-width at half maximum (FWHM) of the quasielastic energy spectrum.[1)]

An "elastic" scattering $I(Q,\omega)$ ($\omega=0$) involves the informatin of the quasielastic part of the scattered neutron due to limitations of the energy resolution. Therefore it is found that the information of the quasielastic neutron scattering could be obtained from the analysis of the "elastic" scattering spectrum. A new method performing neutron elastic scattering measurements with various resolution conditions is applied to measure the Q dependence of the FWHM of quasieastic energy spectrum of H_2O (Fig. 1 (b)). The energy resolutions were varied by changing an incident energy. The other instrumental conditions are the same. The energy dependence of a incident neutron flux need not to be considered in the treatment of the present method.

Elastic neutron scattering measurements of H_2O were carried out using the triple-axis spectrometer (ISSP ND-1) installed at JRR-2 in Japan Atomic Energy Research Institute with three incident energy 13.7, 30.5 and 41.0 meV from the pyrolytic graphite 002 reflection of a double-monochromator system. The energy resolutions of the incident energy were measured to be 0.67, 1.85 and 2.80 meV, respectively. The analyzer crystal was mounted at the fixed angle so as to measure only "elastic" part of the scattering. A plane-shaped Al container having parallel plates distanced by 1 mm was utilized. Double axis neutron diffraction measurements of H_2O were also performed to correct for the absorption and the background of the neutron elastic scatterintg measurements. The obtained Q dependence of the intensity of the neutron elastic scattering is shown in Fig. 2.

From the analysis of the Q dependence of I(Q,0) with the incident energy 13.7, 30.5 and 41.0 meV, FWHM vs. Q curve was obtained. The derived Q dependence of $\Gamma(Q)$ of H_2O is almost the same as that by the constant-Q mode of operation.

The detailed procedure of I(Q,0) by the present method will be reported elsewhere.

1) T. Sakuma, S. Hoshino and Y. Fujii : J. Phys. Soc. Jpn 46(1979)617.

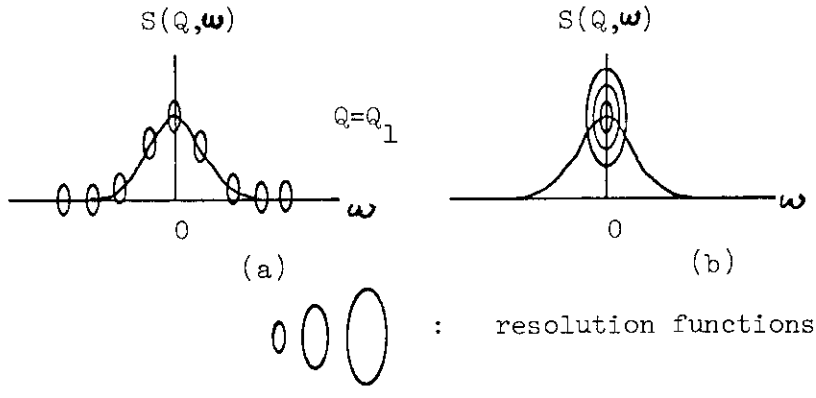

Fig.1 Schematic expressions for (a) constant-Q mode of operation and (b) present method using various resolution functions.

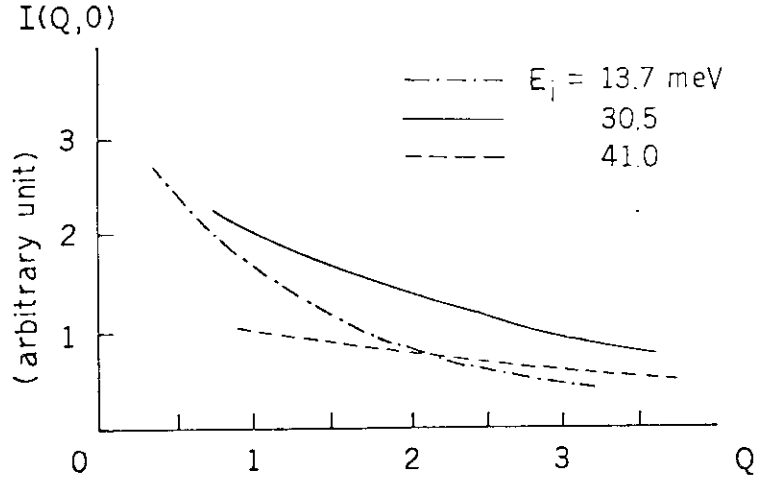

Fig.2 Q dependence of elastic scattering intensity I(Q,0)

VI1

The Very-Small Angle Neutron Scattering from Neutron-Irradiated Amorphous Silica

Toshio Takahashi*, Hiroshi Tomimitsu**, Yoshiyuki Ushigami*, Seishi Kikuta* and Kenji Doi**

* Fuculty of Engineering, The University of Tokyo, and
** Physics Division, Japan Atomic Energy Research Institute.

A neutron version of the 2-crystal diffractometer for the very-small angle scattering (VSAS)[1] is constructed and installed at JRR-2. Two highly perfect Si crystals are oriented for 111 Bragg setting with (+,-) geometry. The sample is placed between the Si crystals, so that the VSAS is observed by rotating the second crystal around the axis normal to the plane of incidence. All the elements of apparatus are installed on a vibration-free measurung table in a enclosure with insulating walls.

The samples examined are plates of amorphous silica ($a\text{-}SiO_2$) with thicknesses ranging from 0.45 to 0.46mm, which are reactor-irradiated in JRR-2 with a thermal neutron of fluence of 3×10^{19} per cm^2, the temperature being maintained at $48° \pm 2°C$

For each run of measurements data points were plotted and examined, eliminating anomalous data possibly affected by accidental eventualities in the measuring conditions. The resultant data points were accumulated until the peak heights attain as high as several 10^3 counts. The data were then Guinier-plotted as shown in Fig.1. Typically a single plot in the figure required about 10 hours. It is seen that the Guinier plots are approximated by straight lines up to the scattering angles of 2 or 3s of arc, and that the half-maximum width of the VSAS's are:

$$\left.\begin{array}{l} 1.41'' \text{ for no specimen (instrumental) (plot (a),} \\ 1.48'' \text{ for unirradiated } a\text{-}SiO_2 \text{ (plot (b))} \\ \text{and} \\ 1.79'' \text{ for irradiated } a\text{-}SiO_2 \text{ (plot (c)).} \end{array}\right\} \quad (1)$$

As plots (a) and (b) are nearly parallel to each other, no VSAS exists for the unirradiated a-SiO_2. For the irradiated a-SiO_2, the plot (c) reveals a VSAS with half-maximum width:

$$(1.79^2 - 1.41^2)^{1/2} = 1.11 \text{ (s of arc)}. \qquad (2)$$

The extraction of structural knowledges of the irradiated a-SiO_2 from the observed VSAS requires particular accounts for multiple scattering and refraction of neutrons[2], which finally yield the figure of radius of gyration: 3×10^5A, the wave length used being 1.9A. It is thus concluded that the irradiation gives rise to structural inhomogeneities of 10^5A in size within a-SiO_2 which has initially no inhomogeneities at all. The conclusion is quite consistent with observation of X-ray VSAS[3] and with optical microscopy.[4] The results have been already published with the details of analysis[4].

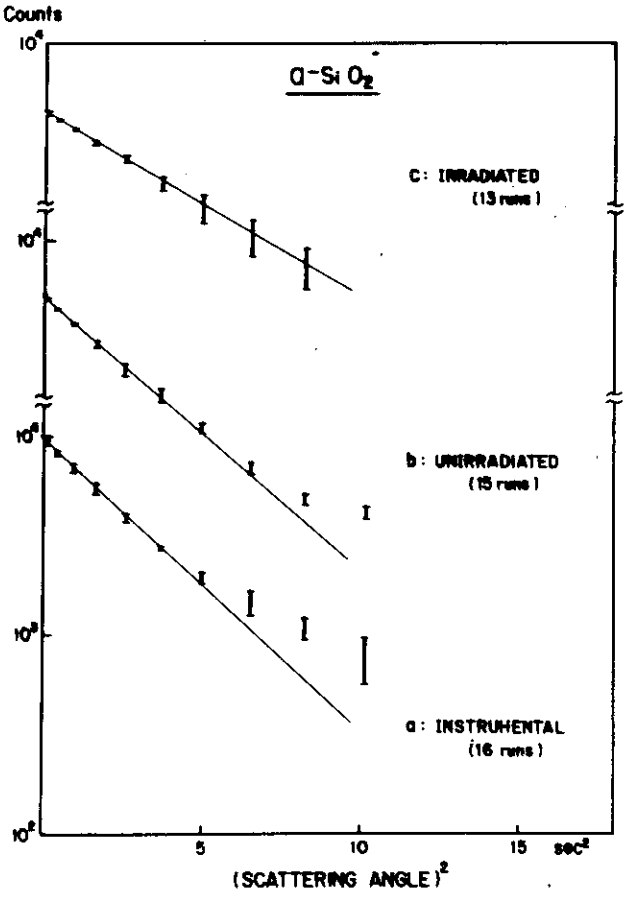

Fig.1. Guinier plots of VSAS's from amorphous silica, before (b) and after (c) the reactor irradiation. (a) is the plot for the trace of direc beam.

(1) U.Bonse & M.Hart: Z.Phys. 189, (1966), 151.
(2) C.K.Suzuki, K.Doi & K.Kohra: Jpn.J.Appl.Phys. 20, 1981), L271.
(3) *idem ibid.*: 19, (1980), L205.
(4) T.Takahashi, H.Tomimitsu, Y.Ushigami, S.Kikuta K.Doi: *ibid.* 20, (1981), L837.

VI2 Observations of Textures in Copper-Alloy Crystals by Neutron Diffraction Topography

Hiroshi Tomimitsu and Kenji Doi

Physics Division, Japan Atomic Energy Research Institute

A characteristic texture has been observed with neutron diffraction topography for a Cu-5%Ge single crystal having a size as large as 3 cm(dia.)×10cm. A layer subtructure normal to [001] and parallel to the [110] growth direction was found extended through the body of the bulky crystal.(1)(2) With a view to establish the model of the texture some novel techniques of observation were applied. Fig.1 shows the results of the simultaneous edge-on observation of the layer-substructure. The neutron wavelength 1.8A was adopted so that the Bragg angle for the 220 reflection is exactly 45°. The neutron beam was incident parallel to the layer plane and to the [100] direction as well. The reflected neutrons emerged from the layer exactly parallel to the [010] direction, of which the intensities were recorded with usual procedures of the neutron topography. Figs.1.a, b, and c are the images thus obtained, where fins are seen attached perpendicularly and symmetrically to both sides of the layer with regular width, height and interval of 0.4-0.5mm. After the geometry of the reflection the fins run parallel to the (010) plane. Furthermore the jag-shaped spaces between those fins are just filled up by other fins attached to the adjascent layers.

Those and other observations finally lead us to the model as depicted in Fig.2. The crystal is constituted of layer-substructure parallel to (001)(Z-sublayer) extending throughout the body of the crystal nearly parallel to the growth direction [110]. Each Z-sublayer is attached with X-plates and Y-plates (fins) which run parallel to [100] and [010] respectively. The interplanar spaces between X- and Y-plates are filled up by other X- and Y-plates attached to the adjascent Z-sublayers. The detailed accounts of the model have already been published.(3)

Similar topographic images were observed for other copper alloy crystals, viz. Cu-10%Ni, Cu_3Au, etc. of which detailed investigations are underway.

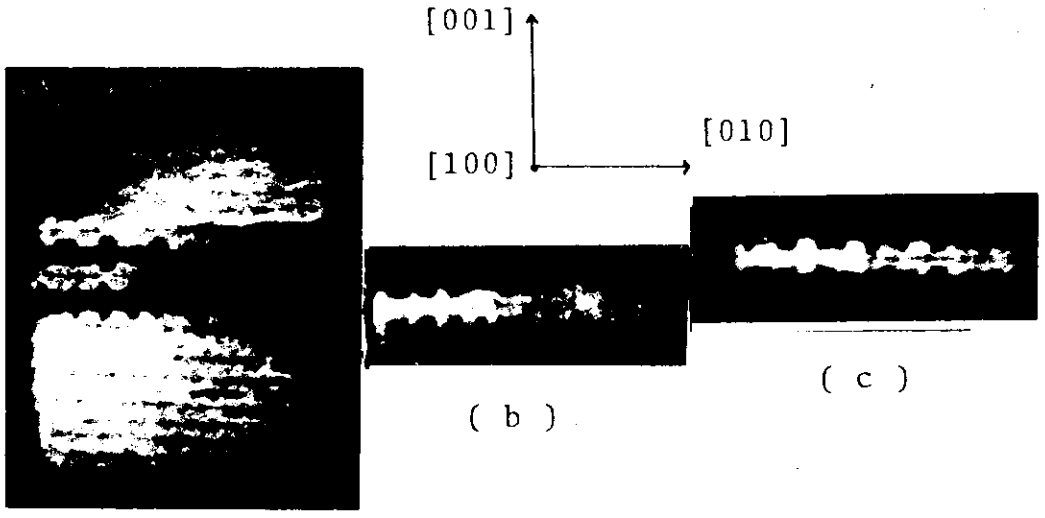

Fig.1

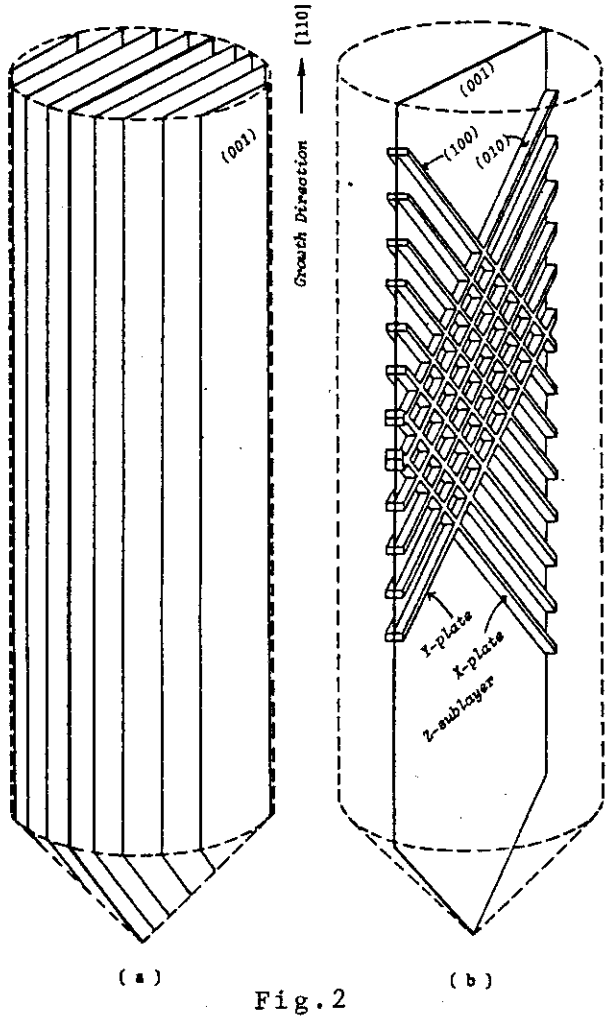

Fig.2

(1) H.Tomimitsu,K.Kamada & K.Doi:Phil.Mag.A,38,(1978),483.
(2) H.Tomimitsu & K.Doi:Sci.Rep.RITU A29,Suppl.1,(1981),47.
(3) H.Tomimitsu: Phil.Mag.A.43,(1981),569.

VI3 High Pressure Apparatus for Neutron Diffraction

Kazuo Kamigaki, Takejiro Kaneko, Shunya Abe and Masayoshi Ohashi

The Research Institute for Iron, Steel and Other Metals, Tohoku University, Katahira, Sendai 980.

A piston-cylinder type high pressure apparatus was designed for the angle dispersive neutron diffraction. Ti-53wt%Zr alloy was used for the cylinder. The performance was tested by observing the strucural transformation under pressure in RbBr from a NaCl-type to a CsCl-type.

1. High pressure cell

The Ti-53wt%Zr alloy was used as a material of the high pressure cell. Mechanical strength of the alloy is moderate, but it has a special characteristic for thermal neutrons. In this composition, the coherent scattering amplitude of thermal neutron is zero, and no coherent peak is observed in the elastic scattering pattern. The alloy was prepared, then remelted and accumulated to a large cylinder; 3-4 cm diameter and 8-10 cm long.

The high pressure cell was a piston-cylinder type, the diameter of the center hole was 6-8 mm. Both ends of the cylinder were inserted into steel binding rings. The pistons were made of alumina, hardened steel or tungsten carbide. Powdered specimen was put into a thin-walled capsule of teflon, CS_2 was used as the pressure medium. The arrangement of the apparatus is shown in Fig.1, a cylinder was blowed out at about 12 kb.

2. Neutron diffraction

The structural transformation under pressure in RbBr was observed for the test of performance. KCl powdere was mixed to RbBr as a reference of pressure. A pattern for NaCl-structure at normal pressure is shown in Fig. 2. In the figure, the background orginated from the incohrent scattering by the Ti-Zr cell is considerably high, but peaks of elastically scattered neutron by RbBr and KCl are clearly identified. With increase of pressure, peaks shift in accordance with a reduction in the lattice spacing. Then, RbBr transformed to a CsCl-type structure as shown in Fig.3.

The variation of volume with pressure in RbBr is shown in Fig. 4 by open circles, the value of pressure was determined by the volume change in KCl. In the figure, the compression of RbBr and KCl measured by Vaidya and Kennedy by X-ray diffraction is shown by solid circles and lines.

The transformation in RbBr occurs at about 4.5 kb and the compression of volume follows the line obtained by X-rays.

3. Discussion

Many materials are rather transparent for thermal neutrons in contrast with X-rays. Hence, the neutron diffraction is powerful for high pressure works, where specimens are surrounded by a mass of medium to generate and to keep pressure. In the present case of Ti-Zr alloy cylinder, no diffraction peak of the cylinder is superimposed and the original pattern of the specimen is not disturbed. The absorption of thermal neutron by Ti-53wt%Zr is ~0.1 cm^{-1}, the value is lower middle in ordinary substances. The apparatus developed here will be applicable for the study of materials under pressure; precise determination of the compressibility and the transformation in the crystal structure.

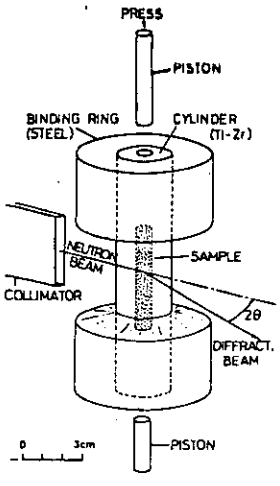

Fig. 1 Arrangement of the apparatus

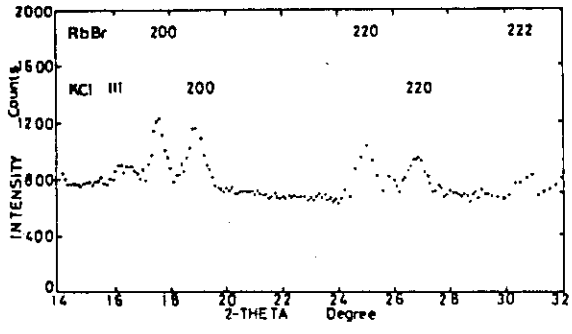

Fig. 2 Diffraction pattern of RbBr KCl mixture at low pressure.

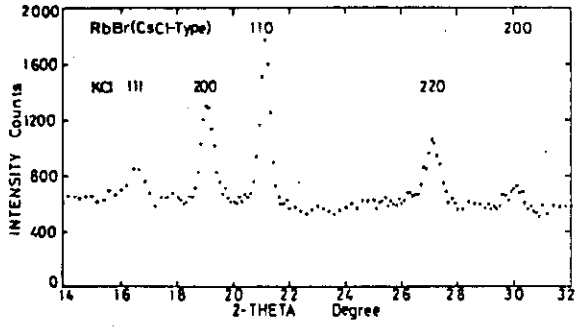

Fig. 3. Diffraction pattern of RbBr-KCl mixture, at high pressure.

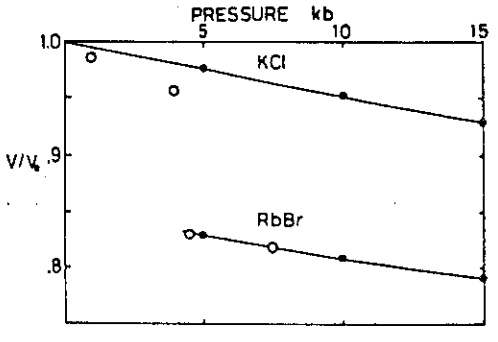

Fig. 4. o Volume compression of RbBr bye the present experiment, and for KCl and RbBr by Vaidya and Kennedy —●— .

VI4

Neutron Spectral Modulation
A New Thermal Neutron Scattering Technique

Yuji Ito, Masakazu Nishi, Kiyoichiro Motoya

Institute for Solid State Physics, the University of Tokyo

We have developed a new thermal neutron scattering technique called "Neutron Spectral Modulation",(NSM).

The principle of the new method is essentially to observe the response of the scattering system to the incident impulse, whose spectral distribution is modulated sinusoidally. This point should be contrasted to the conventional neutron spectroscopy, the principle of which is to see the impulse response of the monochromatic neutron beam.

The impulse response along the time domain can be simulated by the use of the pseudo-random correlation method, by which the duty cycle can be increased as much as 50%. In addition to the time correlation technique, we employed another modulation along the spectral domain by utilizing the neutron spin phase as was first done by the neutron spin echo (NSE).

The two dimensional modulation (in time and in spectral space) as the result increases the neutron economy to a great extent.

The beauty of the new method is that it not only utilizes neutrons of the broader spectral range but also it can improve the energy resolution by one or two orders of magnitude than the conventional triple axis and/or the time of flight techniques.

The NSM also has certain advantages even compared with the NSE. This arises from the fact that in the former, each labelled neutron in the spectral domain can be separately followed in the time domain through the scattering processes, whereas in the latter, only the averaged quantities over the incident neutron spectrum can be measured.

The detailed account of the NSM has been published in ref.1, and some preliminary experiments together with the original developments including resolution problems were reported in ref.2.

The special features of the NSM essentially boils down to the following two points.

The first is the utilization of the zero-crossing points (ZCP) in the spectrum, which correspond to non-modulating neutrons or equivallently to those neutrons whose polarization lie in the scattering plane before its conversion to intensity. In terms of the impulse response picture, at ZCP, the incident neutron intensity becomes identically zero and no scattering takes place.

Under the finite resolution of the practical case, the ZCP's shift their positions very little upon scattering because of its unique resolution cancellation property, and hence are ideally suited to the use as labels for the dispersive scattering processes.

The second feature is the channel Fourier transform scheme,according to which, a desired frequency component of both real and imaginary parts of the scattering function for the non-dispersive processes can be obtained.

This point should be compared with the usual case of the NSE, where only the real part of the non-oscillatory Fourier component of the scattering function can be measured.

We present here the results of theZCP labelling scheme obtained by using the PANSI spectrometer in Fig.1 and Fig.2 for illustration purpose.

In the Fig.1 show the usual cross-correlation results without the NSM,

whereas in the Fig.2 are shown the results with the NSM.

The elastic position was determined by the peak of the (111) Bragg reflection of the Heusler analyzer as the channel #31, with the condition $\vec{H} \perp \vec{K}$.
In the NSM mode, the spin precessing field was adjusted to make the ZCP to coincide at the peak position, that is at the #31 channel.

For the magnon process, instead of the formal NSM arrangement of polarization to intensity conversion, we used the analyzer as the sample, and the field direction at the analyzer was changed to such that $\vec{H}$ be parallel to $\vec{K}$.

In the Fig.1, off-Bragg condition was $+4^{\circ}$ for θ and $+3^{\circ}$ for 2θ, whereas in the Fig.2, they are $+4^{\circ}$ and $+1^{\circ}$ respectively for the magnon observation.

Changes in the sign clearly indicate that these are indeed magnons from the Heusler analyzer. In Fig.1, there are two magnons are expected at 1.16 and 2.06 meV, whereas in Fig.2, they are at 0.60 and 2.55 meV. The 0.60 magnon is clearly seen in the Fig.2, where the energy trasfer of 0.61 meV was obtained from the ZCP in good agreement with the expectation, and demonstrating the power of NSM method for determining the precise dispersion relation.

(1). Tech. Rep. of ISSP, No.1141 June, 1981; and to be published in Nucl. Instrum. and Meth.

(2). Tech. Rep. of ISSP, No.1062 July, 1980.

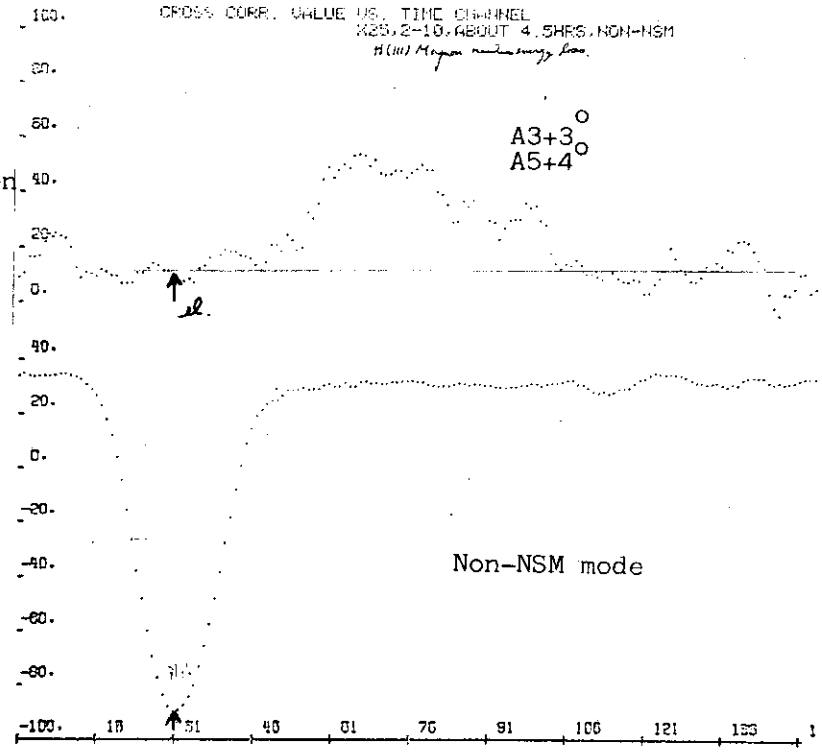

Fig.1. Cross-correlation time spectrum from the Heusler alloy; (111) Bragg reflection (below) and the off-Bragg magnons (above). Arrows indicate the elastic peak positions.

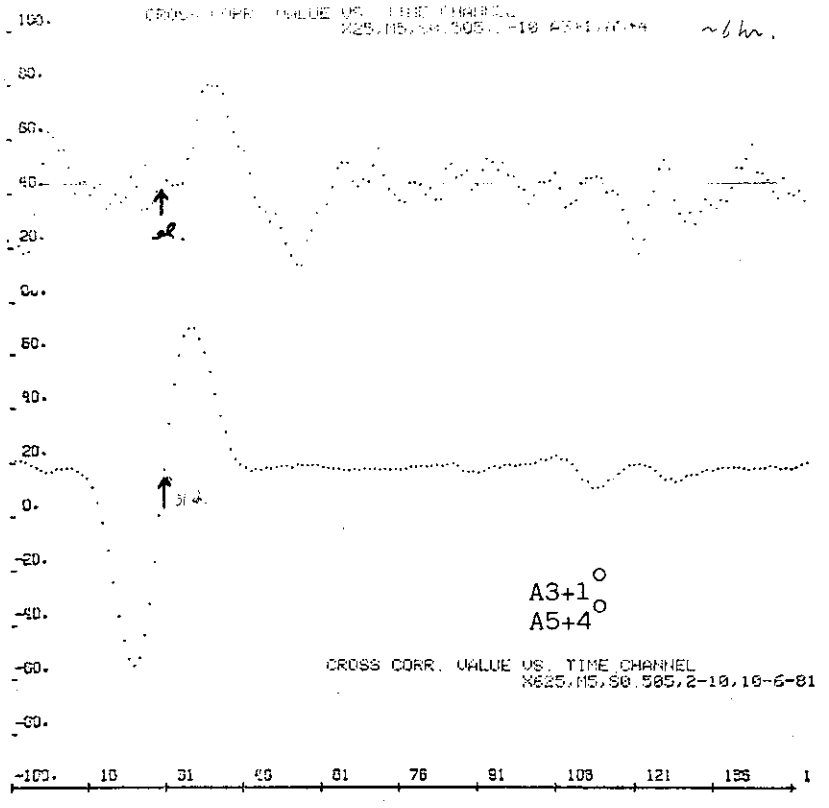

Fig.2. Cross-correlated time spectrum under the NSM mode from the Heusler analyser; (111) Bragg reflection (below) and the off-Bragg magnon (above).

VI5 Monochromator System of Small-Angle Neutron Scattering Instrument at JRR-2

Susumu KATANO, Haruhiko MOTOHASHI,
Nobuaki MINAKAWA and Masashi IIZUMI

Physics Division, Japan Atomic Energy Research Institute

The construction of a small-angle neutron scattering instrument at JRR-2 is in progress. The design of this machine is similar to that of Oak Ridge Research Reactor (ORR).[1] A cooled Be filter and a composite system of double pyrolytic graphite(PG) crystal monochromators are used to obtain the neutron beam with wavelength of about 4 A and with a rather wide wavelength spread. This report describes the monochromator system.

The monochromator assembly is schematically shown in Fig.1. It consists of five pairs of PG crystals. Neutrons are diffracted once by the first crystal then again by the corresponding second one by the same angle. This double crystal scheme produces a beam which is paralled to and displaced from the reactor beam which contains unwanted γ-ray and fast neutron component. The five pairs are fixed to monochromate neutron beams through 73.2°, 74.4°, 75.6°, 76.8° and 78.0°($2\theta_M$) reflections, respectively, and to displace them by 600 mm. The Bragg angles are chosen to generate five monochromatic neutron beams with wavelength from 4.0 to 4.24 A separated by 0.06 A with each other. Since the wavelength spread provided by a single pair of PG monochromators with 0.4° mosaic spread is estimated as 0.04 A, the separation is the least allowable to avoid the substantial overlap in the wavelength region of one pair with those of neighbors. Each crystal is enclosed in an Al case and mounted on a small crystal table. The setting of the crystal plane is made by rotating and tilting of this crystal table. The PG crystals which are used have a peak reflectivity of about 80% at the neutron wavelength of 2.35 A.

The spectrum of reflected and transmitted intensities were measured by changing the wavelength of a neutron spectrometer. The spectrum of the monochromated beam is

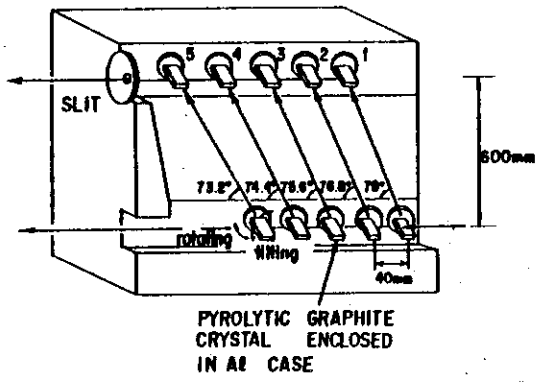

Fig.1. The schematic drawing of the monochromator assembly.

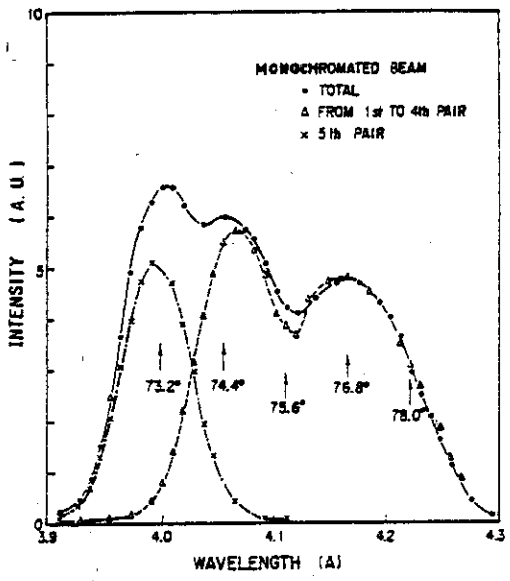

Fig.2. The wavelength spectrum of the monochromated beam. The solid line shows the spectrum of the total monochromated beam. The broken line is the intensity by the fifth pair only and the dotted line is that by other four pairs. The arrow indicates the monochromator angle ($2\theta_M$).

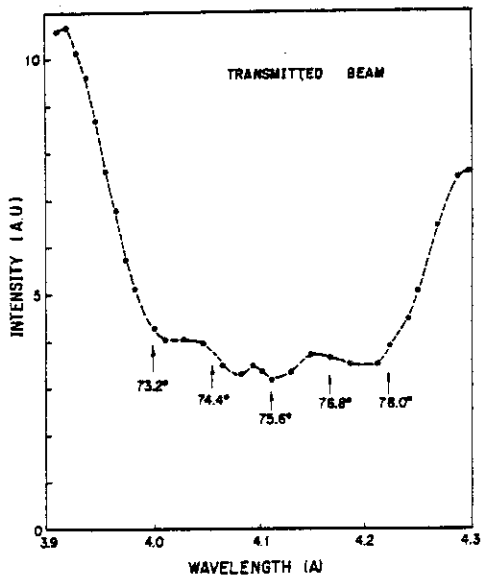

Fig.3. The wavelength spectrum of the transmitted beam. The arrow indicates the monochromator angle ($2\theta_M$).

shown in Fig.2. The arrow indicates the monochromator angle of each crystal pair. The solid line shows the total intensity of the monochromated beam. A rather flat spectrum is obtained compared with the spectrum of the machine at ORR in which three pairs of PG crystals are used.[1] This is probably due to the finite wavelength spread (about 0.06 A) of incident neutrons from the spectrometer used to scan the whole spectrum. The wavelength spread $\Delta\lambda$ is about 0.3 A and the wavelength resoltution $\Delta\lambda/\lambda$ is about 7 %. This is still a little bit smaller than the optimum wavelength spread which is about 10% for ordinary small-angle scattering measurements. It is seen that the intensity by the first ($2\theta_M$ equal 78.0°) and the third monochromater ($2\theta_M$ 75.6°) are a little weak. This is mainly due to the poor peak reflectivity of these monochromator crystals. The monochromated intensity by the fifth pair ($2\theta_M$ equal 73.2°) only is shown by a broken line and that of the total of other four pairs is shown by a dotted line. The spectrum of the transmitted beam is shown in Fig.3. The arrow indicated the monochromator angle of each pair as in Fig.2.

Reference

1) H. R. Child and S. Spooner : J. Appl. Cryst. 13 (1980) 259 .

VI6 Neutron Diffraction Measurement of Texture

Nobuaki MINAKAWA, Susumu KATANO and Masashi IIZUMI

Physics Division, Japan Atomic Energy Research Institute

Measurement of the texture, the grain orientation distribution, of polycrystalline materials has been undertaken by neutron diffraction method in this laboratory. Advantage of the method in the texture measurement has been well recognized. It comes from the high penetrability of neutrons in comparison with X-rays. High absorption of X-rays restricts the thickness of the specimen to less than, say, 0.1 mm and the irradiated volume to less than, say, 0.5 mm^2. And still uncertainty in the absorption correction remains as a problem, especially in measurements with the transmission geometry. The neutron diffraction method is free from these demerits. Therefore it makes it possible to measure an average texture of a thick specimen (about 10 mm thick) containing fairly large grains. Besides, the high penetration of neutrons is also favorable to carry out measurements in a controlled atmosphere (temperature, pressure etc.).

In order to start routine measurements of the texture of engineering materials, such as rolled steel sheets, a texture goniometer (two circle, Eulerian cradle) has been installed on one of the triple axis spectrometers in JRR-2 and a control circuit has been added as shown in Fig. 1. Some preliminary measurements were carried out for a plate of SUS 304 with 5 mm thickness. The pole figures indicating the grain orientation distributions were composed from the diffration intensities measured both for the reflection and transmission geometry. In the reflection method the angles χ and ϕ are used for scanning the pole figure and in the transmission method χ and ω are used instead, as shown in Fig. 2. The controller outputs the intensities on punch tapes which are processed by another computer to compose and plot the pole figures. One of the results, the (111) pole figure of SUS 304 plate, is shown in Fig. 3.

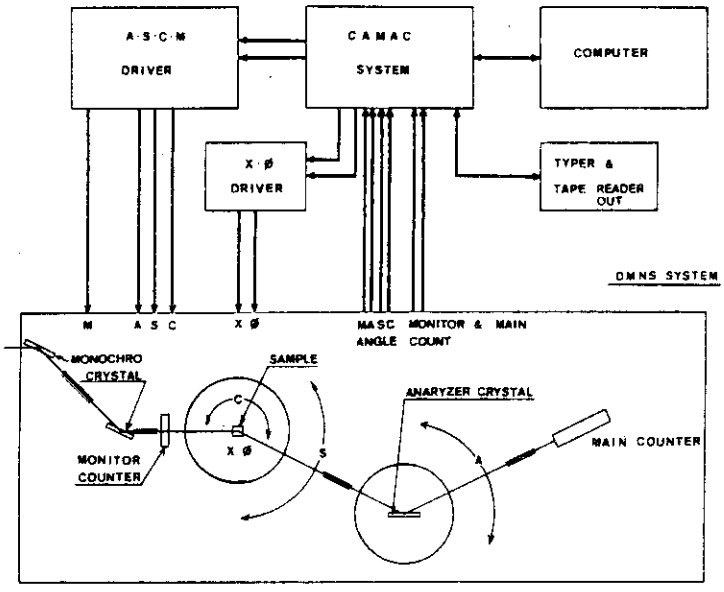

Fig. 1. Control System for Texture Measurements

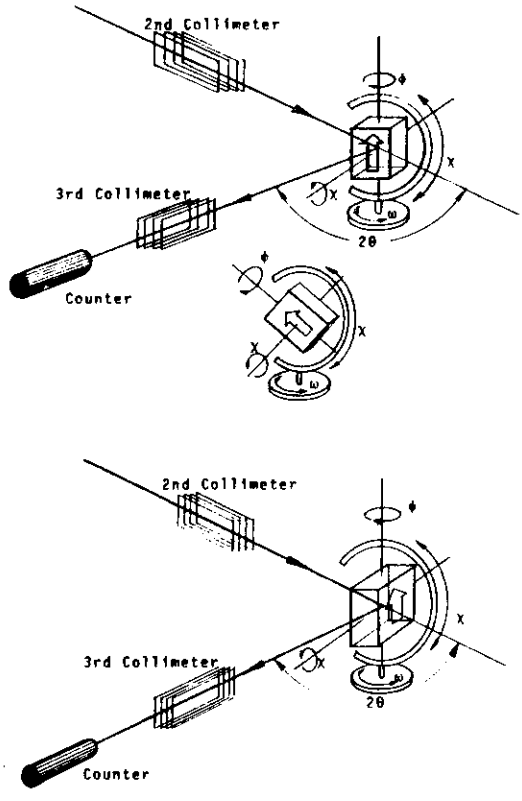

Fig. 2. Transmission (top) and Reflection (bottom) Geometry

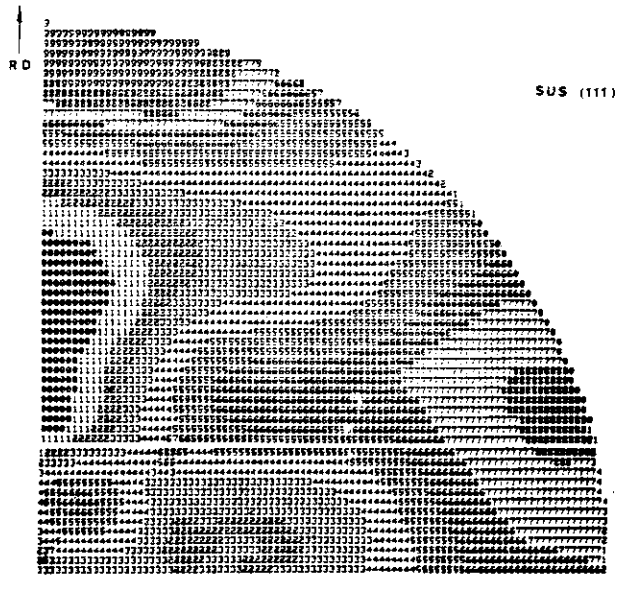

Fig. 3. (111) Pole Figure of SUS 304 Plate

LIST OF PUBLICATIONS

A. Papers Published in Journals

79A40
Y. Endoh, M. Katano, H. Takei, Y. Noda and Y. Ishikawa
Neutron Scattering Study of Cooperative Jahn-Teller Effect in Fe_2TiO_4
J. Mag. Mag. Mat. 14 (1979) 191

79A41
Y. Nakai, I. Tomeno, J. Akimitsu and Y. Ito
Magnetic Form Factor of Ni-Pt Alloy System
J. Phys. Soc. Jpn 47 (1979) 1821

79A42
Y. Tsunoda and N. Kunitomi
Observation of a Resonance-Like Phonon Mode in a force-Constant Disorder System $Pd_{70}Ag_{30}$
Solid State Commun. 31 (1979) 641

80A1
H. Asano, K. Kishi and M. Hirabayashi
Static Displacement of Ta in Ta_2H Studies by Single Crystal X-ray and Neutron Diffraction
Proc. JIMIS-2 Hydrogen in Metals, Minakami, 1979. Jpn Inst. Met. (1980) 93

80A2
Y. Endoh, J. Mizuki and Y. Ishikawa
Spin Density Wave in Dilute Fe and Si-Cu Alloys under High Pressure
J. Mag. Mag. Mat. 15-18 (1980) 501

80A3
S. Funahashi and Y. Hamaguchi
Spin-Wave Dispersion Relations in Mn_2Sb
J. Mag. Mag. Mat. 15-18 (1980) 353

80A4
K. Gesi and M. Iizumi
Study on the Incommensurate Nature of the Intermediate Phase of the $RbD_3(SeO_3)_2$ by Neutron Diffraction
J. Phys. Soc. Jpn 48 (1980) 697

80A5
K. Gesi and M. Iizumi
Neutron DIffraction Study on the Incommensurate Phase in $\{N(CH_3)_4\}_2CuCl_4$
J. Phys. Soc. Jpn 48 (1980) 1775

80A6
M. Hirabayashi
Structural Phase Transitions of Metal Hydrides; V-H and V-D
Proc. JIMIS-2 Hydrogen in Metals, Minakami, 1979. Jpn Inst. Met. (1980) 49

80A7
M. Iizumi and K. Gesi
Neutron Scattering Studies of Ferroelectric Crystals with Incommensurate Phases
J. Phys. Soc. Jpn 49 (1980) Suppl.B 72

80A8
M. Iizumi
Neutron Scattering Studies of Incommensurate Ferroelctrics
J. Mineralogical Soc. Jpn 14 (1980) 319

80A9Y. Ishikawa, K. Tajima, Y. Noda and N. Watanabe
Magnetic Excitations in Ordered Ferromagnetic Alloy Fe_3Pt
J. Phys. Soc. Jpn 48 (1980) 1097

80A10
Y. Ishikawa
Neutron Scattering In magnetic Transition metals
Int. Phys. Conf. Ser. No.55 6 (1980) 357

80A11
M. Kataoka and Y. Endoh
Critical Diffuse Scattering due to Cooperative Jahn-Teller Phase Transition
J. Phys. Soc. Jpn 48 (1980) 912

80A12
M. Kohgi and Y. Ishikawa
Magnetic Excitations in a Metallic Antiferromagnet $FePt_3$
J. Phys. Soc. Jpn 49 (1980) 985

80A13 M. Kohgi and Y. Ishikawa
Paramagnetic Scattering of Neutron from a Metallic Antiferromagnet $FePt_3$
J. Phys. Soc. Jpn 49 (1980) 994

80A14
S. Komura et al.
Spin Wave Excitations in Fe_2P
J. Mag. Mag. Mat. 15-18 (1980)

80A15
N. Kunitomi, Y. Tsunoda and H. Shiraishi
Phonon Dispersion Relations in Cu-Pt -An Evidence of the Effect of the Force constant Disorder-
Solid State Commun. 34 (1980) 519

80A16
T. Tomonao, K. Kikuchi, H. Kondo and Shuzo Sakka
Magnetic Properties of $Cr_{1/3}NbS_2$
Proc. the 3rd Int. Conf. Ferrite (Kyoto 1980) 212

80A17
K. Motoya, M. Nishi, Y. Ito and T. Mizoguchi
Spin Wave Excitations of Amorphous Ferromagnetic $Fe_{40}Ni_{40}P_{14}B_6$
J. Phys. Soc. Jpn 49 (1980) 115

80A18
K. Motoya, M. Nishi and Y. Ito
Polarization Analysis Neutron Scattering of Anomalous Paramagnet FeSi
J. Phys. Soc. Jpn 49 (1980) 1631

80A19
H. Obara, Y. Endoh, Y. Ishikawa and T. Komatsubara
Magnetic Phase Transition of MnP under Magnetic Field
J. Phys. Soc. Jpn 49 (1980) 928

80A20
I. Okada, H. Asano and M. Hirabayashi
Refinement of the Structure of β-V_2D by Single Crystal Neutron Diffraction
Proc. JIMIS-2 Hydrogen in Metals, Minakami, 1979 Jpn Inst. Met. (1980) 89

80a21
T. Sakuma and S. Hoshino
The Phase Transition and the Structures of Superionic Conductor Ag_3SBr
J. Phys. Soc. Jpn 49 (1980) 678

80A22
T. Sakuma and S. Hoshino
Anharmonic Thermal Vibration of Cation in β-Ag_3SI
J. Phys. Soc. Jpn 48 (1980) 1036

80A23
S. K. satija, J. D. Axe, G. Shirane, H. Yoshizawa and K. Hirakawa
Neutron Scattering Study of Spin Waves in 1D Antiferromagnet $KCuF_3$
Phys. Rev. B21 (1980) 2001

80A24
S. K. Satija, G. Shirane, H. Yoshizawa and K. Hirakawa
Neutron Scattering Study of Spin Dynamics in $CsCoCl_3$
Phys. Rev. Letters 9 (1980) 1548

80A25
M. Sato
Low Lying Phonon Dispersion Curves of Rb_xWO_3
J. Phys. C13 (1980) L481

80A26
M. Sato, K. Abe, Y. Endoh and J. Hayter
Magnetisation of Ferromagnetic Metals at the Interface of Other Materials
J. Phys. C13 (1980) 3563

80A27
M. Suzuki, H. Ikeda, H. Suematsu, Y. Endoh, H. Shiba and M. T. Hutchings
Neutron Scattering Studies of the Ordered Structure of $C_{24}Rb$
J. Phys. Soc. Jpn 49 (1980) 671

80A28
K. Tajima, Y. Ishikawa and H. Obara
Neutron Scattering Studies of the Ferro to Spiral Transition in MnP
J. Mag. Mag. Mat. 15-18 (1980) 373

80A29
T. Tawaraya, K. Katsumata and H. Yoshizawa
Neutron Diffraction Experiment on a Randomly Mixed Antiferromagnet with Competing Spin Anisotropies
J. Phys. Soc. Jpn 49 (1980) 1299

80A30
Y. Tsunoda and Y. Nakai
Inclined Spin Axis of Mn-Rich γ-MnCu Alloy
Solid State Commun. 34 (1980) 413

80A31
H. Watanabe, H. Oda, E. Nakamura, Y. Yamaguchi and H. Takei
Magnetic Polarization of Oxygen Ions in $SrFeO_3$
Proc. Int. Conf. Ferrites (Cent. Acad. Pub. Jpn 1980) 381

80A32
H. Watanabe and Y. Yamaguchi
Electronic State of Cations in NiAs type Compounds Containing Mn
J. Mag. Mag. Mat. 15-18 (1980) 863

80A33
H. Watanabe, Y. Yamaguchi, H. Oda and H. Takei
Magnetic and Neutron Diffraction Study of $SrCoO_{3-x}$
J. Mag. Mag. Mat. 15-18 (1980) 521

80A34
Magnetic Disturbance around the Interstitial-Site Mn Atoms in MnSb
J. Phys. Soc. Jpn 48 (1980) 435

80A35
Y. Yamaguchi, Y. Ohishi, M. Ohashi, O. Yamashita and H. Watanabe
Electrical Conductivity and 3d- Elctron Distribution in $CuCr_2Se_{4-x}Br_x$
Jpn. J. Appl. Phys. 19-3 (1980) 291

80A36
H. Yoshizawa, W. Kozukue and K. Hirakawa
Neutron Scattering Study of Magnetic Excitations in Pseudo-one Dimensional Singlet Ground State Ferromagnet $CsFeCl_3$ and $RbFeCl_3$

81A1
H. Asano and M. Hirabayashi
Neutron Diffraction Studies of Metal Hydrides
Metal Hydrides, Proc. NATO Advanced Study Inst. Rhodes, 1980, Ed. G. Bambakidis, Plenum (1981) 81

81A2
Y. Endoh, I. U. Heilmann, R. J. Birgeneau, G. Shirane, A. R. McGurn and M. F. Thorpe
Static and Dynamical Magnetic Properties in the Random One Dimensional Antiferromagnet TMMC:Cu
Phys. Rev. B23 (1981)

81A3
Y. Endoh, Y. Noda and M. Iizumi
Lattice Dynamics and Invar Properties in f.c.c FeMn Alloy
J. Phys. Soc. Jpn 50 (1981) 469

81A4
S. Funahashi, H. Nozaki and I. Kawada
Magnetic Structure of V_5S_8
J. Phys. Chem. Solids 42 (1981) 1009

81A5
M. Hirabayashi and H. Asano
Order-Disorder Phenomena in Metal Hydrides
Metal Hydrides, Proc. NATO Advanced Study Inst. Rhodes, 1980, Ed. G. Bambakidis
Plenum (1981) 53

81A6
Phase Transition of Ag_3SX (X=I, Br)
S. Hoshino et al.
Solid State Ionics 3/4 (1981) 35

81A7
S. Iida, S. Kawarazaki and N. Kunitomi
Neutron Diffraction Study of Chromium-Germanium Alloys
J. Phys. Soc. Jpn 50 (1981) 3612

81A8
S. Iida, M. Kohno, Y. Tsunoda and N. Kunitomi
Strain Waves in Cr, CrMn and CrV Alloys
J. Phys. Soc. Jpn 50 (1981) 2581

81A9
S. Iida, Y. Tsunoda, Y. Nakai and N. Kunitomi
Third Harmonics of Spin Density Wave in Cr and Its Alloys
J. Phys. Soc. Jpn 50(1981) 2587

81A10
M. Iizumi
Fluctuation and Modulated Structures
J. Cryst. Soc. Japan 23 (1981) 140

81A11
Phase Transition in Incommensurate Insulators
JAERI_M 9843 (1981)

81A12
H. Ikeda
Sharp Phase Transition in Two-Dimensional Dilute Antiferromagnets $Rb_2Co_cMg_{1-c}F_4$
J. Phys. Soc. Jpn 49 (1981) 671

81A13
H. Ikeda, T. Abe and I. Hatta
Phase Transitions in Two-Dimensional Random Antiferromagnets $Rb_2Co_cNi_{1-c}F_4$
J. Phys. Soc. Jpn 50 (1981) 1488

81A14
Y. Ishikawa, S. Onodera and K. Tajima
Longitudinal Spin Fluctuations in Invar Alloys of Ordered Fe_3Pt and disordered $Fe_{65}Ni_{35}$
Solid State Commun. 38 (1981) 561

81A15
Y. Ishikawa et al.
Spin Dynamics in the Amorphous Invar Alloy of $Fe_{86}B_{14}$
J. Phys. Soc. Jpn 50 (1981) 1958

81A16
K. Katsumata et al.
Spin-Glass Behabior of a Randomly Mixed Insulating Ferromagnet and Antiferromagnet
Phys. Rev. b24 (1981) No. 11

81A17
M. Kohgi and Y. Ishikawa
Neutron Scttering from FeSi
Solid State Commun. 37 (1981) 833

81A18
J. Mizuki and Y. Endoh
Conventional High Pressure Techniques for Neutron Diffraction
J. Phys. Soc. Jpn 50 (1981) 914

81A19
Y. Nakai and S. Iida
Emperical Relation between Amplitude and Period of Spin Density Wave for Cr(V) and Cr(Mn) alloys
J. Phys. Soc. Jpn 50 (1981) 3637

81A20
O. Okada, T. Miyadai and K. Kikuchi
Magnetic Properties of $Mg_{1-p}Mn_pTe_2$ near p=0.5
J. Mag. Mag. Mat. 22 (1981) 306

81A21
S. Onodera, Y. Ishikawa and K. Tajima
Spin Dynamics in Invar ($Fe_{65}NI_{35}$, Fe_3Pt) and Non Invar ($Fe_{50}Ni_{50}$) Alloys
J. Phys. Soc. Jpn 50 (1981) 1513

81A22
T. Sano, S. Kawarazaki, S. Iida and N. Kunitomi
Neuatron Diffraction Study on the Magnetic Phase Diagram of Cr-Be Alloy
J. Phys. Soc. Jpn 50 (1981) 1203

81A23
H. Suematsu, M. Suzuki, H. Ikeda and Y. Endoh
Phase Transition in the Graphite Intercalation Compound $C_{24}Rb$
Synthetic Metals 2 (1981) 133

81A24
M. Suzuki, H. Ikeda, H. Suematsu, Y. Endoh and H. Shiba
Phase Transition in Rubidium Intercalated Graphite
Physica 105b (1981) 280

81A25
T. Takahashi, H. Tomimitsu, Y. Ushigami, S. Kikuta and K. Doi
The Very Small Angle Scattering from Neutron-irradiated Amorphous Silica
Jpn J. Appl. Phys. 20 (1981) L837

81A26
H. Tomimitsu
Neutron Diffraction Topographic Observation of the {100}-layer Substructure in a Cu-5%Ge Single Crystal
Phil. Mag. A43 (1981) 469

81A27
H. Tomimitsu and k. Doi
Observation of the {100}-layer Substructure in a Cu-5%Ge Single Crystal by Neutron Diffraction Topography
Sci. Rep. RITU A29 Suppl. (1981) 47

81A28 Y. Tsunoda and Y. Nakai
X-ray and Neutron Scattering Measurements in Mn-Rich γ-MnCu Alloy Single Crystal
J. Phys. Soc. Jpn 50 (1981) 90

81A29
Y. Tsunoda and N. Wakabayashi
Phonons and Martensitic Transformation in Mn-Rich γ-MnCu Alloys
J. Phys. Soc. Jpn 50 (1981) 3341

B. Preprints of Papers Submitted for Publication

81B1
K. Hirakawa, H. Yoshizawa and K. Ubukoshi
Neutron Scattering Study of the Phase Transition in Two- Dimensional Planar Ferromagnet K_2CuF_4
Tech. Rep. ISSP, (1981) No. 1148

81B2
K. Hirakawa
Kosterlitz-Thouless Transition in Two-Dimensional Planar Ferromagnet K_2CuF_4
27th MMM Conf. Atlanta (1981) Nov.

81B3
K. Hirakawa, H. Yoshizawa and K. Ubukoshi
Magnetic and Neutron Scattering Study of One Dimensional Heisenberg Antiferromagnet $CsVCl_3$
Tech. Rep. ISSP (1981) No. 1179

81B4
K. Honma and K. Iida
Neutron Diffraction Study on Liquid Mg-Bi Alloys

81B5
S. Katano and M. Iizumi
Neutron Small-Angle Scattering Study of the Decomposition of an Fe-Cr Alloy in the Unstable State
JAERI_MEMO-9801 (to be published in J. Phys. Soc. Jpn)

81B6
T. Moriya and T. Miyadai
Evidencefor the Helical Spin Structure due to Antisymmetric Exchange Interaction in $Cr_{1/3}NbSe_2$
Tech. Rep. ISSP Ser.A No.1185 (1981)

81B7

S. Takeda, Y. Tsuchiya, S. Tamaki and Y. Waseda

Neutron Diffraction of Liquid Pb-Te Alloys

Submitted to J. Phys. C

81B8

N. Wada, K. Ubukoshi and K. Hirakawa

Incommensurate Magnetic Phase Transition in the Triangular XY-like Antiferromagnet $RbFeCl_3$

Tech. Rep. ISSP (1981) No. 1180